Induction welding of high performance thermoplastic composites

Focused heat generation in weld zones of carbon fiber laminates by magnetic field manipulation and carbon fiber susceptors

M.C. Dhondt

Student no: 4274318

TUDelft

DLR

Induction welding of high performance thermoplastic composites

Focused heat generation in weld zones of carbon fiber laminates by magnetic field manipulation and carbon fiber susceptors

by

M.C. Dhondt

to obtain the degree of Master of Science
at the Delft University of Technology,

Student number: 4274318
Project duration: February 18, 2019 – December 20, 2019
Thesis committee: Dr.-Ing. Jan Stüve, TU Delft
Prof. C.A. Dransfeld, TU Delft
Dr.ing. S. Giovani Pereira Castro, TU Delft
M.Sc. Niklas Menke DLR

TU Delft

DLR

Preface

Before you lies the dissertation “Induction welding of high performance thermoplastic composites: focused heat generation in weld zones of carbon fiber laminates by magnetic field manipulation and carbon fiber susceptors”. It has been written to obtain a master’s degree in Aerospace Structures and Materials from the Delft University of Technology. The thesis was sponsored by and executed at the German Aerospace Center (DLR) in Stade, Germany.

This report is written for anybody interested in induction welding of thermoplastic composites with some background knowledge on composites. It can be read to gain knowledge on the principles of induction welding of thermoplastic composites, to get familiarized with its current state of the art, to get to know about the influence the magnetic field direction has on the heating of multidirectional laminates, to learn about what carbon fiber material heats up more than average and whether this can be used as a benefit in induction welding.

I would like to thank Dr.-Ing. Jan Stüve for supervising me as a professor from the TU Delft. I want to thank M.Sc. Niklas Menke and Dipl.-Ing. Hakan Ucan for the helpful supervision from DLR. Furthermore, I thank Dr. Irene Fernandez Villegas for giving me tips on how to find a suitable thesis topic and I thank Prof. Clemens Dransfeld for giving me useful tips on how to further improve and finalize my research.

I hope you enjoy your reading.

M.C. Dhondt
Stade, December 2019

Contents

Abstract

Mass reduction is one of the main drivers for aircraft design. A big potential for saving mass can be found in part joining. Currently, most parts are joined by mechanical fastening. However, mechanical fastening requires labor intensive work and results in a weight increase especially for composite parts that, due to the mass saving they allow, are increasingly used in the aerospace industry. Induction welding of thermoplastic composites shows great potential to limit this mass increase and it can vastly reduce the amount of work that is needed to join parts while improving the working conditions on the shop-floor.

A characteristic of induction welding is that the heating rate goes down with increasing distance to the inductor. This often leads to fully melting the top plate across its thickness. This results in an imperfect weld as pressure is required for proper consolidation which leads to a damaged surface. Therefore, the challenge is to find a way to selectively heat the weld zone, without using a metallic susceptor that can lead to an unreliable joint. Accordingly, the aim of this thesis is to find how induction heating can be used to selectively heat the weld zone of multidirectional carbon fiber laminates with and without using a carbon fiber susceptor material. To this end, three sub-questions are answered. Can specific plies in multidirectional CFRP laminates be heated by manipulation of the magnetic field? Can a carbon fiber material be used as susceptor material in order to increase the temperature at the weld interface? Is it possible to weld parts with lightning strike protection?

Using an infrared camera and fine wire thermocouples of type E to measure the temperature profile across the thickness of the test parts, a dependency of the heating rate on the orientation of the magnetic field was discovered for all parts that were tested. This dependency can indeed be used to selectively heat plies in a specific orientation within the laminate.

Also, the possibility of using susceptors made of carbon fiber to increase the temperature at the weld zone was shown. To this end, susceptors were made of fabrics and of thin-ply material. Further research has to be done to improve these susceptor materials. An increase of the heating benefit they deliver could enable them to be used for more efficient welds in the future.

Finally, by clamping lightning strike protection (LSP) onto the test parts, the temperature profile of parts with LSP was imitated. Striking was that the heat generated in the two CFRP parts went down when the LSP was added. No peak temperature was measured at the side of the LSP but this could probably be explained by the poor contact between the thermocouple in the test part and the LSP. It is recommended to further investigate this topic by consolidation of the LSP onto the test part.

List of Figures

List of Tables

Nomenclature

List of Abbreviations

AE	Aerospace Engineering
AFP	Automated fiber placement
ATL	Automated tape laying
CF	Carbon fiber
CFRP	Carbon fiber reinforced polymer
CFRT	Carbon fiber reinforced thermoplastic
DLR	German aerospace center
DoE	Design of experiments
emf	Electromagnetic field
FBG	Fiber Bragg Grating
FVC	Fiber volume content
Lam.	Laminate
LSP	Lightning strike protection
LWD	Long Way of Design
NCF	Non-crimp fabric
PEAK	Polyaryletherketone
PEEK	Polyetheretherketone
PEKK	Polyetherketoneketone
RTD	Resistance Temperature Detector
TC	Thermocouple
TPC	Thermoplastic composite
UD	Uni-Directional

List of Symbols

μ	Magnetic permeability
ρ	Electrical resistivity
ρ_f	Fiber density
ρ_m	Matrix density
ε_0	Vacuum permittivity

ε_r	Relative permittivity or Dielectric constant
A	Cross sectional area
b	Polymer layer thickness between fibers
C	Capacitance
f	Frequency
K	Thermal conductivity
k	Number of input variables
L	Inductance
l	Length
m_f	Fiber mass
m_m	Matrix mass
N	Amount of experiments to be executed
n	Amount of levels
R	Electrical resistance
$tan\delta$	Loss tangent
v_c	Composite volume
V_f	Fiber volume fraction
v_f	Fiber volume

1

Introduction

In many industries such as the aircraft and car industry, a shift from aluminum structures towards thermoset composite structures takes place [1, 2]. This is because lighter structures can be achieved using composites and therefore lower operating costs are realized due to a reduction in fuel required. The disadvantage, however, of these thermoset composites, is that joining them takes a lot of effort and results in a weight increase [3].

Today, composites are often mechanically fastened which requires holes to be drilled and deburred and fasteners to be installed. Due to these holes, fibres are cut, failures such as delaminations can occur and stress concentrations are imposed [4–6]. Except for the disadvantages regarding the quality of the aircraft, more factors play a role. One factor is that when mechanically fastening a composite structure, carbon fiber dust is created. This is not only very unhealthy for the workers, but it also creates risks as the conductive dust can short circuit machines exposed to the dust. Furthermore, mechanical fastening is very loud and therefore not pleasant for the workers. One alternative to mechanical fastening that eliminates those problems is bonding of thermoset composites. This, however, requires extensive surface treatments, long curing times, it adds weight to the structure and the strength of the bond is unpredictable [4–6].

Research is done into the possibility to join composite structures by welding. Similarly to bonding, this would reduce the effort and risks involved in mechanical fastening but it would also reduce the labor and unpredictability involved in bonding. Welding of composite materials is possible when the thermoset matrix material is replaced by a thermoplastic matrix. Since thermoplastics can be melted, it is possible to join thermoplastic composites (TPCs) by welding, resulting in lighter structures and lower production costs [7].

One of the main reasons to use TPCs is that they can be melted and joined by welding. Even though TPCs are more expensive and suffer from creep as will be explained later, their advantages are numerous. These advantages over thermoset composites include [7–10]:

1. They can be remelted and thus reformed and welded.
2. They require no curing and thus a shorter to no autoclave cycle is required.
3. They have an almost indefinite shelf-life.
4. They do not have to be cooled in storage and thus have reduced storage costs.
5. They have a higher impact resistance.
6. Can be recycled more easily than thermoset composites.
7. TPCs allow for more efficient repairs.
8. They can be processed rapidly.

Except for all the advantages that are listed above, some disadvantages or challenges remain for TPCs. One of those disadvantages of using a thermoplastic matrix includes that higher processing temperatures and pressures are required [10]. This is because the melting temper-

atures are higher for high performance thermoplastics than the curing temperatures for thermosets. Also, the viscosity of molten thermoplastics is higher than for uncured thermosets, requiring a higher pressure to wet the fibers with a thermoplastic matrix properly.

For an aerospace thermoset composite, a normal processing cycle would contain a maximum temperature of 180°C, maximum pressure of 7 bar and a processing time of approximately 6 hours [11]. For thermoplastic composites pressures between 7 bar and 24 bar are found in previous studies at temperatures slightly above their melting temperature [5, 12–14]. The melting temperature of the high performance thermoplastic matrices PEEK, PEKK and PAEK are approximately 350°C, 340°C and 305°C respectively [15]. Processing times of 10-20 minutes have been reported in [5, 12–14]. To these processing times the heating and cooling down time of the autoclave or press used should be added. So, even though the required processing pressures and temperatures for TPCs are higher than that for thermoset composites, the required processing time can be much shorter, depending on the heating technology, which makes the process feasible for automating higher part rates.

Another disadvantage of TPCs is that they suffer from creep. When a material is loaded with a constant force, it quickly deforms to a given strain. Then, it keeps on deforming slowly until failure [16]. This phenomenon is called creep and it is influenced by the lay-up for composites, load, temperature and humidity [17]. This phenomenon is much bigger in thermoplastic materials than in thermoset materials as thermosets have crosslinks that prohibit the movement of the polymer chains, resulting in less creep [16]. Because crystals in thermoplastic materials act like crosslinks in thermoset materials, creep goes down with increasing crystallinity [18]. Because crystals get more time to form when the cooling rate after welding is decreased, the degree of crystallinity increases with decreasing cooling rate [19]. Therefore, reducing the cooling rate after welding results in parts or welds that will experience less creep. The minimum amount of crystallinity required in a weld is still to be determined and is likely to differ for each weld. The effect this crystallinity requirement has on the process time still needs to be investigated.

Finally, a disadvantage of TPCs is that generally the raw-material cost is higher than that for thermoset matrices [20, 21]. However, more costs can be saved by shorter production cycles, joining by welding instead of riveting and the elimination for the need of storing and transporting the pre-preg materials cooled [22].

Beside the fact that thermoplastic material possesses a lot of advantages of their own as was listed above, the advantages gained from the possibility to weld are plenty. These advantages compared to mechanical fastening include [4, 6, 22, 23]:

1. No carbon fiber dust is produced by drilling in the production environment
2. No delaminations occur due to drilling
3. Less stress concentrations are induced
4. Less thermal stresses are induced
5. No galvanic corrosion occurs
6. Less work is required
7. There is no additional weight of the fastening system

In order to utilize the aforementioned advantages, a good welding technique has to be used. As automation becomes more and more important, the industry is looking for techniques that can be made continuous, automated and quality assured and can be combined with other techniques such as Automated Tape Laying (ATL) and Automated Fiber Placement (AFP) that are increasingly used to manufacture parts.

There are a lot of techniques that can be used to weld TPCs. These include resistance-, vibration-, ultrasonic-, induction-, hot plate-, microwave-, high frequency-, spin-, laser- and hot air welding [24, 25]. From these techniques, three are believed to be the most promising for welding TPCs. These include resistance-, ultrasonic- and induction welding [4, 6, 22]:

1. In resistance welding an electrically resistive element is put between the to be welded surfaces [26]. According to Joule's Law, heat is generated when current flows through

the element. This heat melts the matrix and when the current is turned off, a weld is formed while cooling under pressure [26, 27]. A set-up is shown in Figure 1.1 [26].

2. In ultrasonic welding a sonotrode vibrates the to-be-welded materials using a piezo element. Figure 1.2 shows a set-up for sequential ultrasonic spot welding [13]. The material undergoes high frequency stresses due to which the material heats up [4]. By correctly designing the components, the heat is generated at the weld interface through friction and hysteresis [4].
3. In induction welding a coil is put under an alternating current. This creates a magnetic field around the coil. When a conducting or magnetic material is within this magnetic field, eddy currents are generated in conducting materials and hysteresis losses are generated in magnetic materials [28]. Both phenomena heat up the material and can be used for welding. An induction welding setup is depicted in Figure 1.3 [23].

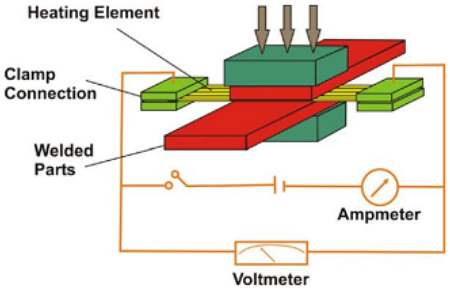

Figure 1.1: Resistance welding [26]

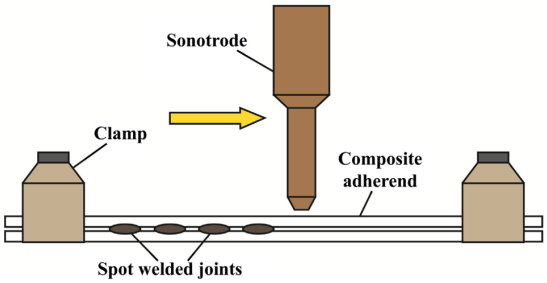

Figure 1.2: Ultrasonic welding [13]

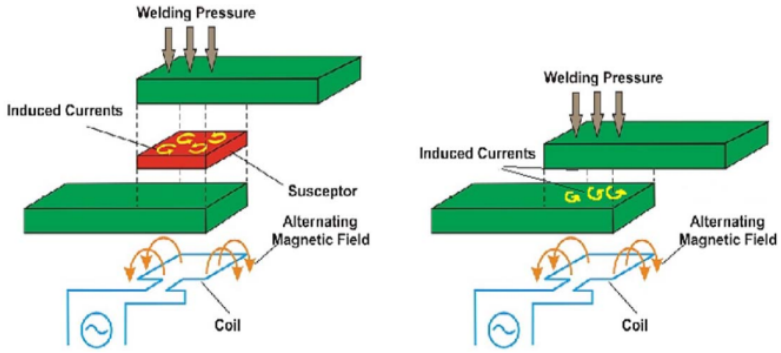

Figure 1.3: Induction welding [23]

The German Aerospace Center (DLR) investigates these three most used welding techniques at different research locations. At DLR in Stade the induction welding process is investigated and therefore this thesis will focus on improving this welding technique. The research question is: how can induction heating be used to selectively heat the weld zone of multidirectional carbon fiber laminates with and without carbon fiber susceptor materials?

First, in Chapter 2, background information is given on induction heating of carbon fiber reinforced thermoplastic composites. Second, in Chapter 3, the state of the art is described. This includes the different strategies that can be followed in order to get a good weld. Third, the research done is explained in Chapter 4, followed by the experimental hardware used in Chapter 5. Then, in order to get first results and to be able to optimize the primary tests, preliminary trials have been executed which are described in Chapter 6. Using the data gathered during the preliminary trials, the primary trials were designed and executed as is outlined in Chapter 7. Then, tests were performed to see whether it is possible to further improve the temperature profile across the thickness of the laminate using a carbon fiber susceptor material in Chapter 8. The possibility to weld parts with lightning strike protection is investigated in Chapter 9, followed by a validation of the test results in Chapter 10. Finally, conclusions and recommendations are given in Chapters 11 and 12 respectively.

2

Theoretical background

In this chapter some theoretical background is provided such that the remainder of the research can be better understood. First, in Section 2.1 the induction heating principle is explained based on the inductor that is available at the German Aerospace Center in Stade, Germany. Then, different methods to measure temperature in electromagnetic fields are explained in Section 2.2.

In order to create a weld, the to-be-welded parts must be heated above their melting temperature. For this, the optimal temperature profile would have the highest temperature at the weld interface, which is at the contact surface where the two parts are to be joined, and a lower temperature at the outer surfaces. This way, the matrix material is melted at the weld zone and the outer surfaces remain solid. Both outer surface areas should be kept under the melting temperature because after melting, pressure needs to be applied during cooling of the parts to allow for good consolidation of material in the weld zone. The application of this pressure is likely to damage the surface when the surface has been molten. Therefore, the optimal temperature profile across the thickness of a laminate is represented by the sketch in Figure 2.1.

Figure 2.1: Optimal temperature profile

2.1. Induction heating principles and characteristics

Materials that heat up under induction are magnetic, conductive or both. Therefore, materials that are magnetic or conductive can be welded without susceptor material. Susceptor materials such as a metal mesh can be used at the weld interface either to weld materials that do not heat up by induction, such as glass fiber reinforced thermoplastics, or to create a better temperature profile across the thickness with the highest temperature at the weld interface. Therefore, when welding carbon fiber laminates (which are conductive enough), it can be chosen to weld with or without a susceptor material. Both have their advantages and disadvantages. By using a susceptor material a better heat profile can be generated but the weld strength and reliability go down due to problems with bonding, thermal stresses, stress concentrations and corrosion [4, 22, 23].

Eddy current generation is possible when closed electrical loops can be formed [29]. These closed loops can be created in CFRT when fibers in different directions either touch each other or are very close to each other. This means that only fabrics and cross plies will heat up when put near an induction coil and stacks of uni-directional (UD) plies in one direction will hardly heat up.

The technique can be made continuous by moving a coil over the surface followed by a cooled tool that provides pressure for consolidation [2, 30]. Additionally, the surface underneath the coil is often cooled using, for instance, an air jet in order to move the hottest point towards the weld zone [21, 31]. The coil heats up the laminate above its melting temperature after which the tool applies pressure and cools the laminate for consolidation [32, 33]. An illustration of this continuous process can be found in Figure 2.2 [33].

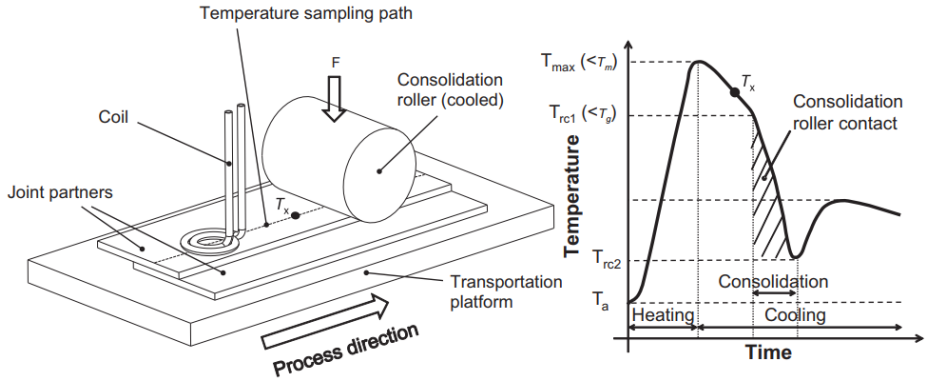

Figure 2.2: Setup example for continuous induction welding [33]

In Figure 2.2, the material is moved underneath the coil and cooled tool (roller). However, it is also possible to move the coil and cooled tool, while keeping the material stationary [2, 8, 30, 34, 35].

Induction heating is based on an alternating current in a coil which generates an alternating magnetic field inducing eddy currents in conductive materials within this field. Inductors come in different shapes and sizes and in Figure 2.3 [36] the inductor is shown that is available at DLR. Here, the current flows through the copper which induces a magnetic field, the ferrite focuses the magnetic field on the CFRP part and the water cools the inductor.

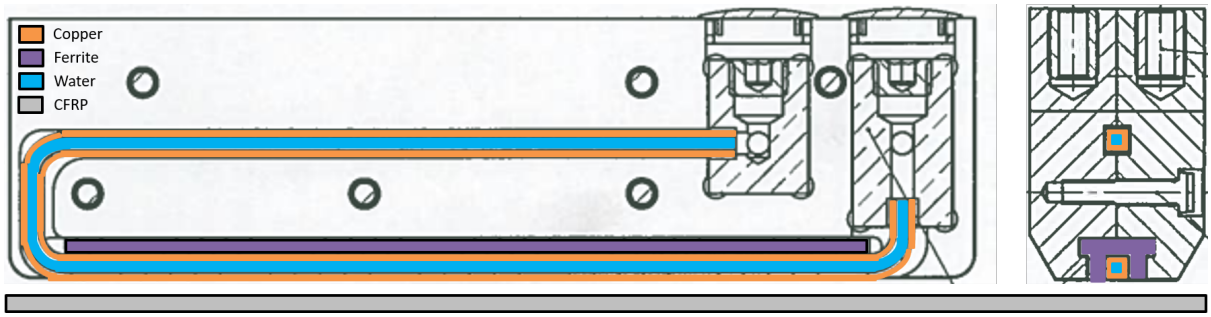

Figure 2.3: Inductor sketch [36]

According to Lenz's law, eddy currents are generated such that their resulting magnetic field opposes the change in magnetic field that caused them [28]. Lenz's law is further explained in Figure 2.4.

The generation of eddy currents is depicted in Figures 2.5a to 2.5c. As can be seen in Figure 2.5a, both the upper and lower copper tube generate a magnetic field. However, as the lower field is focused by the ferrite, the effect of the field generated by the top tube can be

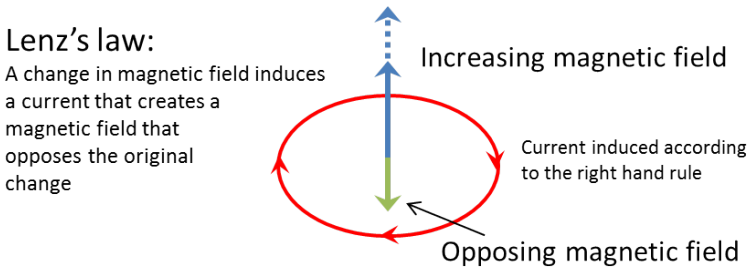

Figure 2.4: Lenz's law - Eddy current generation

neglected as is shown in Figure 2.5b. Then, using Lenz's law, the direction of the eddy is determined and shown in Figure 2.5c.

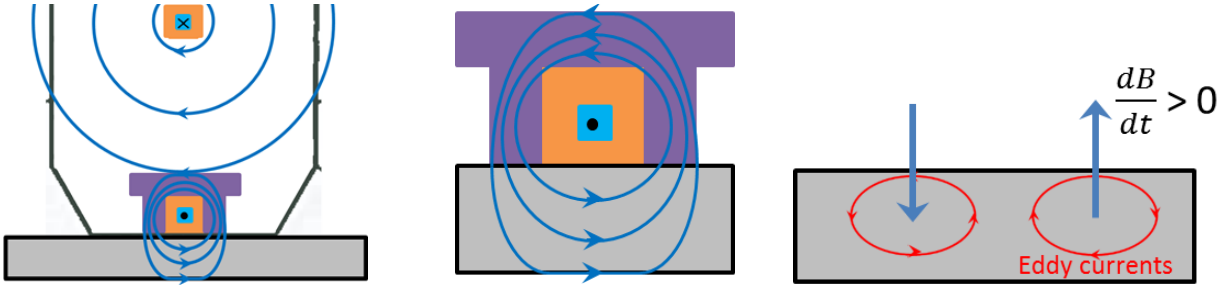

(a) Magnetic field lines by inductor (b) Close-up of magnetic field lines (c) Eddy current generation

Figure 2.5: Eddy current generation according to Lenz's law

Because the eddy currents induce a magnetic field opposing the field that generated them, the penetration depth of the electromagnetic field is limited [33]. This effect is called the "skin effect" and it describes the depth at which the density of the eddy currents has decreased to $1/e = 37\%$ [23]. The skin depth (δ) can be calculated using Equation (2.1) [23, 33].

$$\delta = \sqrt{\frac{\rho}{\mu \cdot \pi \cdot f}} \tag{2.1}$$

Where: ρ = electrical resistivity [$\Omega \cdot m$], μ = magnetic permeability [H/m], f = frequency [Hz]

The current density across the thickness of a laminate was calculated by Schieler [3] and is shown in Figure 2.6. The blue line represents an infinitely thick laminate whereas the red lines represent laminate thicknesses of 0.3, 0.5 and 0.8 times the skin thickness. In a laminate with finite thickness the magnetic waves are reflected by the backside of the material resulting in higher current densities across the thickness of the laminate [3].

It can be noted from Figure 2.6 that the smaller the laminate thickness is compared to the skin thickness, the more homogeneous the current profile across the thickness of the laminate is [3]. Therefore, the heating profile across the laminate thickness will be more homogeneous for decreasing laminate thickness and/or increasing skin depth. A small laminate thickness compared to the skin thickness can be achieved by decreasing the inductor frequency or by decreasing the magnetic permeability of the laminate, increasing its electrical resistivity or by decreasing the laminate thickness.

Schieler [3] showed that when clamping two consolidated laminates together, a discontinuity in the temperature profile can be found at the interface of the two plates which is shown in Figure 2.7. The discontinuity is a consequence of the semi-permeability of the laminate surface which causes the magnetic wave to partially reflect [3]. According to Schieler [3], the second laminate has no effect on the heating of the first laminate with the exception of cooling

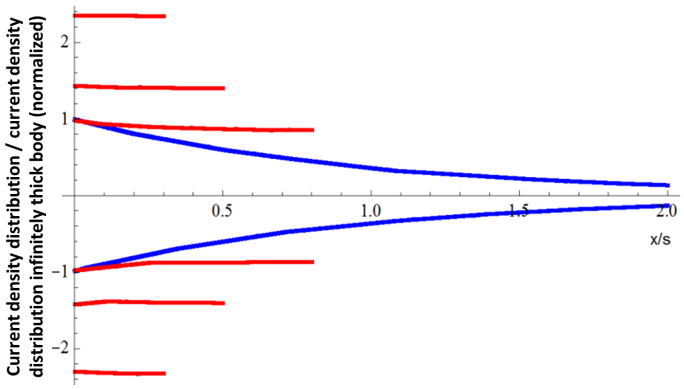

Figure 2.6: Current profile across thickness of laminate (blue = infinitely thick laminate, red = 0.3, 0.5 and 0.8 times the skin thickness) [3]

by conduction. This is contradicted by Duhovic et al. [37] stating that the heat developed in the top plate is affected by the bottom plate. Because the generated eddy currents generate a magnetic field themselves, the eddy currents in the bottom plate can affect the heat generated in the top plate. However, this effect is expected to be very small. The effect of the bottom plate on the top plate should be further investigated.

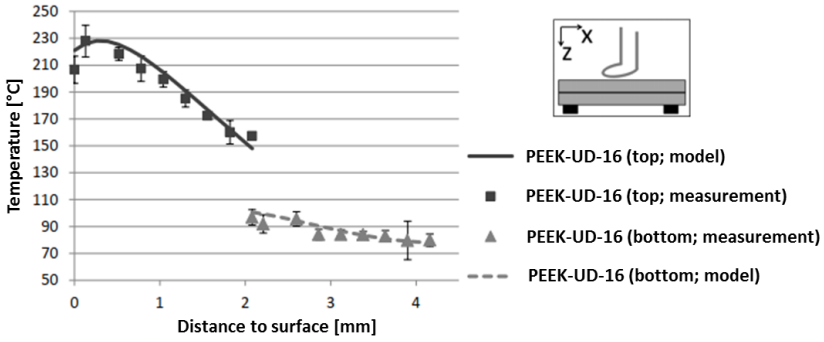

Figure 2.7: Temperature profile of two consolidated laminates pressed together [3]

Because magnetic waves are partially reflected by the backside of the top laminate, a change in temperature profile can be found when heating the samples before and after welding. When the weld is performed, the interface between the two laminates disappears and therefore no partial reflection at the back side of the laminate occurs. The influence on the temperature profile is shown in Figure 2.8 [3]. Here, only the temperature in the top plate is shown in contradiction to Figure 2.7 where the temperature profile in both the top and bottom plate is shown. The change in temperature profile before and after welding could be used to make the process in-line quality controlled [3].

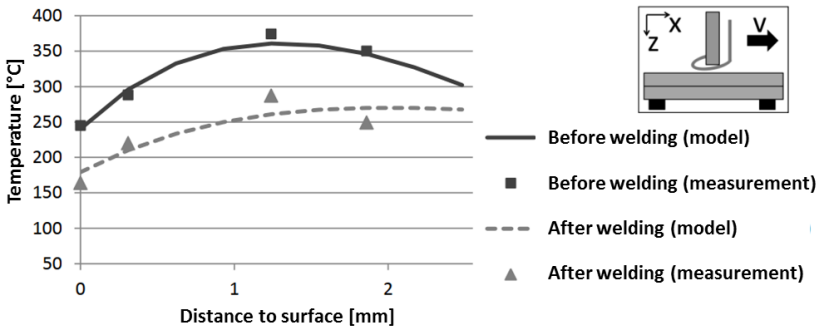

Figure 2.8: Temperature profile of laminate heated before and after welding [3]

Due to the current flowing in the TPC material, heat is generated by three different heating mechanisms. These include Joule losses, contact resistance and dielectric hysteresis heating [8, 38]. Carbon fibers are heated by Joule losses when a current passes through them and this heating is governed by Equation (2.2) [39].

$$R_f = \rho_f \frac{l_f}{A_f} \tag{2.2}$$

Where: R_f is the electrical resistance of a fiber, ρ_f its specific electrical resistance, l_f its length and A_f its cross sectional area.

Junction heating and dielectric hysteresis heating, however, occur at the contact points of the fibers. Dielectric heating occurs when the matrix is dielectric and matrix material surrounds the fibers such that the fibers are not in direct contact [38]. The matrix material acts as a capacitor and resistor and the generation of heat is dependent on the matrix properties and on the frequency [38]. The governing equation is presented in Equation (2.3) [39].

$$R_{jd} = \frac{b}{2\pi f \epsilon_0 \epsilon_r (tan\delta) A_j} \tag{2.3}$$

Where: R_{jd} is the equivalent resistance, b equals the polymer layer thickness between fibers, f is the frequency of the electromagnetic field, ε_0 is the vacuum permittivity, ε_r is the relative permittivity of the matrix, $tan\delta$ is the loss tangent of the matrix and A_j is the projected area between two fibers in the crossing area.

In junction heating the fibers touch each other and the heat generated is dependent on the contact resistance between the fibers [38]. The contact resistance is dependent on a lot of factors and can be determined by the method explained by Yarlagadda et al. [38]. The three heating mechanisms are visualized in Figure 2.9 [38]. The arrow “emf” indicates the direction of the electromagnetic field.

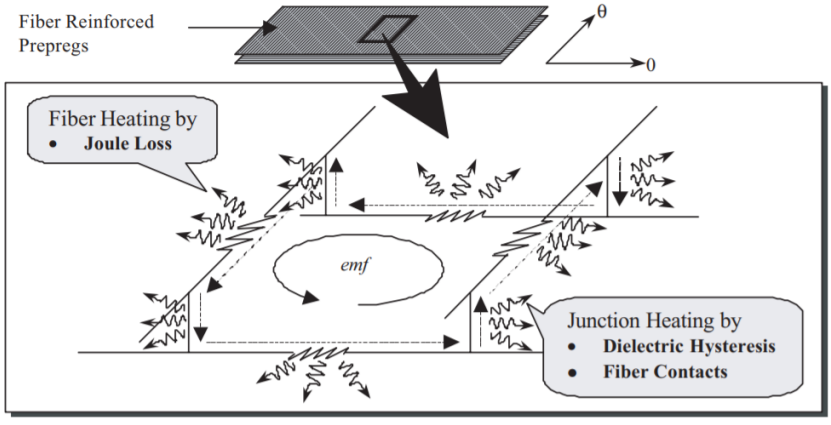

Figure 2.9: Heating mechanisms in TPCs [38]

For metals, only heating by Joule losses and magnetic hysteresis occur as there are no fibers and therefore no contact resistance or dielectric hysteresis heating. For metals, the higher the electrical resistivity is (which is the inverse of electrical conductivity), the higher the heating rate is [28]. This is due to increased Joule losses with higher resistance. Opposing to this, the heating rate of CFRP is increased with increased conductivity (and thus decreased resistivity). Causing this difference is the low conductivity of CFRP compared to metal, and when no electricity is able to flow, no heating takes place. Therefore, an optimum in electrical conductivity should be present. In general, metals heat up better by induction than CFRPs do.

Much research has been done into induction heating of laminates built with CF fabrics [2, 25, 30–32, 40]. However, there are two reasons why researching induction heating of laminates built with CF fabrics is decreasing. First of all, unidirectional reinforcements allow for better mechanical properties than fabric reinforcements do [41]. These improved mechanical properties are needed to compete in the aerospace industry. Second of all, the current trend in many industries is to automate production processes using techniques such as Automated Tape Laying (ATL) and Automated Fiber Placement (AFP). These techniques, however, do not lay fabrics but Uni-Directional (UD) material instead. Therefore, research into the induction heating of CF fabric reinforced laminates is decreasing. As closed loops are required for heat generation, stacks of UD plies do not heat up well [42]. When UD layers are placed in different orientations, closed loops can be formed and heat is developed [43].

Because parts are increasingly often made of cross-plies, it can be investigated whether plies in different directions from the main load carrying direction can be used to generate heat in specific plies close to the weld interface. In order to do this, it is important to understand how and where the eddy currents are generated.

Because both the generation of eddy currents and the skin effect are dependent on characteristics of the magnetic field (frequency and orientation), it is interesting to investigate whether induction heating can be used to target specific plies in a laminate. As to the best of the author's knowledge, this has not been done for cross-plies yet. For fabrics it was tried, but no significant difference could be found [29].

As for every technique, also induction welding has a few challenges that need to be addressed. These include that, because of the skin effect and because the magnetic field near the coil is the strongest, the most eddy currents are introduced near the coil. This results in the most heat generation at the surface closest to the coil. However, as convection cools the surface down, the hottest spot can be found close to, but not on the surface [21]. This means that the weld zone most likely does not have the highest temperature and that there is a risk of damaging the surface.

Further challenges for all TPC welding processes include, but are not limited to [2, 8, 12, 21, 22, 30, 34, 44]:

- The temperature at the weld zone should go over the melting temperature but nowhere over the degradation temperature.
- The degree of crystallinity of the matrix material and thus the quality of the weld is dependent on the cooling rate.
- The edge effect results in a non-homogeneous heating over the weld.
- There are a lot of variables in the material to be welded.

All these challenges make it difficult to design a solid process that can be applied in different circumstances. For this to be possible, research has to be performed to create a thorough understanding of where and how much heat is generated within different laminates, how the edge effect can be predicted or minimized, what the influence is of the cooling rate, welding temperature and pressure on the mechanical properties of the weld and much more.

2.2. Temperature measurement in electromagnetic fields

Various means to measure temperature exist. In order to regulate the welding process, it is important to know the temperature profile over the thickness of the part that is welded. With this temperature profile, it can be investigated what effects characteristics of the magnetic field and layup have on the heat generated across the thickness of a laminate. Measuring the temperature can be done using infrared cameras as is explained in Section 2.2.1, using thermocouples as is described in Section 2.2.2 or using other types of sensors as is outlined in Section 2.2.3. Important is that the electromagnetic field, in which the sensor will be used, does not result in large errors.

2.2.1. Infrared camera

Every object emits infrared energy when its temperature is above absolute zero. An infrared camera measures the infrared energy that is emitted and converts this to a voltage [45]. Infrared cameras are easy to use, can be used in many different settings and create nice visuals that can be used to present the data. However, a disadvantage of using infrared cameras is that only the temperature at the surface of a part can be measured. Therefore, it is a nice tool to use to check the temperature of the surface of the to-be-welded part, but it cannot tell anything about the temperature that can be found in the weld zone or anywhere else across the thickness of the laminate.

In several studies, two infrared cameras were used measuring the temperature at the surface facing the coil and the surface not facing the coil [12, 31, 34, 42].

When using infrared cameras, it is important to note that every material, including different types of CFRPs, has a different coefficient of emissivity. This coefficient is used to determine the temperature of the surface. Therefore, for a quantitative evaluation of the temperature using an infrared camera, the emissivity coefficient should be known and applied in the software. When this emissivity coefficient is not correctly used, the images still show a qualitative picture of temperature differences, but the absolute temperatures are false [46].

2.2.2. Thermocouples

Thermocouples are widely used temperature sensors made of two dissimilar electrical conductive metals. When these dissimilar metals touch, a small open-circuit voltage is created which is dependent on the temperature [47]. This voltage is called the Seebeck voltage and was discovered in 1821 by Thomas Seebeck [47]. Temperature causes the voltage to change in a nonlinear way, however, over small ranges of temperature, the relation can be considered linear. Thermocouples are typically inexpensive and have a large temperature range.

Different types of thermocouples exist that are made of different types of metals. These different types result in different characteristics such as sensitivity and operating windows. These characteristics are given in Table 2.1 [47, 48].

Table 2.1: Thermocouple characteristics [47, 48]

Thermocouple Type	Positive Conductor	Negative Conductor	Temperature Range (°C)	Voltage Range (mV)	Seebeck Coefficient (V/°C)
E	Chromel	Constantan	-270 to 1,000	-9.835 to 76.358	58.70 at 0°C
J	Iron	Constantan	-210 to 1,200	-8.096 to 69.536	50.37 at 0°C
K	Chromel	Alumel	-270 to 1,372	-6.548 to 54.874	39.48 at 0°C
T	Copper	Constantan	-270 to 400	-6.258 to 20.869	38.74 at °C
S	Platinum-10% Rhodium	Platinum	-50 to 1,768	-0.236 to 18.698	10.19 at 600°C
R	Platinum-13% Rhodium	Platinum	-50 to 1,768	-0.226 to 21.108	11.35 at 600°C

Even though the temperature range is large as is shown in Table 2.1, the supplier of the thermocouples, Omega Engineering GmbH, Deckenpfronn, Germany, recommends that the unsheathed fine wire diameter thermocouples are used below the maximum service temperatures stated in Table 2.2 [48–50]. Here, the maximum service temperatures are stated for different wire diameters and the limit of error is stated for the standard variant of each thermocouple type and for the special type. Note that the percentages denoted are the percentages of the temperature in Kelvin and the greater of the two stated values counts. As can be seen, the maximum service temperatures of thermocouple type K and E with a diameter of 0.13mm pose no problems when PEKK is used which has a melting temperature of 340°C. This means that these thermocouples can be laminated in the test parts.

Table 2.2: Maximum service temperature unsheathed fine diameter thermocouples with bead-welded junction and thermocouple accuracy [48–50]

Thermocouple Type	0.13 mm	0.38 mm	0.51 mm	0.81 mm	Limit of error Standard	Limit of error Special
J	320°C	370°C	370°C	480°C	2.2°C or 0.75%	1.1°C or 0.4%
K	590°C	870°C	870°C	980°C	2.2°C or 0.75%	1.1°C or 0.4%
T	200°C	200°C	200°C	260°C	1.0°C or 0.75%	0.5°C or 0.4%
E	370°C	430°C	430°C	590°C	1.7°C or 0.5%	1.0°C or 0.4%
R, S	-	-	1450°C	1450°C	1.5°C or 0.25%	0.6°C or 0.1%
B	-	-	1700°C	1700°C	0.5%	0.25%

Thermocouples should be calibrated before use. This is required for accurate measurements as each thermocouple produces a slightly different voltage for each temperature. Calibration is done in a special oven that can accurately regulate the temperature within a small volume within this oven. The thermocouples are then inserted into this oven in such a way that the hot junction is within this regulated volume. The thermocouples are calibrated by comparing the reference temperature with the temperature measured by the thermocouple. This is done over the range in which the thermocouple is going to be used. From this, a polynomial will result which accurately relates the voltage produced to the temperature.

Because thermocouples are made of electrical conductive metals, they are also affected by the alternating magnetic field resulting in errors as they are heated up via induction themselves [51]. Also, when the inductor is on, a current is induced in the thermocouple producing false readings which disappears again when the inductor is turned off [51]. Schieler [3] investigated how much the different thermocouples of diameter 0.13mm heat up by induction and the different temperatures reached after 5 seconds heating at 99% power is shown in Figure 2.10 [3]. It can be noted that thermocouples of type J and K heat up the most while thermocouples of type E and T heat up the least. This is the case as thermocouples of type E and T are made of alloys that are non magnetic while thermocouples of type J and K are made of magnetic alloys [3]. Type T thermocouples do not withstand the processing temperature of high performance thermoplastic materials (PEEK, PEKK and PAEK), so they cannot be used in this research.

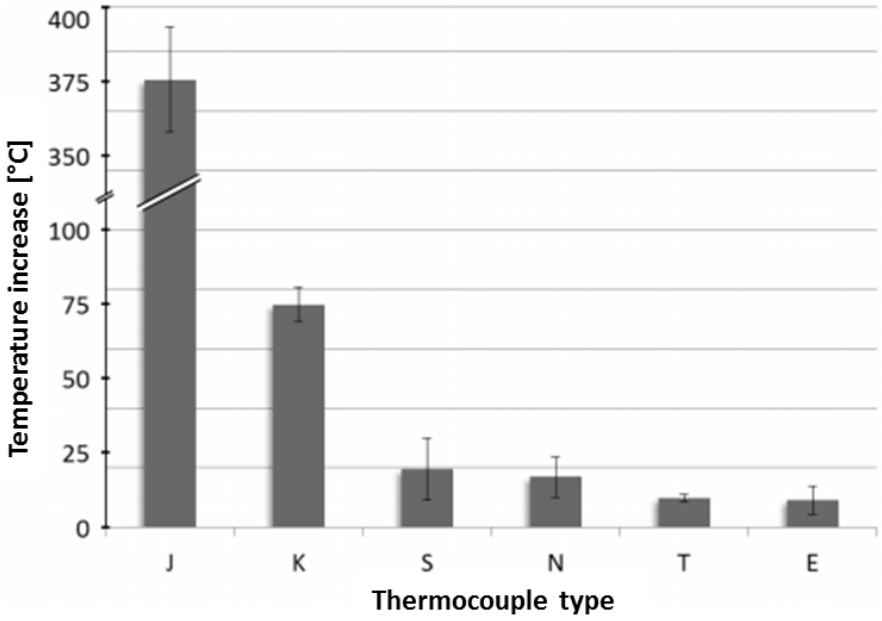

Figure 2.10: Heating of different thermocouple types by induction [3]

Not only the thermocouple type, but also its diameter has an influence on the heating rate of the thermocouple. This effect is further explained in Appendix A. The smaller the diameter of the thermocouple is, the less the thermocouple heats up due to the alternating magnetic field. Therefore, to measure temperature during the induction heating of laminates, thermocouples of type E can be used with a small wire diameter to limit the heating of the thermocouples themselves. This way, the measurements will only contain a small error.

As was mentioned above, two sources of errors exist when measuring with thermocouples in an electromagnetic field. First of all, the inductor introduces errors in the measurement by inducing current in the thermocouple wires when it is turned on. When the inductor is switched off after heating the part, the measurements become reliable again [51]. Second of all, when a small thermocouple is used, the little amount of energy caused by the heating of the thermocouple flows away fast. This means that almost directly after the inductor is switched off, the two sources of error disappear and the temperature increase can be measured reliably.

2.2.3. Other types of sensors

Except for infrared cameras and thermocouples, there are other sensors to measure the temperature too. These include but are not limited to pyrometers, Fiber Bragg Gratings (FBGs) and Resistance Temperature Detectors (RTDs).

Instead of an infrared camera, a pyrometer can be used. This, however, measures the surface temperature at one single spot only and like the infrared camera, no temperature measurement inside the laminate can be done.

Fiber Bragg Gratings can be used as temperature sensors. The advantage of FBGs is that they are not conductive or magnetic and therefore are immune to the alternating magnetic field of the inductor [52]. Because FBGs are also sensitive to strain, it is important to calibrate the sensors after they are built into the laminate. FBGs are, however, much more expensive than thermocouples and the results expected using FBGs do not justify their use compared to thermocouples when the price is taken into account.

Another option is to use Resistance Temperature Detectors (RTDs). When made from platinum, the influence the alternating magnetic field has on the sensor is small [53]. RTDs are generally fragile, bigger and more expensive than thermocouples but cheaper than FBGs [54]. RTDs were not used as no advantages over thermocouples were found that weigh up to their increased cost and fragility w.r.t. thermocouples.

Further options could include Surface Acoustic Wave (SAW) sensors or measuring the difference in electrical conductance due to a temperature change by measuring a difference in impedance of the TPC-inductor combination. The latter option is currently investigated for use in domestic induction hobs for cooking [55]. However, as these sensors are still being developed, these sensors will not be considered in this research due to the lacking reliability of these sensors and the low experience in their use.

3

State of the art

There are different methods of welding thermoplastic composites effectively. All these methods strive a temperature profile where the weld zone temperature is higher than the two outer surface temperatures. There are multiple ways of reaching this goal and those that have been described in literature are outlined in this chapter. Firstly, methods using both metal and CFRP susceptor materials are described in Section 3.1. Secondly, in Section 3.2, methods that can be used to reach the optimal temperature profile without using a susceptor are explained. Thirdly, in Section 3.3, the possibility to weld with lightning strike protection is discussed. Finally, a summary is given in Section 3.4.

3.1. Welding with susceptor material

In order to avoid heating up the entire laminate, but to focus the heat generation at the weld interface, a susceptor material can be used that heats up more than the laminate does. This is wanted as the goal is to melt the material at the weld zone while keeping the outer surfaces solid such that no damages or deformations are imposed. This can be done in several ways. A metallic mesh or a film with metallic particles can be added on the weld interface such that heat is generated by conduction, magnetic hysteresis or both [28]. By doing this, a foreign material stays at the interface which can cause problems with corrosion and thus reliability [4]. Also, problems with adhesion, stress concentration and residual thermal stress after cooling can occur [56].

A cleaner way to generate heat at the weld interface is by using a susceptor made of carbon fiber (CF). By using CFs that heat up faster than the laminate, it could be possible to achieve the highest temperature at or near the weld interface without having a foreign material at the weld interface.

In this section, first literature on metallic susceptors is reviewed in Section 3.1.1. Because, as to the best of the author's knowledge, no literature can be found on using CF susceptor materials, Section 3.1.2 reviews literature that can be used to design a good CF susceptor.

3.1.1. Metallic susceptor material

Metallic susceptor materials can be used to focus the heat generation at the weld interface as they generally have a higher heating rate under induction than CFRPs do. A metallic susceptor material can be heated using two different principles. It can be heated when the metal is conductive only (such as copper and some stainless steels) or magnetic too (such as some types of steel, nickel and iron). According to Ahmed et al. [23], the frequency required to weld with a metallic susceptor is generally an order of magnitude higher than when fibers are used.

Heating by conduction

Heating by conduction is typically done using a metal mesh. Also, particles or short fibers can be used to form a conductive network [57]. First the research done into metallic meshes is discussed followed by the research done into films with metallic particles or short fibers.

Metallic mesh

Rodriguez-Senín and Villegas [58] investigated the heating rate of three different meshes heated by induction including two of stainless steel with different wire diameter, thickness and mesh width and a mesh of galvanized steel. The conclusion was that when having a small mesh of test-coupon size, the galvanized steel performed better and for larger meshes, the stainless steel mesh with larger diameter performed better [58].

In the article by Rodriguez-Senín and Villegas [58], nothing is said about the used sample size, the location of the coil above the small meshes and a possible interference of the magnetic field with the thermocouples used. The location of the coil above the small mesh is of importance as the heat generation is often a mirror image of the coil and therefore when the mesh was put in the center of the coil, not much heat would be generated and this would then explain the lower temperatures reached in the small meshes than in the large meshes. Further research was not found comparing different metallic meshes in the induction welding process. Therefore, there would be room for further investigating this subject.

There has been research done into adjusting the metallic mesh such that the edge effect is limited. Here, parts of the mesh are cut away in order to achieve a homogeneous temperature distribution [59].

Dubé et al. [60] showed that the fatigue level of resistance welded joints was about 25% of the single lap shear strength. Poor adhesion between the heating element and the matrix was observed from the fracture surfaces [60]. Even though this study is about resistance welding, when induction welding with a metal mesh, a similar behavior is expected. This means that higher fatigue limits can be established when the bonding at the interface is improved by for instance using a CF susceptor instead.

Metallic films

For a metallic film to be conductive, the percolation threshold needs to be exceeded. This threshold is a percentage of particles or short fibers that needs to be reached in a material after which the material starts to conduct because a network is formed. For spherical particles, this percolation threshold is around 33 vol% and, because of their high density, this results in a lot of extra weight [33]. Therefore, particles with a high aspect ration, such as coated short carbon fibers, are preferred as the percolation threshold goes down with increasing aspect ratio [57].

Except for electrical conductivity, thermal conductivity of a mesh or film is also wanted. As a thermally conductive material transports heat, a homogeneous temperature distribution can be reached more easily [57]. The thermal conductivity can be enhanced by using thermally conductive fillers such as metal particles, carbon nanotubes, carbon fibers, carbon black, graphite or ceramic particles [57].

Heating by magnetic hysteresis

When magnetic materials are put in an alternating magnetic field, atomic dipoles turn such that they are aligned with the magnetic field. When the magnetic field is switched off, the material stays magnetized and a reversed magnetic field or heat is needed to demagnetize the material. With an alternating magnetic field, the material is magnetized and demagnetized constantly and therefore the atomic dipoles change direction continuously. This results in heating and is called hysteresis loss [57, 61]. In Figure 3.1 a sketch of a hysteresis loop is shown where H represents the magnetic field and B the magnetization of the material [62]. In Figure 3.1, the initial magnetization is started at (0,0) and the loop is followed anticlock-wise.

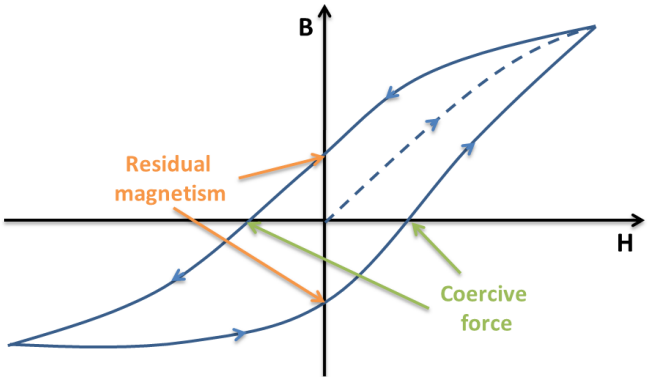

Figure 3.1: Example hysteresis curve

For hysteresis heating to occur, no electrical percolation threshold needs to be reached. Therefore, heating by magnetic hysteresis can also be done with particles of low aspect ratio. Often nickel is used as the magnetic material. This can be in the form of particles or coated carbon fiber, coated carbon nanofibers or coated carbon nanotubes [57].

3.1.2. Carbon fiber susceptor

Different types of carbon fiber (CF), with a different weave pattern, fiber volume content, titer and thread count have different heating rates when heated by induction [12, 34]. Therefore, CF plies with a distinctively high heating rate can be used as susceptor materials. This can be done when the rest of the laminate consists of plies with limited heating rates such that the most heat is generated by the CF susceptor at the weld interface. The advantage of this is that no foreign material is left in the weld and therefore a reduction or elimination of the problems with matrix-susceptor bonding and fatigue as was shown by Dubé et al. [60] is achieved. Different types of CFs can be used to this end such as non-crimp fabric, woven fabric, thin-ply CFRP and highly conductive CFs.

Woven and non-crimp fabric

Because closed loops need to be formed for eddy currents to flow, a woven fabric shows great potential for being used as a CF susceptor. Because in a weave fibers go in perpendicular directions and because the fibers touch each other, eddy currents can flow in circles by flowing from one fiber to the other.

The weave style has an influence on the contact between the fibers and therefore also on the heating rate. There are many types of weaves and the most common weave styles are presented in Figures 3.2a to 3.2c [63].

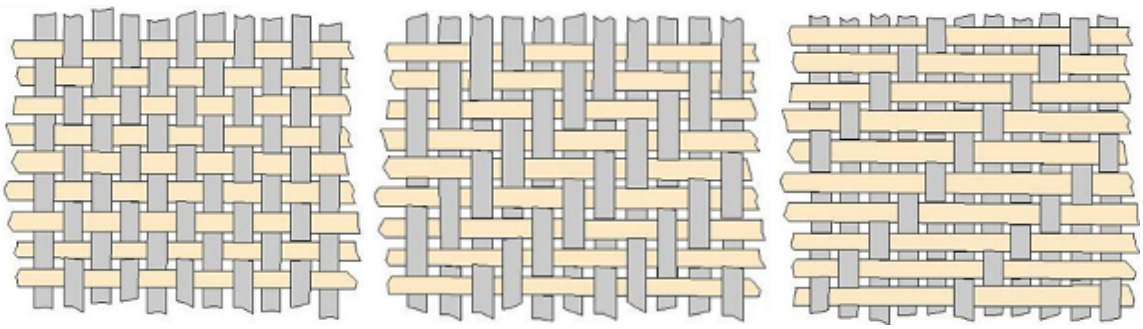

(a) Plain weave (b) Twill 2x2 weave (c) 4H Satin weave

Figure 3.2: Different weave styles [63]

Becker and Mitschang [34] investigated the effect of the weave style on the heating rate of CFRT laminates. The textiles under investigation had different weave styles, titer, thread-count and thus area weight. Here, titer is defined as the weight per unit length in "tex" where $1tex$ equals $1g/1000m$. Thread-count is the sum of the threads woven in a square inch. This includes the threads in both (weft and warp) directions. The different reinforcement textiles tested by Becker and Mitschang [34] are shown in Figure 3.3. The non-crimp fabric (NCF) consists of layers of UD material in two directions and is stitched together with a thread compatible with the matrix material such that it melts away.

No.	Weave	Area weight in g/m²	Titer		Thread-count		Matrix	Producer
			Warp direction in tex	Weft direction in tex	Warp direction in Threads/cm	Weft direction in Threads/cm		
1.	Twill 2/2	200	200	200	5	5	PA66	
2.	Twill 2/2	160	200	200	4	4	PA66	
3.	Twill 2/2	245	200	200	6.1	6.1	PA66	
4.	Twill 2/2	285	200	200	7	7	PA66	
5.	Twill 2/2	400	400	400	5	5	PA66	Made by IVW
6.	Twill 2/2	630	800	800	4*	4*	PA66	
7.	Plain	200	200	200	5	5	PA66	
8.	Satin 5H	290	200	200	7*	7*	PA66	
9.	±45° non-crimp fabric	200	800	800			PA66	
10.	Twill 2/2	200	200	200	5	5	PA66	BL

Figure 3.3: Carbon fiber reinforcements tested by Becker and Mitschang [34]

The heating rate was measured using two infrared cameras. Data on the experimental setup used and the laminate thicknesses and fiber volume contents can be found in Appendix B.

First, Becker and Mitschang [34] investigated the influence of the thread count on the heating rate. The results are shown in Figure 3.4. As can be seen, the heating rate increases with decreasing thread count. When the thread count increases, the width of the compacted rovings decreases, resulting in a lower contact area with the fibers in perpendicular direction [12]. This leads to less electricity flow and therefore less heat generation. Becker and Mitschang [34] performed the same test but then with a generator power of 15% instead of 40%. Here, a limit could be found at the Twill 200 with 5 threads/cm. The authors state that this is due to lower heating rates and therefore "the heating behavior is slurred by the relative long heating time" [34]. However, the optimum at Twill 200 at 15% power can also be caused by a too low thread count. When the thread count becomes too low, spaces between the rovings will exist because the rovings cannot be squeezed any flatter during consolidation. This results in less contact points, less electricity flow and thus less heating.

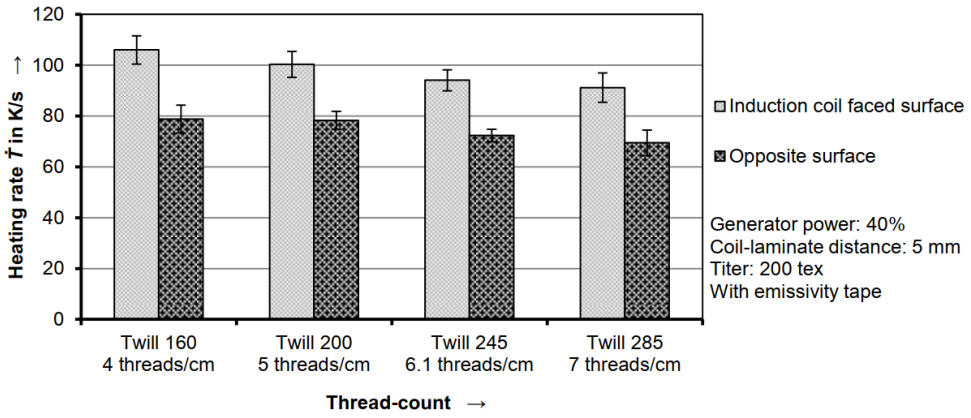

Figure 3.4: Influence of thread-count on heating rate [34]

In Figure 3.5, it can be seen that the heating rate increases with decreasing titer [34]. Here, the thread count is remained constant. Increasing the titer, and thus the diameter of the roving, probably has a similar effect as increasing the thread-count. When increasing the titer, the rovings cannot be flattened easily because there is no room.

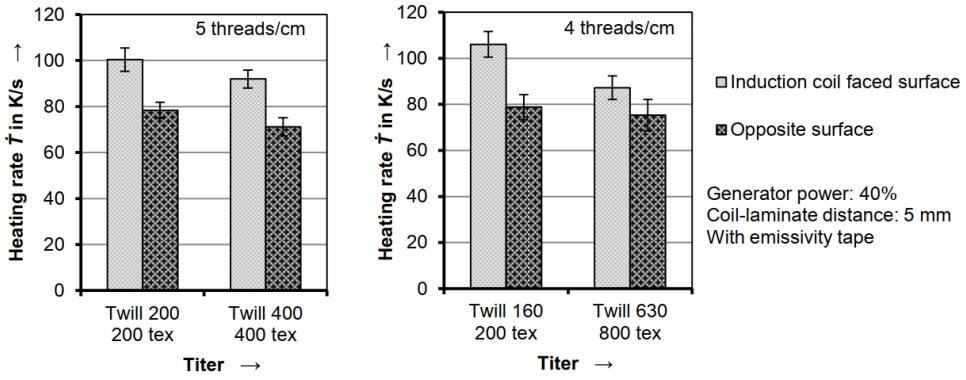

Figure 3.5: Influence of titer on heating rate [34]

In Figure 3.6 the heating rate of the different weave styles is shown [34]. Fabrics with the same area weigh of $200 g/m^2$ are compared. As no 5H Satin weave was tested of $200 g/m^2$, it was compared with a twill weave of the same weight for reference.

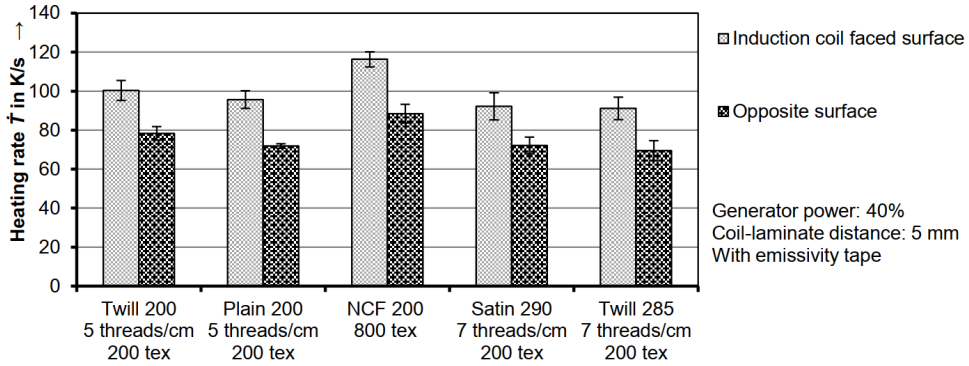

Figure 3.6: Influence of weave style on heating rate [34]

As can be seen in Figure 3.6, the NCF has the highest heating rate of all fabrics. This contradicts the findings by Rudolf et al. [29] who found that UD cross plies took longer to heat to 300°C than the other fabrics. More information on the research of Rudolf et al. [29] can be found in Appendix C. The difference in heating rates observed can be explained by the fact that Rudolf et al. [29] used a FVC of 50% while Becker and Mitschang [34] used a FVC of 58%. Both used CF with a Polyamide 6.6 matrix, but Rudolf et al. [29] did not state any more details on the fibers such as titer and area weight and on the dimensions of the laminates. Also, the difference can be caused by using different processing conditions such as coil, frequency, power and distance to surface.

Furthermore, in Figure 3.6, hardly any difference in heating rate can be found between the Satin 290 and the Twill 285 weave. Comparing the Twill 200 and Plain 200, it can be seen that the Twill 200 has a higher heating rate. Therefore, it can be concluded that either the Twill 200 or a (to be tested) satin weave with an area weight of $200 g/m^2$ such as the HexForce 286 4H Satin [64] produces the highest heating rate.

Using the insights gained with the research reviewed above, Becker and Mitschang [34] designed a laminate that would produce more heat near the weld interface and less heat close to the coil. It exists of Twill 160 plies near the weld interface and Twill 630 plies close to the coil. More information on this laminate design can be found in Appendix B.

Becker and Mitschang [12] further investigated the effect of laminate properties on the heating rate. Here, the influence of the FVC on the heating rate is studied. The same fabrics as shown in Figure 3.6 were used to create laminates with three different FVCs (30%, 45% and 60%). These laminates were then heated by induction and the heating rates of the different laminates were plotted. These plots can be found in Figure 3.7 [12].

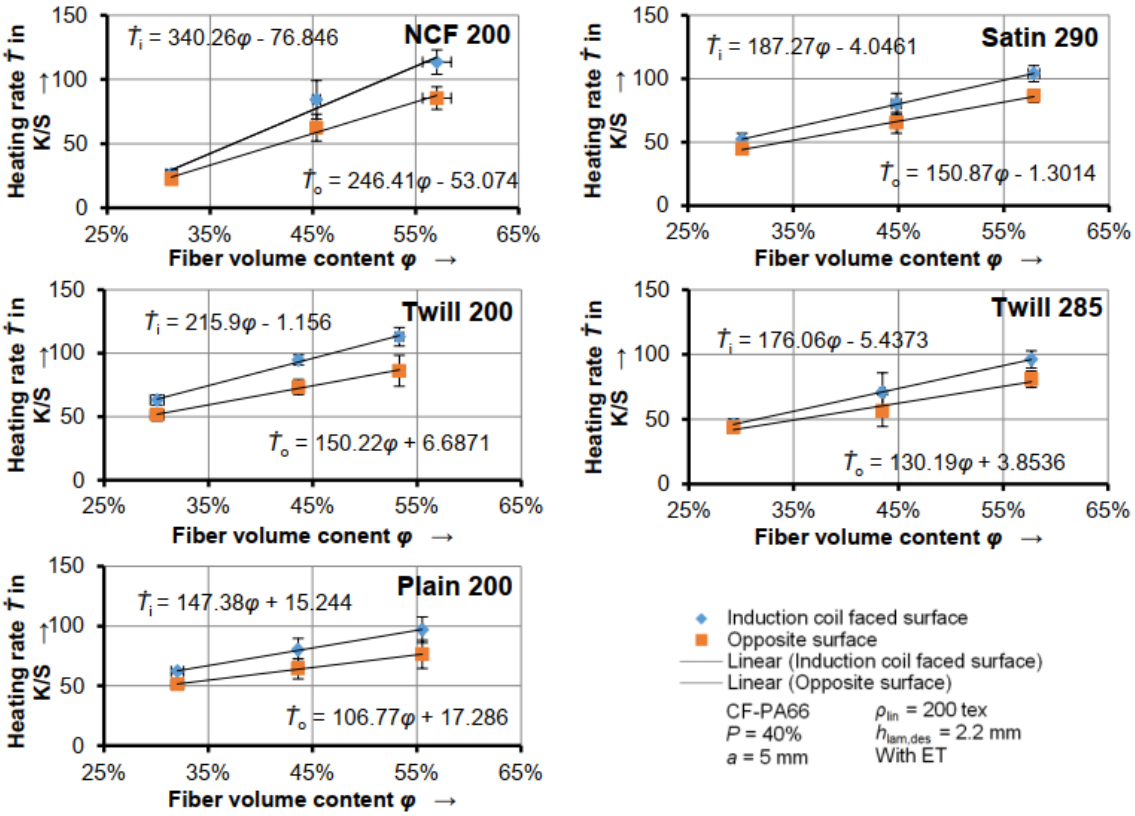

Figure 3.7: Influence of FVC on the heating rate of different laminates [12]

In Figure 3.7, the lines are linear and they follow the three data points well. This means that the influence of the FVC on the heating rate can be approximated by a linear equation which can be used to better understand the heating characteristics of the different laminates. These linear equations are also shown in the graph in the form of Equation (3.1).

$$\dot{T}_o = \mathbf{a}\varphi + \mathbf{b} \tag{3.1}$$

Here, **a** is the slope and **b** is the y-intercept. When first looking at the y-intercept **b**, big differences can be found ranging from -53 to +17 K/s. When approaching the y-intercept, and thus approaching a FVC of 0%, there is so much matrix material around the fibers such that the fibers are not pushed towards each other. However, when the fibers are woven, they will always have some contact points whereas non-woven fabric or NCF do not have contact points with fibers in a different orientation to form closed loops for eddy currents to flow. Therefore, it can be seen that the fabric with the most cross-overs (Plain 200) has the highest y-intercept followed by the Twill 200 and 285, Satin 290 and NCF 200 respectively.

The slope **a**, ranges from 107 to 246 $K/(s \cdot FVC)$ in the sequence: Plain 200, Twill 285 and 200, Satin 290 and NCF 200. Here, it seems that the lower the amount of cross-overs is, the higher the slope is. When increasing the FVC, a force is used to compact the layers. Therefore, the contact points between the fibers are enlarged and new contact points will arise [12]. This results in more eddy current being able to flow through the laminate and hence a higher heating rate.

When a fabric has less cross-overs, the contact between the different layers of fabric is more efficient as the fibers are straighter. Also, with an increasing FVC, layers of matrix between the fibers will reduce which increases the in- and out-of-plane contact areas much more than for woven fabrics [12].

Concluding the research of Becker and Mitschang [12, 34], non-crimp fabrics result in the highest heating rates when FVCs normal to the aerospace industry are used (>50%). Also, as non-crimp fabric exists of layers of UD fibers with different orientations, this can be laid using ATL or AFP which simplifies automation. Furthermore, the titer should be minimized for high heating rates and when a woven fabric is used, the thread count should be minimized too [34].

Thin-ply composites

Thin-ply composites are made from CFRP plies that are much thinner than the standard in engineering. Their thickness is about a fifth of that of standard plies (areal weight of $\approx 40 g/m^2$ versus $194 g/m^2$). Thin-ply composites are used not only to create thinner laminates, but also to produce stronger laminates with a higher damage resistance [65]. These improved properties can be attributed to positive size effects and an increase in design space due to the ability to have layers in more directions [65].

Because thin-ply composites are so thin, many more cross-overs of single filaments are created within a laminate of equal thickness as one made from regular plies. This allows thin-ply composites to heat up faster under induction than normal composites do. This was also explained in Section 3.1.2. Therefore, thin-ply composites can be ideal to use as susceptor material in induction welding as they heat up faster than normal plies, they are thin resulting in a minimum amount of peel stresses and they have a high damage resistance which helps to reduce the damage growth in the weld zone.

Highly conductive CFRP

When more eddy currents would flow in CFRTs during induction, it would heat up more. Creating more eddy current flow could be possible by making the CFRT more conductive. Therefore, it could be possible to use highly conductive CFRT as a susceptor material at the weld interface. This could, like using special fabrics that heat up faster, create more heat generation at the weld interface such that the matrix at the interface is melted while keeping the rest solid.

Several studies have been done in order to increase the electrical conductivity of CFRPs [66–68]. This was mostly done in order to decrease the extent of lightning strike damage. One strategy to enhance the electrical conductivity of CFRT is to manufacture conductive steel fibers that are integrated in the CFRP along the carbon fibers [66]. Another strategy that can be followed is to increase the conductivity of the matrix material [67]. Finally, the electrical conductivity of NCF can be increased by using silver-coated yarns to knit the different layers together [68].

It still needs to be investigated whether using highly conductive CFRT actually would increase the heating rate of CFRP. Valery Rudnev [28] namely states that the higher the electrical resistivity of a metal is (which is the inverse of its electrical conductivity), the higher the heating rate is under induction. Meaning that a high heating rate is achieved in poorly conducting metals. On the other hand, if a material does not conduct, it is not heated by induction meaning that an optimum should be present.

These highly conductive CFRPs show potential for being used as susceptor material. The disadvantage is that these materials are difficult to obtain as they are still being developed. Also, steel or silver wires integrated in the CF can result in unwanted effects and it is not guaranteed that it would increase the heating rate. Therefore, and because it is a complex topic that could be researched as a big project on its own, it is chosen not to investigate the possibility of using highly conductive CFRP in this thesis.

3.2. Susceptorless welding

Welding without susceptor material shows great promise as no foreign material is left at the weld zone. It is not a new technique, but there are a lot of possibilities to further enhance the process. Currently, either problems arise while the whole laminate is heated instead of the weld zone only, or tricks are used such that the maximum temperature is found at the weld zone. This, however, often includes waste of energy, trial and error for each new configuration, the addition of unwanted materials or laminate manipulation which sets even more rules to laminate design. In this chapter, research done into how the highest temperature is created close to the weld zone is reviewed in Sections 3.2.1 to 3.2.3 followed by a theory on how specific plies can be targeted by magnetic field manipulation in Section 3.2.4.

3.2.1. Active cooling

Because of the skin effect, the most heat is generated at the surface closest to the coil. Due to convection, the maximum temperature cannot be found at the surface, but slightly under this surface [21]. This effect was used by Schieler et al. [21] to move the highest temperature closer to the weld zone by increasing the heat drainage due to convection using active cooling.

Active cooling was done using an air jet with varying flow rate and flow temperature. The temperature between the plies was measured using Type E thermocouples from Omega Engineering GmbH, Deckenpfronn, Germany, with a diameter of 0.13mm [21]. Figure 3.8 shows the temperature profile across the thickness of the laminate after heating for 2s with 10% power on a laminate with 8 plies using an air jet with an air temperature of 20°C [21].

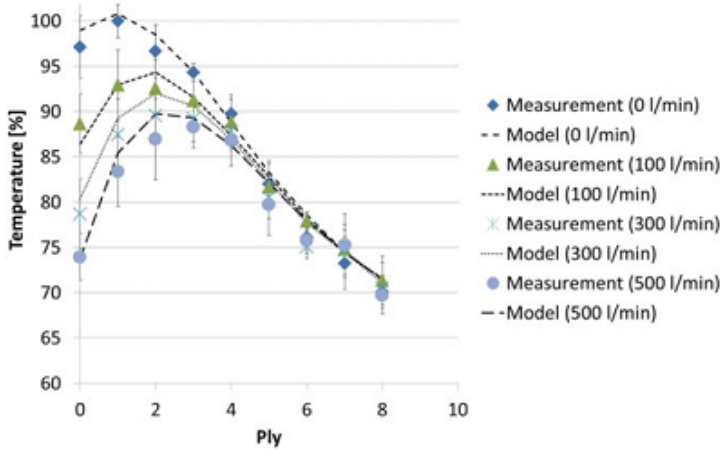

Figure 3.8: Through-thickness temperature profile with varying air jet volume rates by Schieler et al. [21]

Both the values produced by a model created by Schieler et al. [21] and the measured temperatures with the thermocouples are plotted in Figure 3.8. It can be seen that the highest temperature across the laminate shifts away from the surface (and towards the weld zone) with increasing airflow.

Not only the air jet flow, but also the flow temperature can be regulated. More information on tests done on this topic by Schieler et al. [21] can be found in Appendix A.

3.2.2. Layer insulation

Except for draining the excess heat as is done by Schieler et al. [21], it is also possible to avoid generating heat in the laminate facing the coil. This was done by Worrall and Wise [42] by insulating the different UD cross-plies. By insulating the plies in different orientations, no closed loops are available for eddy currents to flow, resulting in the absence of heat generation. This can then be used in the laminate facing the coil. In the other laminate insulation of

the layers is not necessary as the highest temperature will be generated closest to the coil, now meaning at the weld zone. The setup and the following temperature profile is given in Figures 3.9a and 3.9b respectively [42]. It can be seen that the top plate stays cool while the bottom plate heats up.

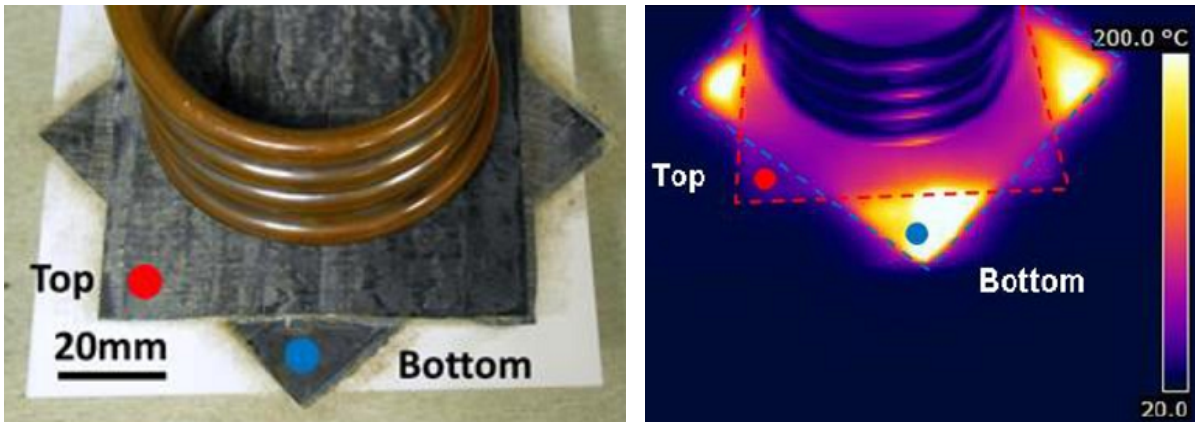

(a) Photo of test setup (b) Infrared image of test

Figure 3.9: Layer insulation by Worrall and Wise [42]

A downside of this solution is that the layers have to be insulated by e.g. a layer of glass fiber. Not only is this heavy, it is also difficult to include in the manufacturing process as the ATL or AFP machines have to deposit two dissimilar materials.

3.2.3. Adjustment of layup

Additional methods are conceivable in addition to the state of the research. As was already described in Section 3.1.2, specific CF materials heat up more than others do under an alternating magnetic field. Therefore, this can be used in order to design a laminate such, that material that heats up the most is used near the weld zone. Care has to be taken that no problems resulting from coupling effects will occur.

However, when the layup is to be automated using ATL or AFP, the use of UD material is favored over the use of fabrics. On top of that, UD materials are favored because of their increased mechanical properties.

In UD material, closed loops can only be generated at the interface where two layers of UD material have a different orientation [43]. This principle can be used to manipulate the laminate such that the optimal temperature profile is approached. Such a laminate would have relative thick stacks of UD material with the same orientation close to the induction coil and many thin stacks of UD material in different orientations near the weld zone. However, as symmetry in a laminate is wanted, thin stacks of UD material in different orientations can be used close to both surfaces and thick stacks in one orientation can be used at the core of the laminate. This way, the core does not heat up, the weld zone heats up and the heating of the surface under the coil can be counteracted by cooling.

Again, when using AFP or ATL it is not favoured to use dissimilar materials. Therefore, the extra heat generation should be achieved by creating more interfaces between the different layers instead of using a finer material close to the weld zone.

A disadvantage of adjusting the layup is that it will impose new design rules on the laminate, meaning that the efficiency of the structures are likely to decrease. Furthermore, when adjusting the layup, care must be taken that no unforeseen coupling effects will occur.

3.2.4. Magnetic field manipulation

The direction of the magnetic field can have an influence on the heating rate of the different plies. When this is the case, it can be used to target specific plies. This has been tested by Rudolf et al. [29] for the induction heating of fabrics using a hairpin inductor. However, no measurable effect could be found. This might be different for UD plies with a different number of plies in different directions or the effect might be measurable with newer techniques as this research stems from the year 2000.

Not only the orientation of the magnetic field can play a role, also the frequency can be used to target different plies. As the frequency of the magnetic field influences the skin depth, the frequency can be adjusted to create the highest temperature near the weld zone.

If it is possible to target specific plies using magnetic field manipulation, the induction welding technique will consume less energy and will be more predictable than what is currently the case. This would allow the process to reach a higher technology readiness level.

3.3. Welding with lightning strike protection

Aircraft are struck by lightning approximately once a year [69]. Because composites are much less conductive than metals are, the damage done to a composite structure that is struck by lightning is much bigger than for metal structures when no protection is applied. The lightning strike enters the aircraft at one point and leaves the aircraft at another point [1, 69]. Between those points, it is important that the immense current can flow. Lightning Strike Protection (LSP) consists of a conductive mesh, film or particles that provides this conductive path. LSP prevents extensive damage caused by the current and following temperatures of several thousands degrees Celsius such as matrix evaporation, destruction of the reinforcement or even ignition of the structure [70, 71]. For a well functioning LSP, both the electrical conductivity as the thermal conductivity should be high [71].

In the aerospace industry the 3CU7-100FA from Dexmet Corporation, Wallingford, England is a standard LSP which is tested in this research. It is made of flattened and annealed copper. Its properties are listed in Figure 3.10a [72]. Here, LWD stands for Long Way of Design and is schematically shown in Figure 3.10b [72].

	3CU7-100FA
Weight g/m^2 ($\pm$ 10%)	195.3
Original metal thickness ($\pm$ 10%)	0.076 mm
LWD ($\pm$ 5%)	2.54 mm
Overall thickness ($\pm$ 0.025 mm)	0.076 mm
Open area ($\pm$ 5%)	70%

(a) LSP property table

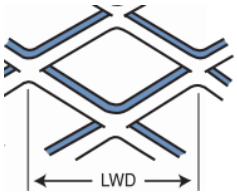

(b) LWD definition

Figure 3.10: LSP properties [72]

As was already explained in Chapter 8, a material can be heated using induction when it is conductive, magnetic or both. Therefore, as a requirement for LSP is that it has to conduct electricity better than CFRP does, it is inherent that LSP heats up by induction.

LSP is often made of copper and will heat up more than CFRP under the same magnetic field. However, since copper is a diamagnetic material, it opposes the magnetic field [73]. This is in contrast with paramagnetic materials such as the stainless steels of grade 304(L) which were previously used in susceptor materials by Rodriguez-Senín and Villegas [58], Ahmed [74]. Stainless steels of this grade are austenitic and therefore paramagnetic which means they are weakly attracted to a magnetic field. However, ferritic and martensitic stainless steels are ferromagnetic and strongly attract the magnetic field [75]. Austenitic stainless steels can be made ferromagnetic by applying cold work [75]. This means that it is unclear whether the materials used by Rodriguez-Senín and Villegas [58], Ahmed [74] were paramagnetic or

ferromagnetic, but in any case, they attract the magnetic field and do not repel the magnetic field as diamagnetic materials like copper do. This means that copper reduces the strength of the magnetic field which could lead to limited heating. Also, since the electrical resistivity of copper is about $2.6 \cdot 10^{-8}\Omega \cdot m$ compared to $72 \cdot 10^{-8}\Omega \cdot m$ for 304(L) stainless steel, copper will heat less than 304(L) stainless steel [76]. Therefore, both the repelling of the magnetic field and the lower electrical resistivity of copper make copper heat less than stainless steels and therefore it could be possible that welding with LSP does not pose such big a problem as was thought.

Even though copper is likely to heat up more than the TPC under induction, it could be possible to weld from the side where no LSP is attached. The strength of the magnetic field could namely be sufficiently decreased over the thickness of the laminate to avoid overheating of the LSP because of both the skin effect and the decreasing magnetic field intensity with distance. Several possible welding configurations are schematically shown in Figure 3.11.

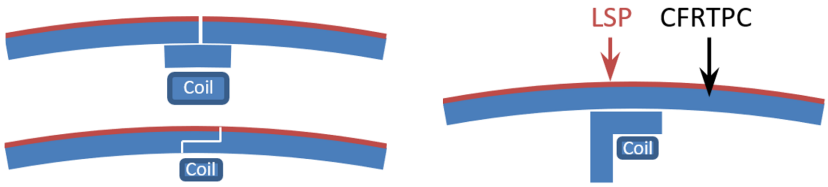

Figure 3.11: Weld configurations for welding with LSP

When it is deemed impossible to weld with LSP, it is possible to manufacture parts without LSP and applying a LSP layer after joining by heating with a laser, by induction or by conduction. These options are, however, not favorable as the techniques are not yet widely used and would require investments to get it up and running.

3.4. Summary

Different methods can be used to weld thermoplastic composites inductively. The two major groups include welding with and without a susceptor material. When using a susceptor material, the temperature at the weld zone is increased by using a material at the weld zone that heats up better than the laminate material does. This material can, however, have a big influence on the joint reliability.

Research has been done into using metallic susceptors such as metallic meshes and films that heat by conduction, magnetic hysteresis or both. A topic that has not yet been researched is using susceptors made of carbon fiber materials that heat up better than the carbon fiber material of which the laminate is made of. Research has shown that carbon fiber heats up well when many crossing points are formed such that eddy currents can flow in loops [34]. Many crossing points can be created using fabrics or by using thin-ply composites made of UD material in multiple directions. Also, a high fiber volume fraction results in an increased heating rate [12]. Furthermore, it can be investigated what effect increased conductivity has on the heating rate of CFRP under induction.

For susceptorless welding, four main strategies were found in literature. The first strategy moves the hottest point across the laminate thickness away from the inductor, and therefore towards the weld zone, using active cooling of the surface. The second strategy electrically insulates the differently oriented layers in the top part using e.g. glass fibers. This way, hardly any heat is produced in the top part and the hottest point across the thickness can be found at the weld interface. The third strategy adjusts the layup such that more crossing points are available close to the weld zone such that the most heat is generated there. Finally, the fourth and least researched strategy is to manipulate the magnetic field in order to improve the temperature profile.

4

Research proposal

In this chapter, first, the gap found in the published research on induction welding of TPCs is outlined in Section 4.1. From this gap in the research, research questions, aims and objectives are formed in Section 4.2. To answer the research questions and to fulfill the objectives, the research strategy is explained in Section 4.3. In order to efficiently perform the tests required, the Design of Experiments (DoE) method is used which is explained in Section 4.4. Then, the prognosed results, outcomes and relevance is described in Section 4.5.

4.1. Gaps in research done

In order to start a research, and to avoid doing double work, it is important to find what has been researched already and what has not. This was done by studying literature as is described in the previous chapters. By studying the literature, gaps within the literature on induction welding of TPCs have been found which can be filled by this master's thesis in order to add something to the body of science. These gaps found in the literature include:

1. Manipulation of magnetic field direction and frequency to target specific plies
2. Using a susceptor made of carbon fiber (CF)
3. Improve induction heating for laminates made with uni-directional plies instead of laminates made with fabric material
4. Using thin-ply or highly conductive CFRP to improve the temperature profile
5. Welding with lightning strike protection

4.2. Research question, aims and objectives

In this thesis it is investigated whether a near-optimal temperature profile can be generated by using a CF susceptor or by selective heating of specific plies through manipulation of the magnetic field orientation. The frequency of the magnetic field generated by the available inductor at DLR in Stade, can currently not be changed and therefore no research is done into the effect of changing the frequency of the magnetic field. Also, no highly conductive CFRP was available to perform tests. Combining the gaps in the research with the boundary conditions imposed by DLR, the main research question is:

How can induction heating be used to selectively heat the weld zone of multidirectional carbon fiber laminates with and without CF susceptor materials?

The sub-questions are:

1. Can specific plies in multidirectional CFRT laminates be heated by manipulation of the magnetic field direction and power?
   (a) Do specific plies heat up more at a given orientation of the magnetic field?
   (b) How does the temperature profile relate to the power of the magnetic field?
2. Can a CF material be used as a susceptor to effectively generate a near-optimal heat profile across the thickness of an aerospace laminate?
   (a) What carbon fiber material allows for the best heat generation?
   (b) Can a CF susceptor be so effective that the most heat is generated by this susceptor at the weld zone instead of the laminate nearest to the coil?
3. Can TPC structures with LSP be welded inductively?

The objective of the research is to investigate the possibility of using induction to selectively heat the weld zone of multidirectional carbon fiber laminates with and without CF susceptor materials by examining the influence of changes in orientation and power of the magnetic field on the temperature profile across the thickness of the laminate. This is first done for different laminates with a standard thickness. Testing whether it is possible to extend this selective heating to laminates with a different thickness will be done in a later research project.

The first goal is to better understand the effect of changing the direction and power of the magnetic field on the heating of different cross plies in the laminate. In order to do this, first a temperature sensor has to be chosen that can be used to measure the temperature profile across the thickness of the laminate. The knowledge gained can then be utilized to target specific plies in a laminate to achieve an appropriate heating profile for welding. When manipulating the magnetic field does not result in a good temperature profile, a good temperature profile is targeted by changing the laminate itself. The next aim is to find whether CF susceptor materials can be effective and, finally, the goal is to see the effect LSP has on the heating behavior of the laminate.

This is, to the best of the author's knowledge, still a gap in the research as no reports on CF susceptors have been found nor has anybody reported on the influence of the direction of the magnetic field on the heating rate of multidirectional UD plies. Furthermore, no reports were found on induction heating with LSP present.

4.3. Research strategy

The research strategy that is followed is the experimental research strategy. Using this strategy the following hypotheses are tested:

1. Specific plies can be targeted with induction heating by manipulating the orientation and power of the magnetic field.
2. A carbon fiber susceptor material can be used to generate the highest temperature at the weld zone.
3. TPC structures with LSP can be welded inductively.

In order to start the experiments, first a temperature sensor is chosen which can be used to measure the temperature profile in thickness direction. In literature thermocouples have been used to this end [8, 21, 25, 32].

All measurements are done below melting temperature such that the specimen can be tested with different magnetic field characteristics without the need for making new specimen and thus the introduction of more uncertainties (difference in test specimen) is avoided.

4.4. Design of experiments

The technique Design of Experiments (DoE) is used to map out the parameters that are tested. In DoE, the input variables for the experiments that need to be performed are mapped out in advance in order to get the most information out of the minimum amount of tests. Mapping out the input variables can be done using different DoE methods. These methods include orthogonal and random designs. In an orthogonal design, the input parameters are statistically independent and therefore uncorrelated and can be changed independently [77]. Examples of these orthogonal designs include full- and fractional factorial designs. In random designs, the input parameters are chosen randomly. The most common used random design is the Latin hypercube design.

The most used designs, including the full factorial design, the fractional factorial design and the Latin hypercube design, are further explained in Sections 4.4.1 to 4.4.3 respectively. In Section 4.4.4, a motivation is given for the DoE design that is used to execute the experiments.

4.4.1. Full factorial design

In a two level full factorial design, all input parameters are given a low and a high value and all possible combinations are tested. An example of a three factor two level full factorial design is given in Figure 4.1a. Here, the blue dots represent the experiments to be executed and the axes A, B and C represent the different input variables. With this design, only linear relations can be observed. When higher order relations are to be detected, a three or higher level factorial design can be used. This, however, results in a lot of experiments that have to be executed. The amount of experiments that need to be executed for a full factorial design are given by Equation (4.1).

$$N = n^k \tag{4.1}$$

Where: n = amount of levels, k = number of input variables

In a full factorial design, the effects of each factor is investigated independently but also interaction effects between the different factors can be detected. A disadvantage of the full factorial design is that the number of experiments required increases exponentially. The number of experiments can be reduced in three ways [77]:

1. Use a minimum amount of levels for each input variable (e.g. n=2)
2. Reduce the amount of input variables (reduce k)
3. Use a fractional factorial design (see Section 4.4.2)

4.4.2. Fractional factorial design

In a fractional factorial design, a fraction of the full factorial design is tested. Mostly it uses half of the experiments of a full factorial design, but smaller fractions are possible too. An example of a 2^{3-1} fractional factorial design is given in Figure 4.1b. Again, the blue dots represent the experiments that need to be executed and the axes represent the input variables. The number of experiments required with a fractional factorial design is given by Equation (4.2).

$$N = n^{(k-p)} \tag{4.2}$$

Where: n = amount of levels, k = number of input variables, p = integer defining the fraction

In a fractional factorial design, different numbers of variables and fractions result in different design resolutions. These design resolutions result in different levels of accuracy that can be

retrieved. The higher the amount of input variables is, the more accurately a fractional factorial design can predict effects. A minimum resolution of III is required which is achieved by a 2^{3-1} design which has three input variables. For such a design, main effects are confounded with two-factor interactions [77]. For higher resolution designs, less effects are confounded and thus the model becomes more accurate. A design with resolution I or II is useless as main effects confound each other. A summary of different design resolutions is given in Appendix D.

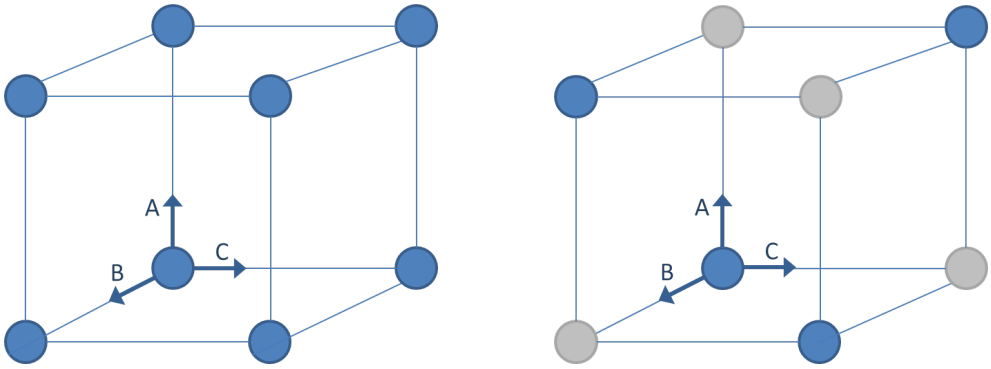

(a) Two level full factorial design (b) Fractional factorial design

Figure 4.1: Factorial design

4.4.3. Latin hypercube design

The Latin hypercube design is based on a Latin square which is an n x n matrix filled with n distinct symbols. Here, each value appears only once in each column and each row.

In Latin hypercube sampling the amount of experiments (N) is chosen and is independent of the amount of input variables. The range of the variables is divided by N and on every row or column that is generated, a random value is picked such that no value is in the same row or column. An example of such a sample is given in Figure 4.2. Here, Figure 4.2a shows a 3D plot including three variables and Figure 4.2b shows the same variables in a 2D plot. Especially in Figure 4.2b, it can be seen that the samples are randomly divided with one sample in each row and column.

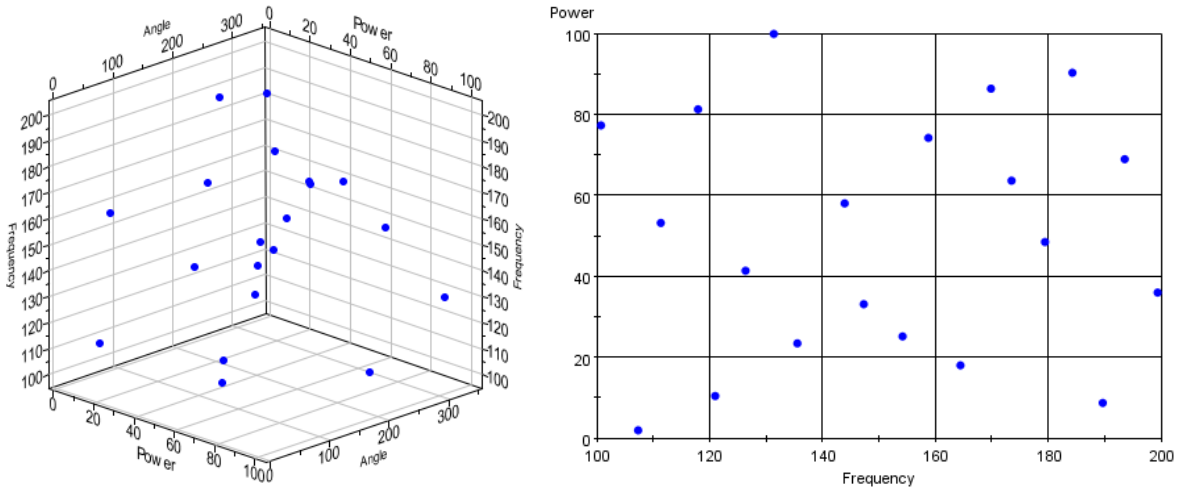

(a) Latin hypercube design 3D plot (b) Latin hypercube design 2D plot

Figure 4.2: Latin hypercube design

4.4.4. Motivation for chosen design

In order to choose a DoE method for the experiments that are executed, first the input variables are investigated. These input variables are:

- Laminate number/layup
- Coil orientation
- Power
- LSP
- Susceptor

From these input variables, the variables that are likely to have a continuous and linear effect on the measured temperature profile are chosen as input variables for the DoE method. This includes power only. The other input parameters, including laminate number, coil orientation, the presence of LSP and susceptor, have a nonlinear effect on the temperature profile.

Next, the relations that are needed to answer the research questions are identified. In order to see the effect of the coil orientation on the temperature profile across the different laminates, the relation between these two parameters is investigated extensively. Then, in order to see the effect of the power on the temperature profile, it is sufficient to test one laminate with multiple power settings. The same holds for the presence of LSP. Therefore, power, susceptors and LSP are tested separately for one specific laminate and inductor orientation.

This results in DoE's with 2 variables only. As was explained in Section 4.4.2, this means that a fractional factorial design is not desired as with two variables the main effects confound each other. Even with three variables the main effect would be confounded with two-factor interactions which would still produce relatively big errors.

Because most variables are discontinuous, result in a nonlinear response or cannot be varied to every possible value, a Latin hypercube cannot be designed the way it is supposed to. Also, because of the random selection of input variables, effects of certain variables are not easily isolated from the other effects when one big Latin hypercube design would be made. Because of those two reasons, it is decided not to use a Latin hypercube design.

Because both a fractional factorial design and a Latin hypercube design are not favourable, it is decided to use the full factorial design.

4.5. Results, outcome and relevance

The results of the experiments contain temperature profiles across the thickness of CFRT laminates, with and without CF susceptor and with and without LSP, under different magnetic field orientations. These temperature profiles are analyzed and a strategy is sought to approach the optimal temperature profile as depicted by Figure 2.1.

The outcome could be that a CF susceptor performs well and creates the highest temperature at the weld zone. It could also be possible that the heat generated by the CF susceptor is negligible. The next outcome could be that particular layers can or cannot be targeted by altering the orientation of the magnetic field. Finally, a conclusion is formed on how likely it is to be able to weld CFRT structures with LSP using induction.

The relevance of this thesis is that it further advances the knowledge on the induction welding process. It becomes clearer whether it is possible to efficiently heat an aerospace laminate by generating most heat at the weld zone by using either a CF susceptor or magnetic field manipulation. This is new as currently the industry gets rid of the excess heat near the surface by active cooling using compressed air which is hard to control and wastes a lot of energy or the industry uses metallic susceptors which can cause different unwanted effects. Furthermore, the relevance of investigating the possibility of welding with LSP is that the LSP in composite aircraft is currently applied before joining and therefore, when it is not possible to join parts that already have LSP, induction welding will be less interesting to the aerospace industry as the LSP has to be attached after the parts have been joined.

5

Experimental Hardware

All experiments were executed at the German Aerospace Center (DLR) in Stade, Germany. The available equipment used to perform the tests are described in this chapter. Firstly, in Section 5.1 the material used and the consolidation process of the material is described. Secondly, the general setup is explained in Section 5.2. Thirdly, in Section 5.3, the inductor is described and its advantages and disadvantages are explained.

5.1. Material and its consolidation process

The material that was used is CF UD tape with matrix PEKK (Teijin HTS45 194gsm – dry fiber weight). The thickness of the material is 0.2mm and the width of the tape is 300mm. It has 34weight% of matrix material which corresponds to a 58volume% of carbon fibers as is calculated in Equation (5.1). Here, the void volume is not taken into account.

$$V_f = \frac{v_f}{v_c} = \frac{v_f}{v_f + v_m} = \frac{m_f/\rho_f}{m_f/\rho_f + m_m/\rho_m} = \frac{0.194 \cdot 1m^2/1780}{0.194 \cdot 1m^2/1780 + 0.194 \cdot 1m^2 \cdot \frac{34}{66}/1278} = 58\% \quad (5.1)$$

All parts have been consolidated in an autoclave. The temperature and pressure were controlled as follows:

1. 2 bar[1] pressure in autoclave during heating to 380°C
2. Increase pressure in autoclave to 7 bar[1] after 15 min at 380°C
3. Keep pressure and temperature for 20 minutes
4. Cool with 3K/min
5. Relieve pressure

5.2. General setup

The experimental setup is depicted in Figure 5.1. The cooled inductor is attached to a pneumatic cylinder such that pressure can be applied for consolidation after welding. A frame is built around this cylinder to distribute the forces. The inductor can be rotated 360°. The CFRP parts are placed below the inductor. A ceramic tile is placed below the CFRP parts because, contrary to metal, a ceramic tile does not heat by induction nor does it attract the magnetic field and therefore has a limited effect (conduction only) on the heating of the test parts.

[1]The pressures stated are gauge pressures meaning that they represent the amount of bars above ambient pressure. This means that 2 bar pressure, with the vacuum bag in the autoclave, represents a differential pressure of 3 bar.

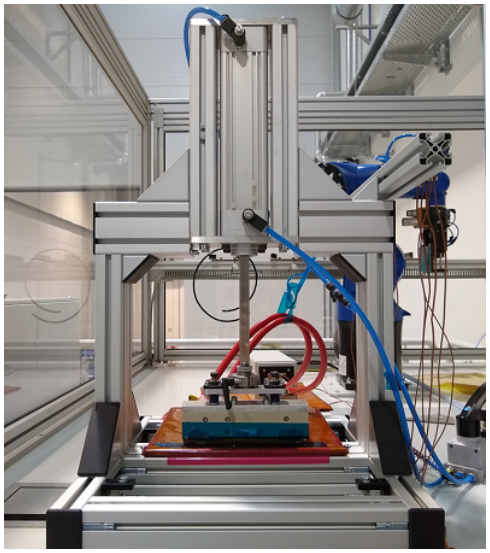

Figure 5.1: Experimental setup

For the preliminary tests, the edges of the test parts are aligned with the edge of the inductor. An infrared camera is positioned such that it captures the sides of the test parts. Thermocouples are placed between the inductor and test part, between the two test parts and between the ceramic tile and test part as close to the edge as possible.

In the primary tests, thermocouples are built throughout the thickness of four different laminates. Another four laminates with the same layup as the ones with thermocouples are built. These laminates are put below the part with thermocouples to simulate a welding setup. Every thermocouple is targeted separately with the inductor to create the same magnetic field and cooling effect for every thermocouple. Every thermocouple is targeted with the exact middle of the inductor.

5.3. Inductor

The inductor used for the experiments is a cooled hairpin coil from COBES GmbH, Ettenheim, Germany (Linear, 1-Wdg., t=170mm). This inductor, as is depicted in Figure 5.2, is pressed onto the laminate. This way, the three requirements for effective welding are fulfilled simultaneously.

The inductor:

1. heats up the parts
2. cools the top surface
3. provides pressure for consolidation

This inductor design is new, as until now, a setup as is depicted in Figure 2.2 has been described in literature [2, 30, 32, 33]. In the setup that has been used in literature, the three functions are fulfilled with three separate parts. The coil heats up the parts, the surface is cooled using an air jet and pressure for consolidation is applied using a roller.

A big advantage of this inductor is that it does not need an air jet to cool the top surface. Compressed air is extremely energy inefficient as only 10-20% of the energy used to compress the air is used in a useful way [78]. Most of the rest of the energy is lost into heat and leakages [78]. Except for the inefficiency of using compressed air, using compressed air is loud, the airflow and therefore the cooling rate cannot be easily controlled when multiple machines are attached to the same compressed air line and it can blow dust particles in the air which can contaminate the to-be-welded surfaces or can be inhaled by the workers.

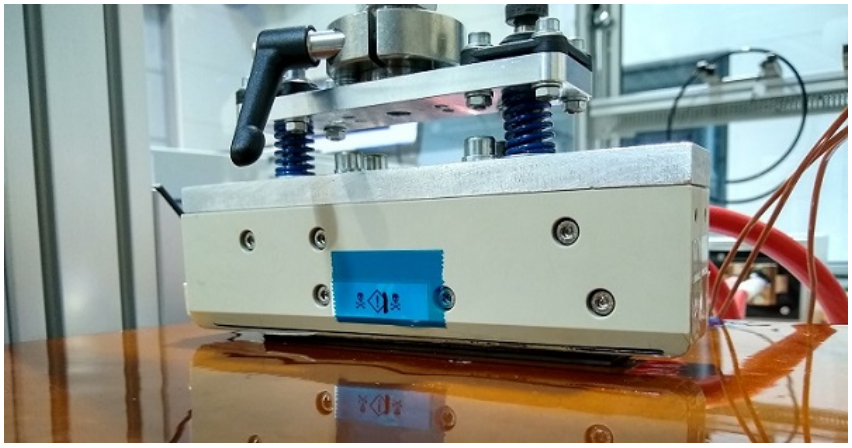

Figure 5.2: Cooled hairpin inductor from COBES GmbH, Ettenheim, Germany

A disadvantage of this inductor design is that it is currently not able to make a continuous weld. To automate the welding, either the inductor has to be changed such that continuous welding is possible, or sequential welding should deliver a high quality weld without much irregularities.

In order for the inductor to work, an induction generator is required. During the experiments use is made of a COBES I-Class 10-12kW induction generator with a frequency range of 50-500kHz cooled by a system cooler of “ers Energie- und Kältetechnik GmbH”, Straßenhaus, Germany, type SC 2.5 VS. A constant force by the inductor was achieved by installing the coil on a pneumatic cylinder that could be regulated automatically. The nominal pressure of 8 bar inside the compressed air lines resulted in a force of 2494N which corresponds to a pressure of 5.25 bar on the CF parts for the geometry of the inductor used.

Capacitors within the induction unit determine the frequency that is produced. These capacitors can be changed by opening up the induction unit and installing different capacitors. The resonant circuit is shown in Figure 5.3 [79].

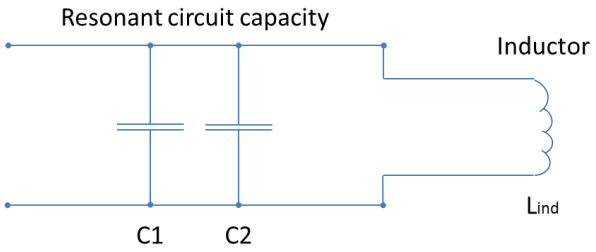

Figure 5.3: Resonant circuit inductor [79]

Using Equations (5.2) and (5.3), the frequency produced by the inductor can be calculated [79].

$$f = \frac{1}{2 \cdot \pi \cdot \sqrt{L_{ind} \cdot C_{tot}}} \tag{5.2}$$

Where: L_{ind} is the inductance of the inductor and C_{tot} is the total capacitance of the capacitors which is calculated with:

$$C_{tot} = C_1 + C_2 \tag{5.3}$$

Two capacitors with a capacitance of 0.17µF were installed because of their capability to withstand high voltages at high frequencies. These capacitors resulted in a frequency of 422kHz.

5.4. Temperature measurement

In order to obtain the temperatures measured by the thermocouples, the data produced by the thermocouples has to be read. This was done using a CompactDAQ and the program LabVIEW, both from National Instruments (NI). This CompactDAQ is connected to a computer. In LabVIEW a program was written to record the data. The measurements were saved in text files including the heating parameters, test piece, date and time.

(a) Thermocouple module [80] (b) CompactDAQ [81]

Figure 5.4: National Instruments data recording hardware

Because one temperature profile requires multiple tests to be performed, data of multiple measurements have to be joined in one graph. This was done using a second program written in LabVIEW where the text files could be added together.

More information on how the program functions and figures of the front end can be found in Appendix E.

6

Preliminary trials

Preliminary trials were performed in order to test hypotheses and to improve the design for the primary tests. First, the trials performed on the heating of thermocouples (TCs) is described in Section 6.1. Second, it is tested whether unsheathed TCs can be used to measure the temperature inside a laminate. Unsheathed TCs are small and their effect on the heating of the plies is therefore limited. Third, the heating of the laminates is examined using an infrared camera and separate TCs. Here, the effect of size, single or double laminate and magnetic field orientation is investigated.

6.1. Thermocouple heating

In order to test whether it is reasonable to use TCs to measure the temperature in the laminate, separate TCs were heated by induction to see the temperature increase produced by the TC itself. The inductor turned up the voltage for 1s from 0% to 40% and was kept at 40% for 2s. These are the inductor settings that are used for both the preliminary and primary trials. Table 6.1 shows the measured values, the average of those values and the maximum temperature increase per TC type. As can be seen, the TCs hardly heat up. This can be attributed to the fact that they are so small (wire diameter of 0.13mm). Only one measurement per TC orientation was done because the values were low, and even when some values might be twice as high, still no problems would arise.

Coil orientation	Type E (°C)	Type K (°C)	Type T (°C)
0°	0.64	1.45	1.07
45°	0.08	0.68	1.14
90°	0.46	0.28	0.20
-45°	0.05	0.14	0.43
Average	0.30	0.63	0.71
Maximum	0.64	1.45	1.14

Table 6.1: Temperature increase of heating separate TCs in different orientations

Looking at the values presented in Table 6.1 it can be seen that type E heats the least of the types tested. Therefore, and because Schieler [3] came to the same conclusion that type E TCs could be used best for this purpose, type E TCs were chosen.

During the temperature measurement an error is created in the measurements when the inductor is on. This is because a current is generated in the TCs by the inductor and this is measured as a temperature increase or decrease. An example of the temperature measured over time is given in Figure 6.1. This figure shows the heating of part 1 with the inductor

settings as were previously described. TC 0 is located under the inductor, TC 1 between the two plates and TC 2 below the second plate.

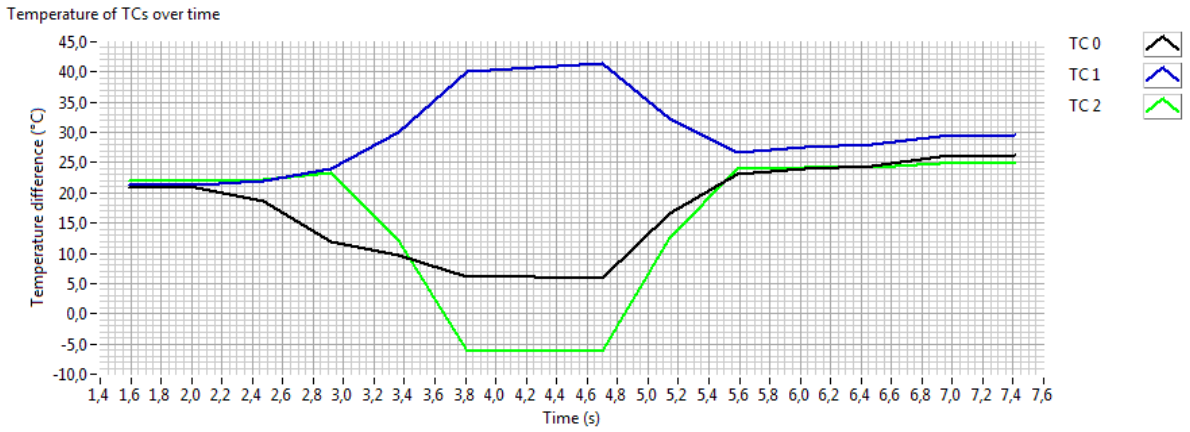

Figure 6.1: Temperature over time in °C (double lam, part 1, 0°)

As is shown in Figure 6.1, the error created while the inductor is on is big. But, when the inductor is switched off, the error dissipates and the temperature is measured reliably [51].

6.2. Testing with unsheathed thermocouples

In order to limit the effect of the TCs on the heating of the laminate, it was tested whether unsheathed TCs could be used within the laminate for temperature measurement. It was tested whether the CFRP would make a short circuit between the two TC wires. To this end, unsheathed TCs of type E with a wire diameter of 0.13mm were used which were supplied by the firm Omega Engineering GmbH, Deckenpfronn, Germany. TCs of type E have a limit of error of 1.7°C or 0.5% (in degree Kelvin). In order to verify the error produced by the TCs, a few TCs have been calibrated before they were built in the test parts. The calibration process performed is explained in Appendix F. The maximum error was found to be less than 1.0°C or 0.15% and was therefore well below the maximum error allowed. This error is small enough such that the experiments can be performed without any problems. To see if unsheathed TCs could be used in a CF part, test parts were manufactured and tested as is described in Sections 6.2.1 to 6.2.3 and results are given and discussed in Sections 6.2.4 and 6.2.5.

6.2.1. Strategy

In order to find a way to target specific plies in a laminate by altering the magnetic field direction and power, first simple laminates were built. These help figure out if and how the magnetic field heats up different plies. For these simple laminates, the same amount of layers were used as in the common aerospace laminate that were tested later. It was chosen to keep all laminates symmetric as is usually done for structural laminates in order to avoid membrane-bending coupling effects [82]. These simple laminates have the following structure and are visualized in Figures 6.2a to 6.2e.

$[90\ 0\ 0\ 0\ 0\ 0]_S$	→	Different orientation at weld interface
$[0\ 90\ 0\ 0\ 0\ 0]_S$	→	Effect of number of interfaces
$[0\ 45\ 0\ 0\ 0\ 0]_S$	→	Effect of relative angle between plies
$[0\ 45\ -45\ 0\ 0\ 0]_S$	→	Effect of ± 45 layers
$[0\ 45\ 90\ -45\ 0\ 0]_S$	→	Effect of gradual change in angle of plies

It is believed that when measuring the temperature profile of these laminates under different magnetic fields, a better understanding of the effect of the parameters is generated.

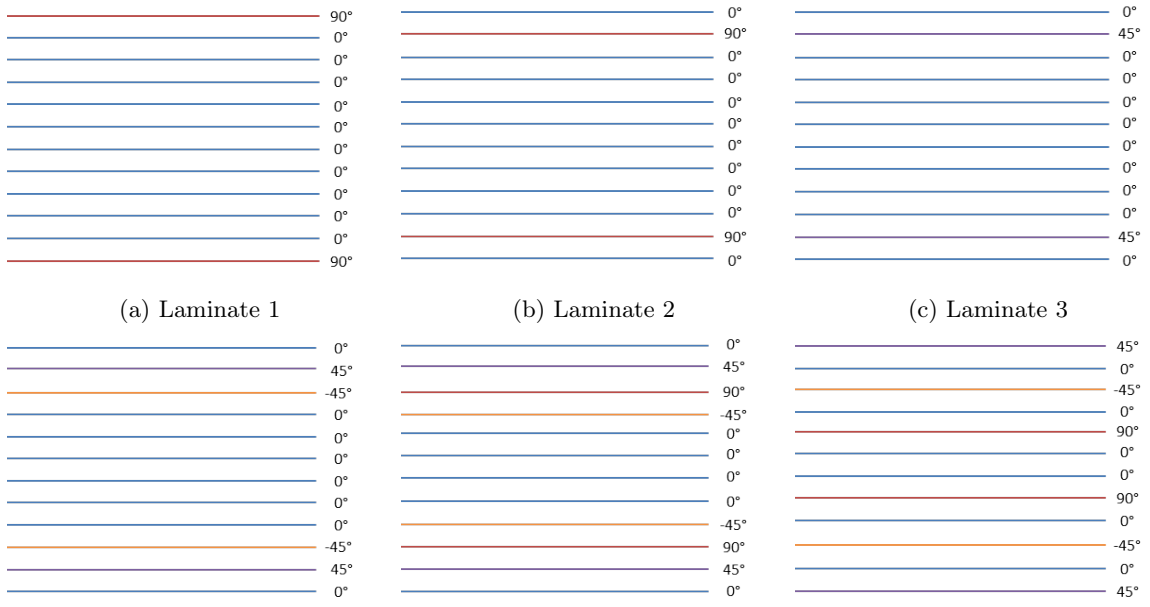

(a) Laminate 1 (b) Laminate 2 (c) Laminate 3

(d) Laminate 4 (e) Laminate 5 (f) Lam. 6: AE laminate (2x)

Figure 6.2: Layup of test laminates

A common aerospace laminate was built with the same thickness as the simple laminates. By adjusting the magnetic field, it was investigated whether targeted heating is possible. If it is possible to target specific plies, it might be possible to create a near-optimal temperature profile without excessive cooling, insulating or using a susceptor material. The common laminate has a layup of (45 0 -45 0 90 0)s and is shown in Figure 6.2f.

The primary test setup is shown in Figure 6.3a. As is shown in Figure 6.3a, two laminates were placed on top of each other to simulate reality during welding. Also, a single laminate was tested as is shown in Figure 6.3b. This was done to investigate whether Schieler [3] is right by claiming that the second laminate has no effect on the heating of the first laminate or whether Duhovic et al. [37] is right by stating that the bottom plate does have an influence on the heat generated in the top plate.

(a) Test setup 1 (b) Test setup 2

Figure 6.3: Test setup

The bottom plate, or base laminate, has the same layup as the top laminate. This requires two test parts for each layup. This was done this way, because when the base laminate has a layup that heats up better, the total temperature profile would improve and when the base laminate would heat up less, the total temperature profile would worsen.

For testing the effectiveness of a carbon fiber susceptor first a control group was made where the temperature profile across the thickness was measured using no susceptor. Then, the temperature profile achieved using several different CF susceptors was measured. These include different fabrics and thin-ply materials.

In order to limit the amount of materials needed to manufacture parts, the tests with LSP were performed by clamping the LSP below the part. This way, no extra parts for the LSP tests needed to be fabricated.

6.2.2. Preparation

The seven laminates depicted in Figure 6.2 were built with integrated TCs. First, the location of the TCs within the test parts is justified, followed by an explanation of how the test parts were built.

Thermocouple location in laminates

A division was made between simple laminates where it was more straightforward to distinguish the cause of the heat generation and a more complex, common aerospace laminate. Because of this difference, it was chosen to save some TCs in the simple laminates by applying them only between layers of interest as is shown in Figure 6.4.

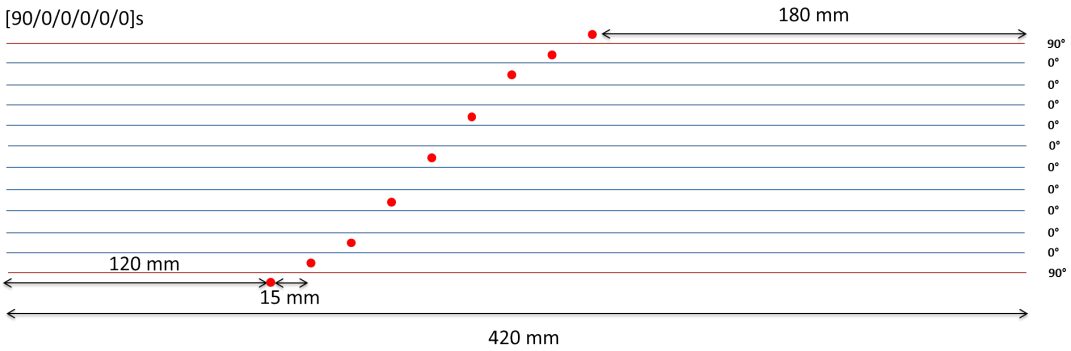

Figure 6.4: Test setup - sensor location

It was chosen to keep the distance between the TCs the same and thus shift the location of the next TCs when a TC is left out. It was chosen not to shift the TCs to the center of the test piece because, this way, the magnitude of the edge effect can be predicted by comparing the test results from heating from one side with heating from the other side.

In the common laminate the sensors are positioned through the whole thickness of the laminate. The setup for the common laminate can be found in Figure 6.5. Here, the induction coil was rotated to see if the orientation of the magnetic field has an effect on the heating of specific plies. Also the voltage setting is changed.

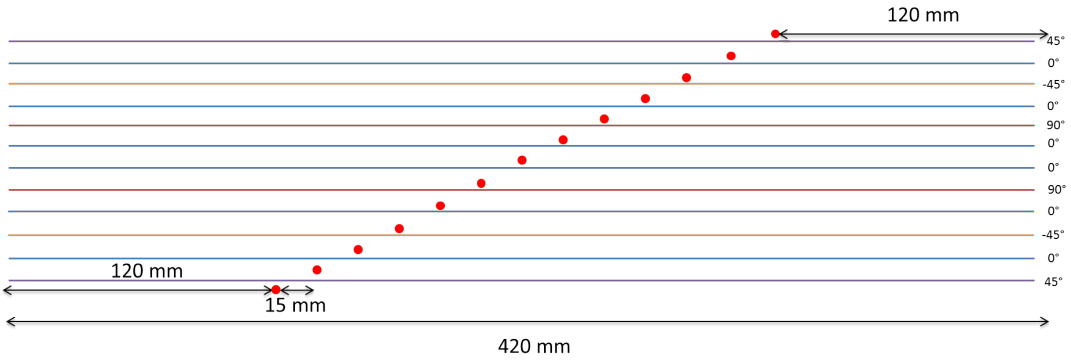

Figure 6.5: Common laminate test setup - sensor location

Building test parts

The test parts were made with Teijin HTS45 300mm wide PEKK UD Tape with $194 g/m^2$ dry fiber weight. The theoretical thickness is 0.2mm but when measuring the part thickness after consolidation a layer thickness closer to 2.3/12=0.19mm was measured. The resulting

part thickness is variable and dependent on several factors including the pressure in the autoclave. The pre-preg material has 34weight% of matrix material which results in a fiber volume fraction of 58% as was calculated in Equation (5.1).

In order to insert the TCs in the test parts in a controlled way without adding material that can influence the heating of the test part, a way had to be found to fasten the TCs. As was already done by Schieler [3] for CF with a PEEK matrix, the TCs were fastened between the layers in the test part using a soldering iron. It was noted that the TCs could be fastened parallel to the fibers with a soldering iron of 450°C. This temperature does not cause degradation as decomposition of PEKK starts at around 500°C [83]. The soldering iron was cleaned well before use, such that no remaining solder could end up in the material. Use was made of a template in order to position the TCs efficiently.

After soldering the TCs onto the layers of the test parts, the parts were laminated and consolidated in the autoclave. This was done according the setup as is shown in Figure 6.6 and the cycle presented in Figure 6.7.

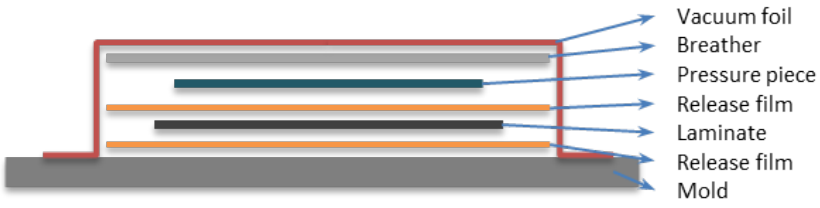

Figure 6.6: Vacuum bag setup

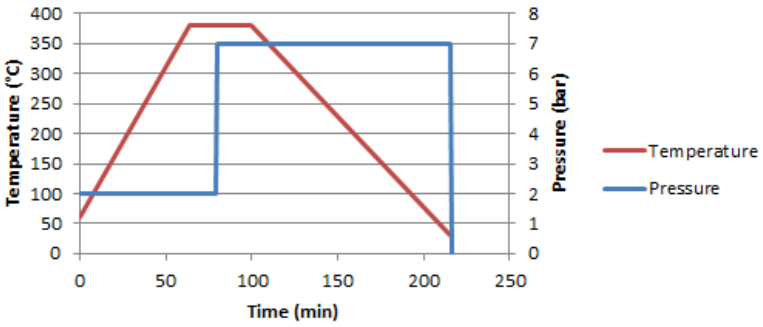

Figure 6.7: Autoclave cycle

The TC wires that came out of the test parts were isolated and a plug was installed as is shown in Figure 6.8. It was made sure that the wires within the tape do not touch each other such that the measuring tip would remain at the desired location within the test part and would not relocate to within the wires.

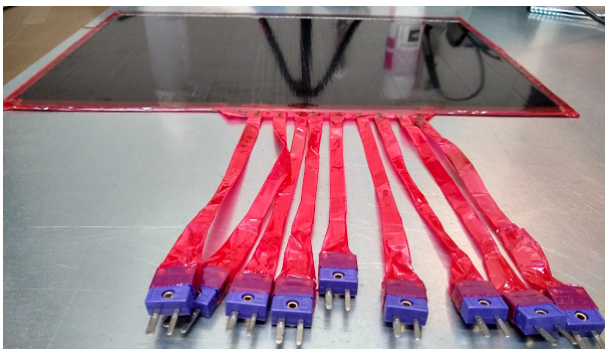

Figure 6.8: Isolation of thermocouple wires

6.2.3. Procedure

The location of TCs in the test parts that are described above were first marked at the surface. Since the TCs are located in a row, and not above each other, the plate is heated multiple times in order to create a temperature profile over the thickness. The data from the measurements were put together and graphs were plotted and saved via LabVIEW. Using the TC location marks, the plates could be positioned w.r.t. the inductor. Every TC was tested separately in order for the magnetic field and the cooling to be the same for each TC measurement.

6.2.4. Results

Heating the test plate by induction showed that the two surfaces heated the most, followed by their neighbouring layers. The core did not seem to heat up. The temperature profile measured is shown in Figure 6.9. The graph shows heating part 6 at 20% Voltage for 7s. In

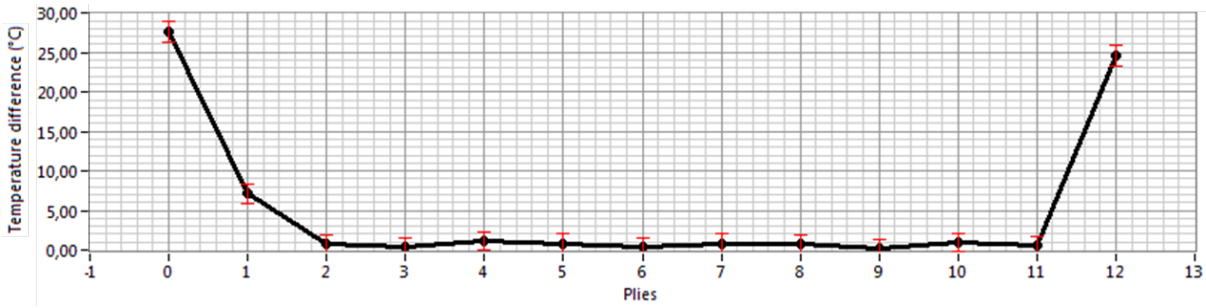

Figure 6.9: Measure through-thickness temperature distribution

order to test whether the results presented in Figure 6.9 resembled reality, a flat iron was used to heat up the laminate. This way, the temperature distribution measured by the TCs should roughly resemble a linear temperature decrease as is shown in Figure 6.10a. Figure 6.10b shows the heat profile as was captured with an infrared camera.

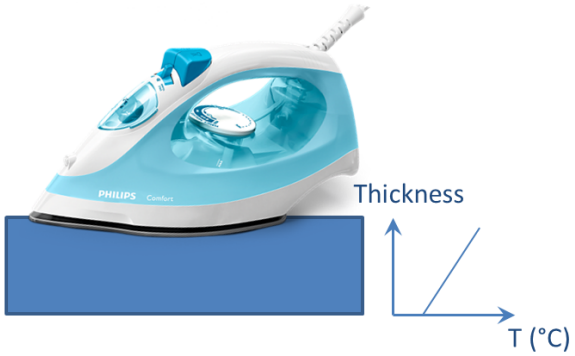

(a) Temperature gradient flat iron [84]

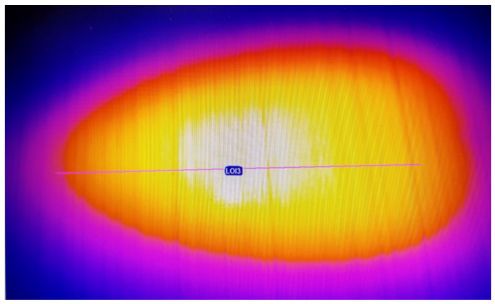

(b) Heat profile by infrared camera

Figure 6.10: Heating with flat iron

In Figure 6.11 the temperature measured by the TCs is depicted over the time that the test part was heated using the flat iron. Here, “TC separate bottom” and “TC separate top” are TCs that were put on top of the surface, but were not consolidated in the material. “TC separate top” was put below the inductor and “TC separate bottom” was put below the part. Furthermore, “TC1” is consolidated within the laminate, but above the first layer and “TC8” is below the last layer. All other TCs are located in in the laminate between the multiple layers.

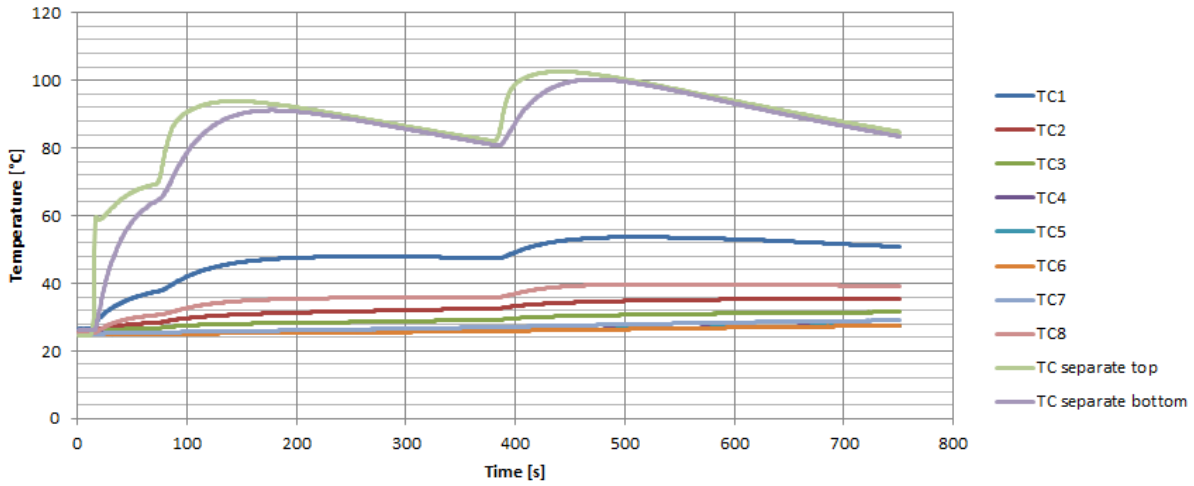

Figure 6.11: Measured temperature during heating with a flat iron

6.2.5. Discussion

As can be seen in Figure 6.11, the temperature shown by the two separate TCs rises quickly. Contrarily, the temperature of the other TCs rises slowly and stops rising after approximately 500s. The temperature measured by the TCs within the laminate should be between the temperature measured by "TC separate top" and "TC separate bottom". This is not the case and thus something in the measuring system is failing.

The cause of the malfunction in the measurement system was that unsheathed TCs were used. Because carbon fiber is conductive, the carbon fibers create a short circuit between the wires of the TC and they show the temperature at the first point where the wires are connected. This is likely to be at the edge and, as can be seen in Figure 6.10b, the temperature at the edge is lower than under the flat iron directly. The cause of the waves seen in Figure 6.11 is the thermostat switching the heating of the iron on and off.

6.3. Identification heat generation with infrared camera and thermocouples

New laminates were built with isolated thermocouples to measure the temperature profile over the thickness for the primary tests. In the meantime, the heating of the different laminates under investigation were recorded using an infrared camera from the side and separate TCs on the surfaces. Section 6.3.1 describes the procedure followed, Section 6.3.2 provides the results and a discussion of the results can be found in Section 6.3.3.

6.3.1. Procedure

The test parts that were used for the tests described in Section 6.2 were cut into smaller parts that could be used to see the heat generation between the layers using an infrared camera that records the temperature at the cut ends from the side. The test setup is shown in Figure 6.12. Even though edge effects are likely to have an influence on the actual temperature measured, it was assumed that the relative temperature distribution is meaningful. Therefore, the actual temperatures measured from the side, are not likely to equal those at the center of a part, but the relative temperature profile was still assumed to resemble the temperature profile that can be found at the center of the part. Using this, preliminary observations on the heat generation were done that were validated using TCs between each layer in a later stage[1].

[1] During validation it was shown that the anisotropic heat conductance led to false conclusions during some of the preliminary tests. Only the tests where the same part orientations are used to compare results are meaningful.

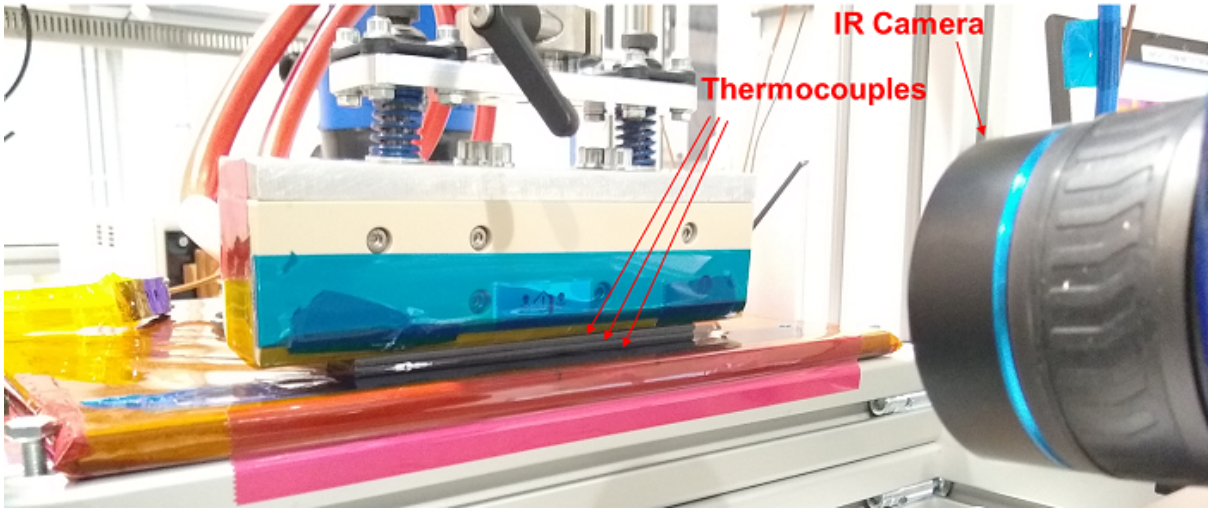

Figure 6.12: Preliminary test setup

On top of using the infrared camera that measures the temperature at the cut edges of the test parts, additional TCs were used to measure the temperature at the surface below the inductor, at the interface between the two to-be-welded parts and below the to-be-welded parts.

In order to test whether the direction of the magnetic field has an influence on the heating of the parts, parts had to be cut that can be tested in the 0°, the 90°, the +45° and the −45° direction. To this end, two square pieces of 14cm x 14cm were cut that could be tested in both the 0° and 90° direction. For the ±45° direction, one square of the same dimension as for the 0/90° samples was cut in the 45° direction and one triangular sample with half the size of the other samples was cut. The parts were cut as is shown in Figure 6.13.

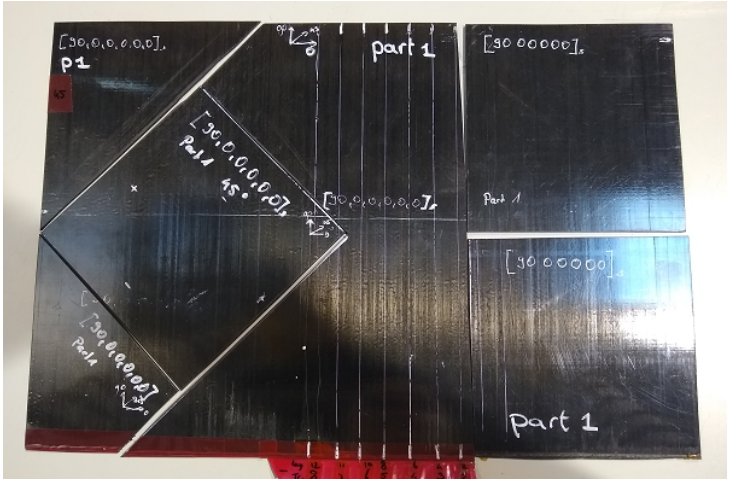

Figure 6.13: Division of laminate in smaller test parts

In order to know more about the distribution of the test values, all tests that are documented below have been performed five times. These five measurements included re-positioning the TCs, using different TCs, turning and shifting the part under the inductor. From these five measurements, the average, the standard deviation and the margin of error for a confidence level of 95% was calculated. This margin of confidence is plotted as the error bars in the figures in Section 6.3.2.

6.3.2. Results

In this section the results of the preliminary trials are given. Some effects have been measured using separate TCs and some effects have been measured using an infrared camera.

Skin effect

Because the electrical resistivity and magnetic permeability of the material used is not known, the skin depth of the material used in this thesis (unidirectional carbon fiber PEKK) could not be determined. However, Becker and Mitschang [39] state that with a CF PPS, PP or PA66 matrix with a thickness between 1.2mm and 3.2mm the skin depth is a multitude of the laminate thickness due to which its effect is negligible. This is confirmed by Rudolf et al. [29] and Duhovic et al. [85]. Therefore, no problems resulting from the skin effect were expected when welding a laminate with a thickness of approximately 2.3mm that was used in the tests. Here, it is assumed that the matrix material and the type of fibers (e.g. woven or UD) has no major influence on the relevant material properties.

In order to see whether the skin effect indeed poses no problems in the heating of the test parts in this thesis, the temperature profile at the edge of the test parts were measured with an infrared camera. Even though, the temperature measured at the side does not resemble the absolute temperature at the center of the part, the relative temperature profiles over the thickness were assumed to be comparable if the heat is generated at the edge the same way as it is at the center of the part. Only if the heat generation at the edge deviates from the center of the part, anisotropic conduction of the heat due to the different fiber directions will have an effect on the temperatures measured. This will be further discussed in Chapter 10. As was already expected, no real skin effect over the thickness of the laminate can be seen in Figure 6.14. A slight increase in temperature can be seen in the top part due to the cooled conductor. In the bottom part a slight decrease in temperature can be seen because of the increasing distance to the inductor and the heat conduction from the part to the tile underneath the parts.

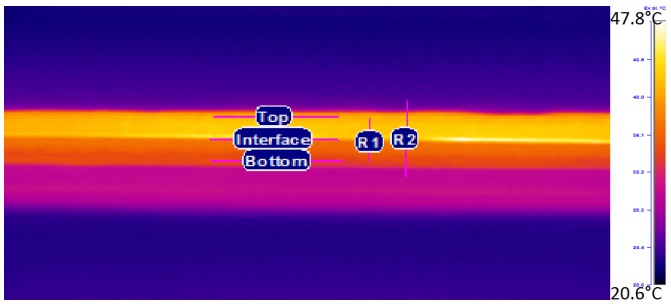

Figure 6.14: Infrared camera picture part 6, double laminate, 0° inductor orientation

Voltage test

A voltage[2] test was performed to see the effect the voltage has on the temperature profile. This voltage test was both performed with separate TCs and the infrared camera. The results can be found in Figure 6.15 and Figure 6.16 respectively. The tests have been performed with a voltage increase from zero to the target voltage in one second and keeping the voltage for another two seconds. A short cycle was chosen because this way, the location of the heat generation could be more easily distinguished. As can be seen in Figures 6.15 and 6.16, increasing voltage results in an increase in generated heat. Furthermore, no big change in the shape of the temperature profile occurs.

[2]The inductor is not power controlled but voltage controlled. The reason for this is that the power is dependent on both the voltage and current ($P = U \cdot I$). The current is dependent on the impedance which varies for each workpiece. Therefore, for different workpieces, different voltages and currents set when the system is controlled via power. On top of that, it is

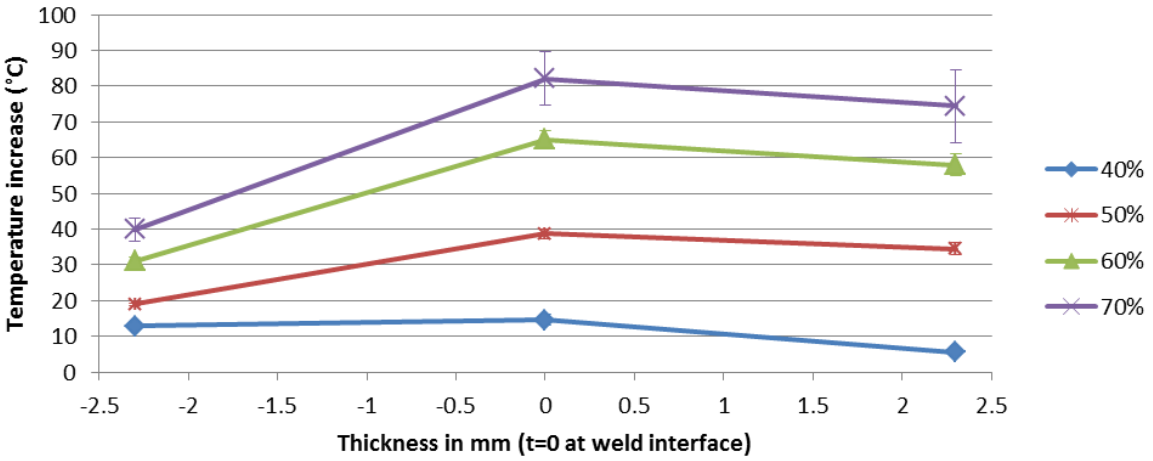

Figure 6.15: Voltage test - thermocouples

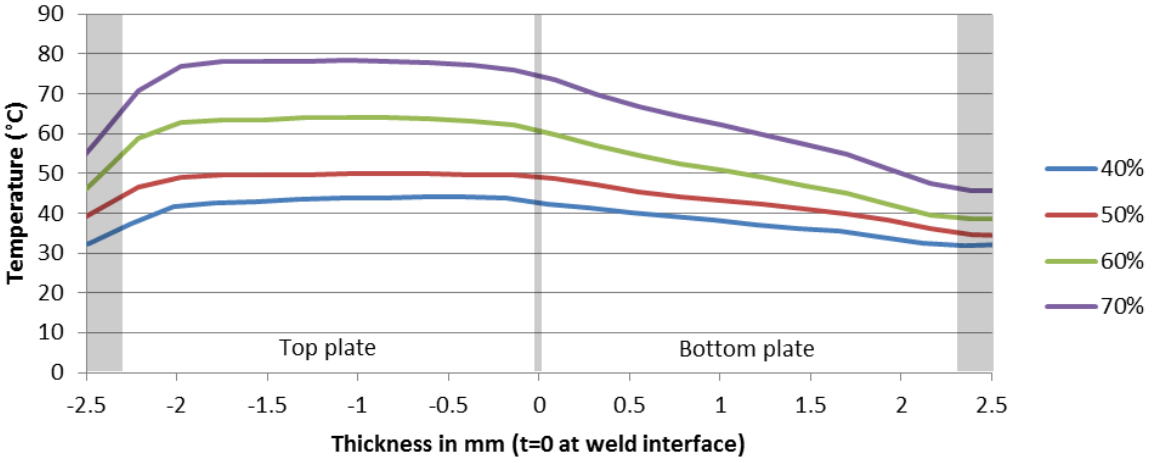

Figure 6.16: Voltage test - infrared camera

Another goal of the voltage test was to choose a voltage setting that could be used for the remainder of the preliminary tests. The voltage setting should:

- Allow for all parts to be tested with the same settings
- Allow for performing the preliminary trials fast
- Reduce handling risks (burning)
- Not melt any part of the test parts (also when LSP is applied)

A voltage setting of 40% was chosen because with a higher voltage some parts would melt when LSP was applied and this voltage setting would increase the amount of tests that could be performed.

Size effect

Different sizes of test pieces heat up differently under induction. The effect of the size on the heating of the test parts was tested using the same inductor settings on two different part sizes. The small test parts consisted of the three squares that can be seen in Figure 6.13. The big test part used was the remaining part that is located at the center of Figure 6.13 with edges in different angles. The effect of the size on the heating of single plates was tested for part 1 and 6 and can be seen in Figure 6.17.

possible that when regulating by power, the necessary current is not reached even at maximum voltage due to high system impedance. Voltage is the only independent variable and thus the best variable upon which the system can be controlled.

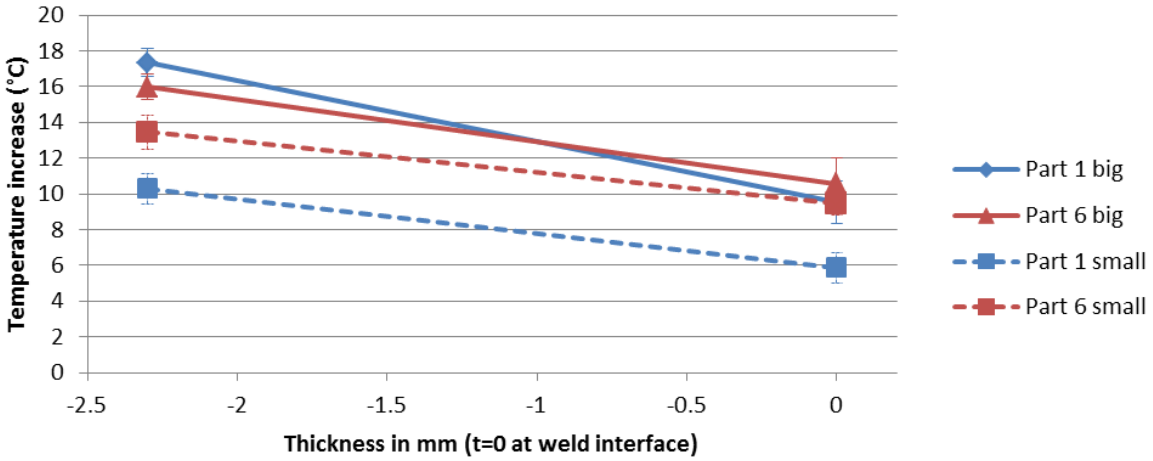

Figure 6.17: Size Effect - 40%V, 2s, 45°

In Figure 6.17 it can be seen that the bigger parts heat up faster than the smaller parts do. Therefore, it is important that all the tested samples have the same dimensions in order to be able to compare them. The difference can be caused by the difference in length of the fibers in the parts. When the fibers are longer, more electricity can flow. The dimensions of the big parts were not equal and therefore no conclusion can be drawn on the difference in magnitude the size has on the temperature increase between the two plates.

Single versus double plates

Next, the influence of a second plate on the heating of the first plate was investigated. Here a single plate was heated with the same settings as the double plate configuration. One TC was put below the inductor and one TC was put below the first plate. For the double plate configuration this means that the second TC was located between the two plates. Figure 6.18 shows the results of testing part 1 and 6 in a single and double configuration.

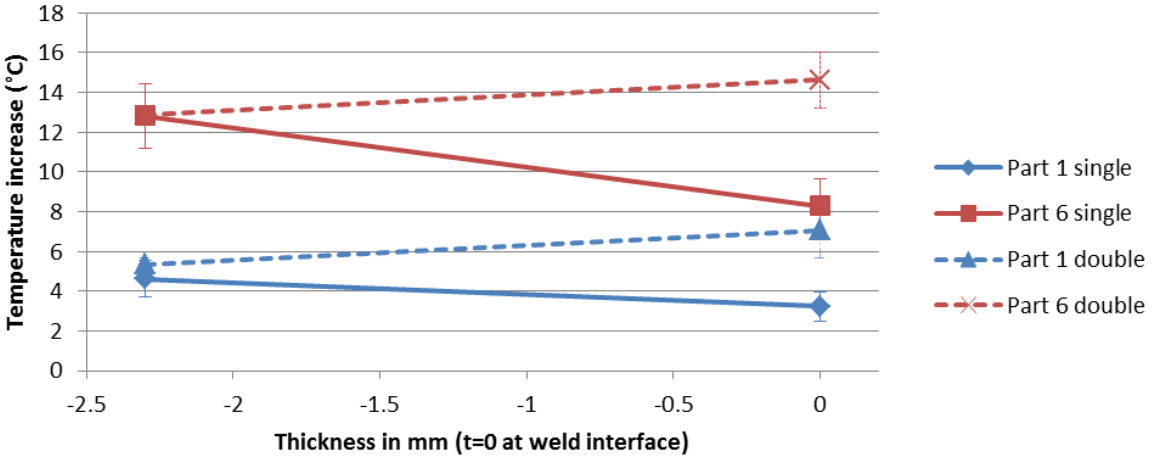

Figure 6.18: Single versus double plate - 40%V, 2s, 90°

As can be seen in Figure 6.18, the second plate has no influence on the heating of the surface directly below the inductor. This can be noted as the measurements below the inductor intersect for the single and double plate configurations. What can be noted in the graph, is that the second plate does have a positive influence on the temperature at the weld interface. The interface is now heated from two sides and can therefore reach a higher temperature than directly below the cooled inductor.

This effect, together with the size effect can be combined to create an optimal temperature profile. To this end, the size of the to-be-welded parts can be used to determine the side from which the welding should take place. This effect is plotted in Figure 6.19. The square parts as shown in Figure 6.13 were compared with the rest pieces with different angles.

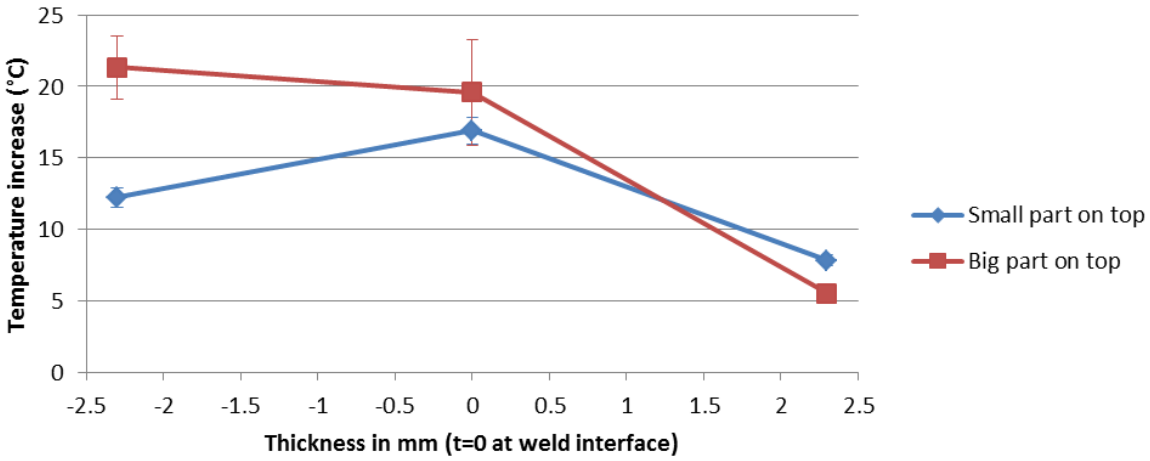

Figure 6.19: Size effect in a double laminate - part 1, 40%V, 2s, 45°

Figure 6.19 shows that, even though higher temperatures are reached when the big part is placed on top, the more optimal temperature distribution can be reached when the small part is on top. When the big part is on top, it produces so much heat, that it cannot be cooled by the cooling system within the inductor sufficiently. When the big part is below, the cooling system has to cool down less and the highest temperature can be found at the weld interface.

Magnetic field orientation

It was tested whether the direction of the magnetic field has an influence on the heating of the part. To this end, every part was heated in -45°, 0°, 45° and 90° angles. The orientation convention used is shown in Figure 6.20. The direction of the 0° fibers shown resemble the direction of the fibers at the center of the laminate which are all aligned with the length of the test part.

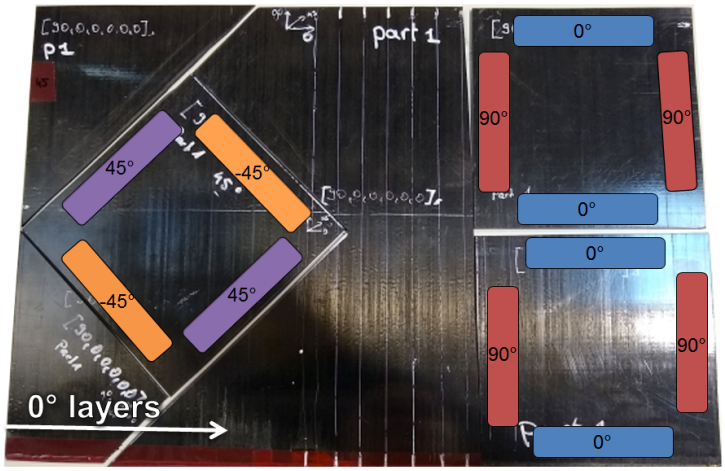

Figure 6.20: Inductor orientation for -45°, 0°, 45° and 90°

The influence of the magnetic field orientation on the heating of part 1 can be seen in Figure 6.21. It can be noted that an inductor orientation of ±45° results in a higher edge temperature than an inductor orientation of 0° or 90°. This means that the edge of the sample heats

up more when all the fibers in the circle in which eddy currents flow are at a ±45° angle. This is depicted in conclusion A. in Figure 6.33.

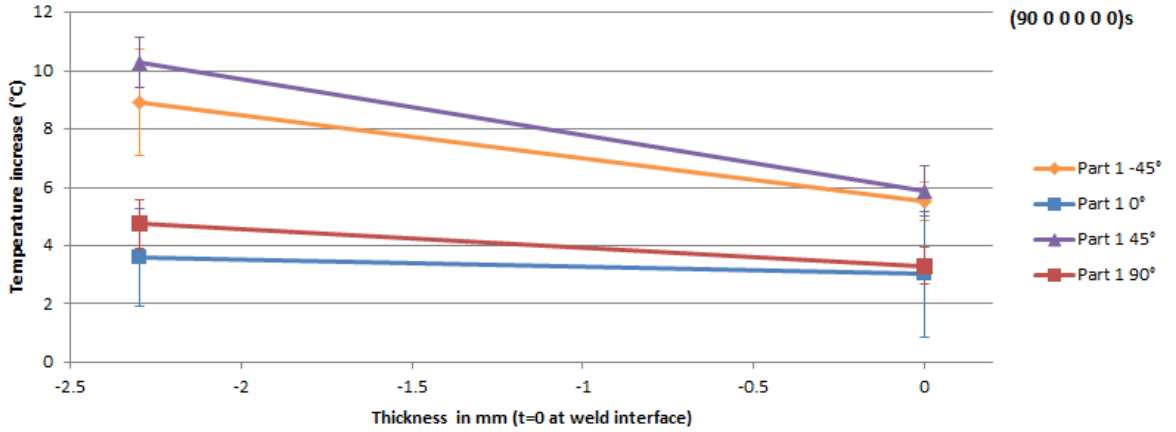

Figure 6.21: Effect of magnetic field orientation part 1

The influence of the magnetic field orientation on the heating of part 2 can be seen in Figure 6.22. Here, only the 0° and 90° angles are plotted as, due to unforeseen reasons, no sample of the same size could be cut in the ±45° direction from part 2. What can be seen in the plot is that the edges of the 90° samples heat up more than the 0° samples. This effect is visualized in point B. in Figure 6.33.

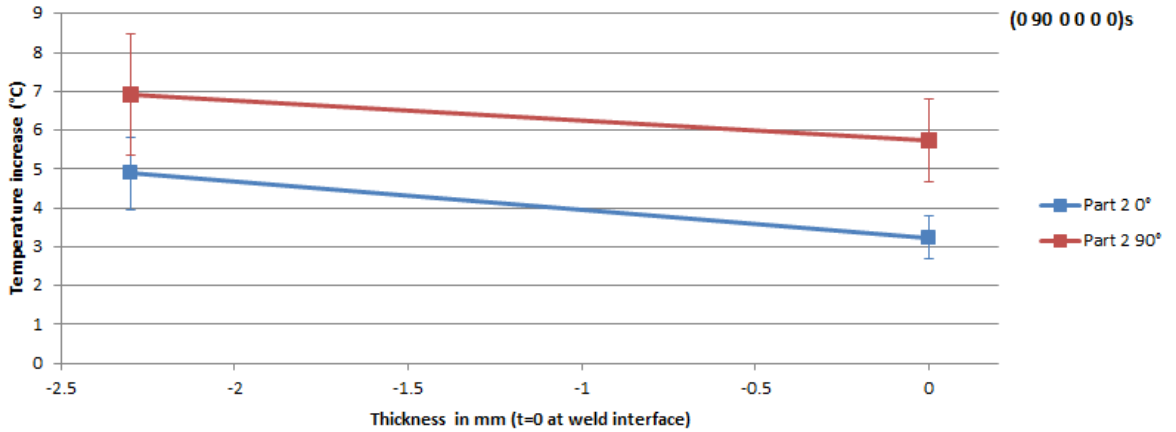

Figure 6.22: Effect of magnetic field orientation part 2

When comparing Figure 6.21 with Figure 6.22, it can be seen that the edge of part 2 heats up more with the 0° and 90° inductor orientations than part 1 does. This is likely due to the fact that part 2 has two interfaces between differently oriented plies generating heat, while part 1 has only one interface between differently oriented plies generating heat. This is visualized in point C. of Figure 6.33.

The temperature increase for the edge of part 3 under different magnetic field orientations is plotted in Figure 6.23. Two things stand out in this plot. First, the edge of the laminate is hardly heated by the 45° magnetic field. Second, the magnetic field in 0° and in -45° heat up the laminate by approximately the same amount. The layer orientations w.r.t. the magnetic field orientations can be found in point D. of Figure 6.33. No clear reason for these effects could be found using the theory presented above. The thicker blue lines denote that, at the interface(s), two layers are in this direction.

The resulting temperature increase of the edge of part 4 for different magnetic field orientations is depicted in Figure 6.24. In point E. of Figure 6.33 the relative angles of the plies w.r.t. the

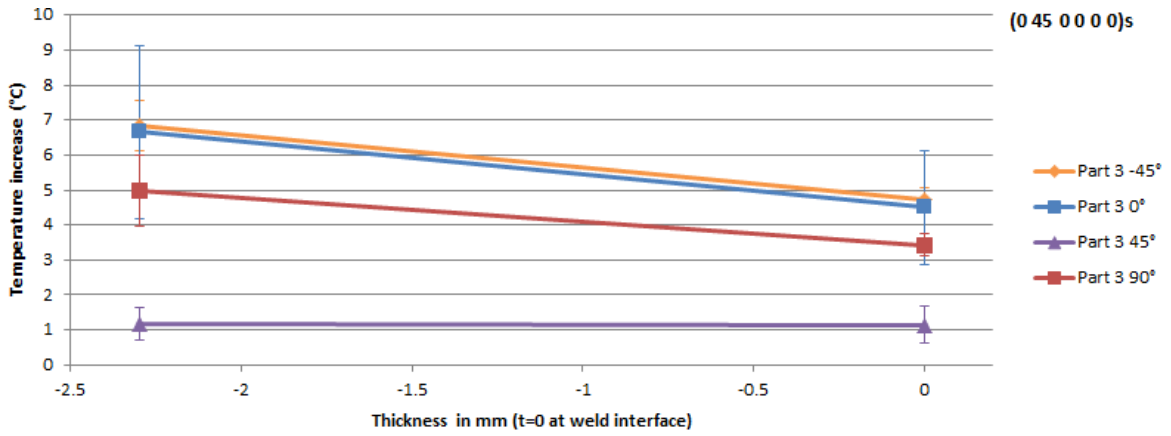

Figure 6.23: Effect of magnetic field orientation part 3

inductor can be seen. Now, as was already noted in point A., plies in the ±45° direction w.r.t. the inductor cause a higher temperature increase at the edge than plies in the 0/90° direction w.r.t the inductor. That is why, for this laminate with ±45° layers, the magnetic field in the 0° and 90° direction causes a bigger temperature increase at the edge of the laminate than the magnetic field in the ±45° direction. The edge heated with the 90° inductor orientation is likely to heat up more than the edge heated by the 0° inductor orientation due to the fact that it has plies perpendicular to the inductor instead of parallel to the inductor. The latter effect could already be seen in point B. in Figure 6.33.

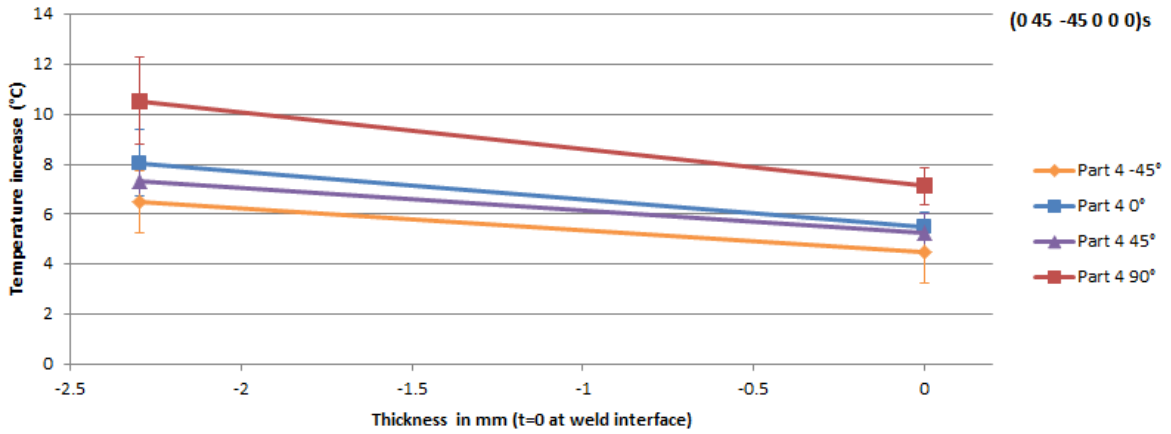

Figure 6.24: Effect of magnetic field orientation part 4

Figure 6.25 shows the temperature increase caused by different magnetic field orientations for the edge of part 5. In Figure 6.33 point F. the layer orientations w.r.t. the inductor are shown. Here it can be seen that the orientation with two layers at the interface is decisive. The edge of the part heats up the most when these are perpendicular to the inductor and the least when they are parallel to the inductor.

The temperature increase of the edge of part 6 due to induction is shown in Figure 6.26. Here it can be seen that a magnetic field in the ±45° direction heats up the edge of the laminate the most. What can further be noted is that the maximum temperature increase of part 6 is lower than for part 5. Part 5 and 6 have the same layer orientations but in a different sequence. Part 6 has one interface between differently oriented plies more than part 5. The number of interfaces has an effect on the heating of a laminate where an increasing number of interfaces increases the temperature increase.

In Appendix G the temperature increase per orientation of the inductor for each part is shown.

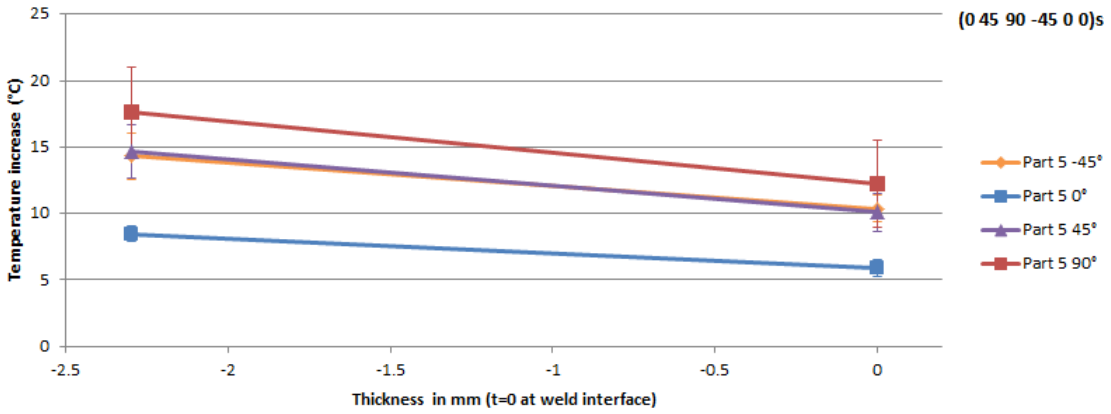

Figure 6.25: Effect of magnetic field orientation part 5

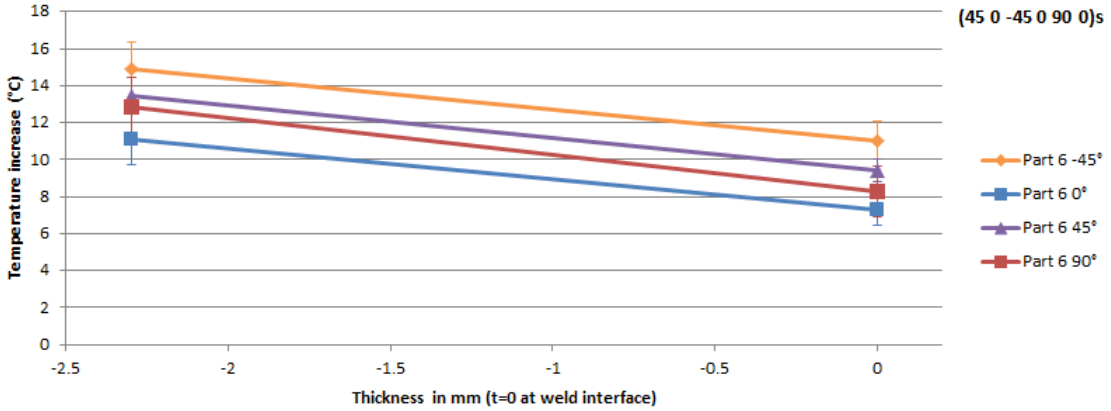

Figure 6.26: Effect of magnetic field orientation part 6

Stacking of different layups

Since different layups heat up differently, the stacking sequence of the layups can be used to generate a good temperature profile. This means that when two parts with different layups need to be welded together, the fact can be used that one layup heats up more than the other under the same magnetic field. This way, it can be ensured that the top plate does not melt, while the bottom plate heats up most. Now, the weld interface reaches the highest temperature and the other surfaces can remain solid with the right inductor settings. This phenomenon is depicted in Figure 6.27 where part 1 and part 2 are stacked in changing order.

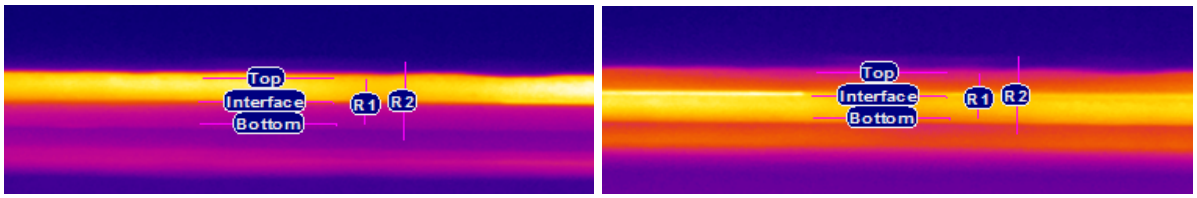

(a) Infrared picture part 2 on top, part 1 below (b) Infrared picture part 1 on top, part 2 below

Figure 6.27: Heating of part 1 and 2 stacked differently

Effect of first plate on heating of second plate

As was already explained and can be seen in Figure 6.14, the skin effect has no big influence in the tests performed. To further investigate if the hypothesis that the lower temperature in the second part compared to the first part can be attributed to the increased distance to the

inductor, a test with a double plate as is shown in Figure 6.28a and with a single plate with a distance of one part thickness between inductor and laminate as is depicted in Figure 6.28b was performed. To create a distance of one part thickness between the part and the inductor, four small plates (two on each side) were used to set the distance. These plates were also used for the double laminate setup to eliminate the possible effect these small parts have on the heating of the to be investigated parts. A $[(0\ 90)_3]$s layup was used for these tests to limit the effect of the layup on the temperature profile.

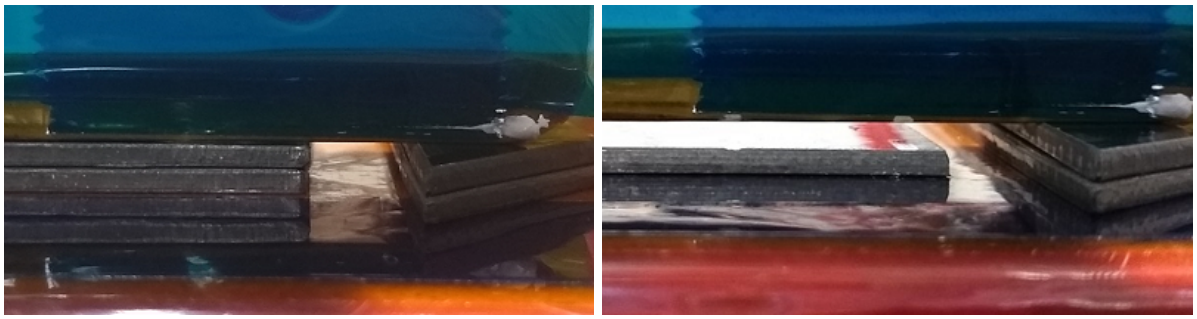

(a) Double laminate (b) Single laminate

Figure 6.28: Test setup - effect of first plate on heating of second plate

In Figure 6.29 the infrared pictures of the test performed are shown. Both have the same colour scale where 20°C has the colour black and 50°C has the colour white. The pictures show the same location of the part and inductor. Figure 6.29b is mirrored for better comparison. As can be seen in Figure 6.29b, the upper surface of the plate gets hot and looks like a second plate in the picture. This is however not the case, the hot surface as is seen Figure 6.29b is the upper surface of the single part. In Figure 6.29a, a small discontinuity in temperature across the two plates can be noted. The pink colour at the bottom of the pictures is a reflection of the heat on the release film that is wrapped around the ceramic tile.

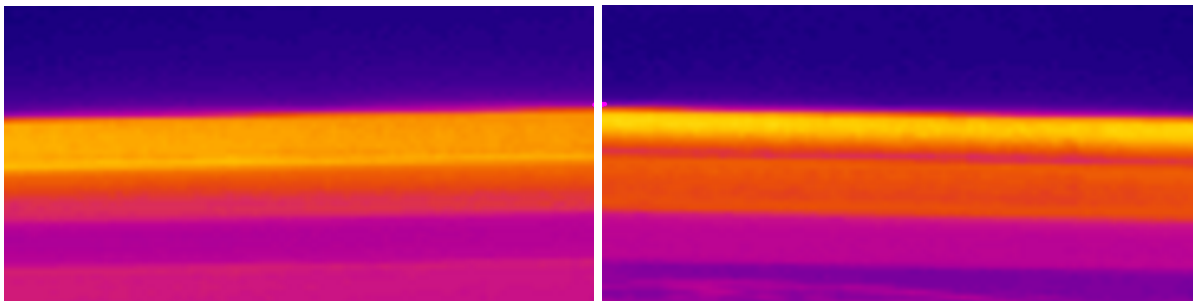

(a) Double laminate (b) Single laminate

Figure 6.29: Infrared picture of $[(0,90)_3]$s, single with distance of one plate thickness to inductor vs double

Figure 6.30 shows the average graph of the temperature measured by the infrared camera starting from the inductor to below the bottom part. A sample size of five was used. The data of which the average was calculated was generated by repositioning and turning two plates. The measured data had little scatter with an average sample standard deviation of 0.3 for the single plate and 1.0 for the double plate. Here, one thing stands out that can also be spotted in Figure 6.29 when taking a closer look: for the single plate the temperature over the thickness stays relatively constant while the temperature over the thickness for the double plate clearly decreases. The non-averaged data is plotted in Appendix H in Figure H.1.

There are two reasons for the change in temperature profile in the bottom plate when a top plate is added. First, heat is conducted from the first plate to the second plate which increases the temperature in the second plate close to the weld interface. Second, the inductor exerted a force on the double plate configuration, but no force was exerted for the single plate configura-

tion. Therefore, the contact with the ceramic tile, and therefore the heat conductance towards this ceramic tile was much more efficient for the double plate configuration. This makes the temperature close to the ceramic tile in the double plate configuration lower than for the single plate configuration. Furthermore, the almost equal average temperature in the bottom plate confirms, or at least does not contradict the hypothesis that the lower temperature measured in the bottom plate is due to the increased distance to the inductor.

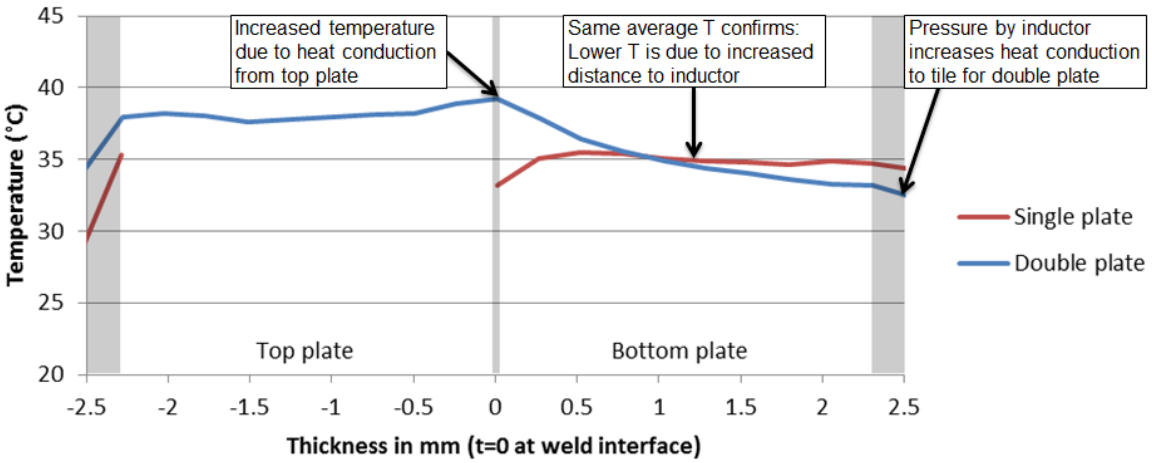

Figure 6.30: Temperature profile across thickness measured with infrared camera

Effect of second plate on heating of first plate

As was mentioned in Chapter 2, Schieler [3] states that the second laminate has no effect on the heating of the first laminate with the exception of cooling by conduction. He states the second laminate has no influence on the current density in the first laminate. According to Schieler [3], the upper laminate cools by conduction to the second laminate. Duhovic et al. [37] states that the heating of the top plate is reduced by the magnetic field created by the eddy currents in the second plate. These two statements contradict each other and therefore tests to clarify the topic have been performed.

Again a $[(0\ 90)_3]$s laminate was used to perform the tests in order to limit the influence of layup properties on the results. The data of the double plate that was discussed in "Effect of first plate on heating of second plate" was compared to the heating data of a single plate without a gap between the inductor and the plate. The data produced with the infrared camera is shown in Figure 6.31. Again, a sample size of five was used. The average sample standard deviation for the single plate was 1.1 and for the double plate 1.3.

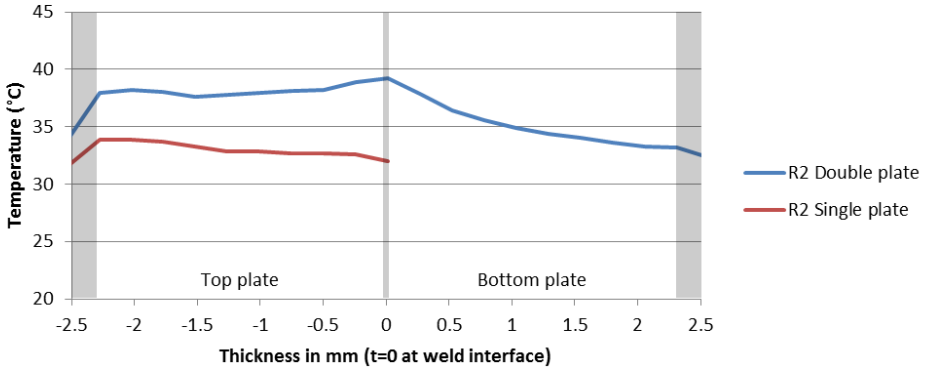

Figure 6.31: Temperature profile across thickness measured with infrared camera

As can be seen in Figure 6.31, the top plate of the double configuration became warmer than the temperature for the single plate. What can be seen is that for the double configuration,

the temperature rises near the interface with the second plate. This is not the case at the bottom of the single plate where it gets colder. Because the temperature in the first plate for the double configuration is much warmer than for the single plate configuration, it is not likely that, as was described by Duhovic et al. [37], the eddy currents of the second plate reduce the magnitude in the first plate enough in order to see its effect. Also, the statement of Schieler [3], where the top plate cools by conduction to the second plate, does not seem to have a big effect as the temperature increases towards the interface.

A possible explanation for the temperature increase consists of two effects working simultaneously. The first effect is that the heating due to induction decreases exponentially when moving away from the surface [28]. The second effect is that cooling a surface of a material leads to a linear decrease in temperature. When superimposing these two effects, a temperature profile as can be found in the top plate of the double plate configuration can be created. This superimposition is depicted in Figure 6.32.

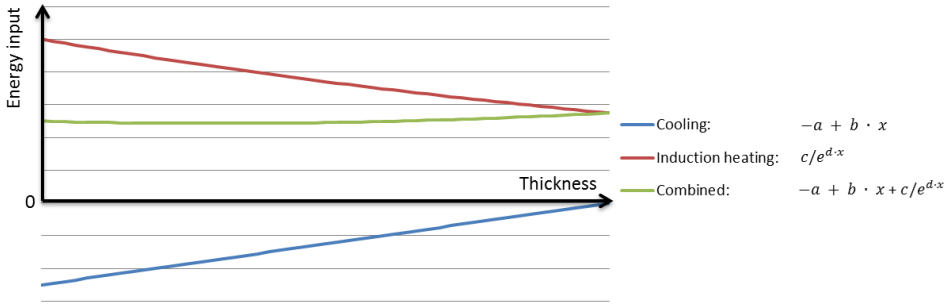

Figure 6.32: Reason for temperature increase towards interface

6.3.3. Discussion

The results stated in Section 6.3.2 are summarized in Figure 6.33[3]. Except for point D, it shows that heating the test parts such that both fiber directions are under a 45° angle results in the highest temperature at the edge. Also, again except for point D, Figure 6.33 shows that the tests where the fiber direction is present two times perpendicular to the inductor have the highest temperature at the edge, followed by the tests where this direction is diagonal to the inductor[3]. Point D. cannot be explained by the theory presented above. In Section 7.1 the reason for this is explained.

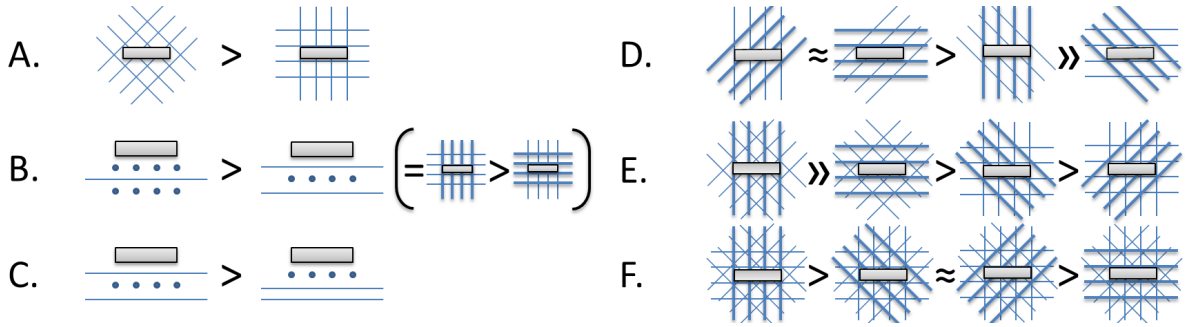

Figure 6.33: Visualization of conclusions made on the influence of magnetic field orientation on laminate heating

[3]During the preliminary trials it was falsely concluded that the electricity is generated in the fibers perpendicular to the the inductor and that the temperatures measured at the edge are therefore the highest with many fibers perpendicular to the edge. However, the highest temperature at the edge is caused by a more efficient heat transport towards the edge when many layers with fibers perpendicular to the edge are present. Therefore, point D can be explained by the fact that the second configuration generates the most heat but can transport this heat to the edge very poorly while the configuration in the first diagram generates less heat, but can transport it to the edge more efficiently. This will be further explained in Section 7.1

7

The effect of the magnetic field properties on the heating of different laminates

In this chapter the effect the direction of the magnetic field has on the heating of different laminates is investigated in Section 7.1. Then, in Section 7.2, the change in temperature profile for different voltage settings is presented.

7.1. Effect of magnetic field orientation

In this section the effect the magnetic field orientation has on the heating of the different laminates, which were proposed in Chapter 6, is investigated. First, the the design of the new test laminates is explained in Section 7.1.1. Second, preparations done in order to be able to perform the tests are outlined in Section 7.1.2. Next, in Section 7.1.3, the procedure used to obtain the data is described. Then, in Section 7.1.4, the acquired results are presented followed by a discussion of the results in Section 7.1.5.

7.1.1. Test laminate design

After the first conclusions on the heating of specific plies in different orientations were made, new layups were designed to further understand the heating of specific plies and laminates under different magnetic field orientations[1]. Except for part 1, all the previously used layups had a 0° layer at the surface of the part. In Figure 7.1 it is explained why this is unwanted.

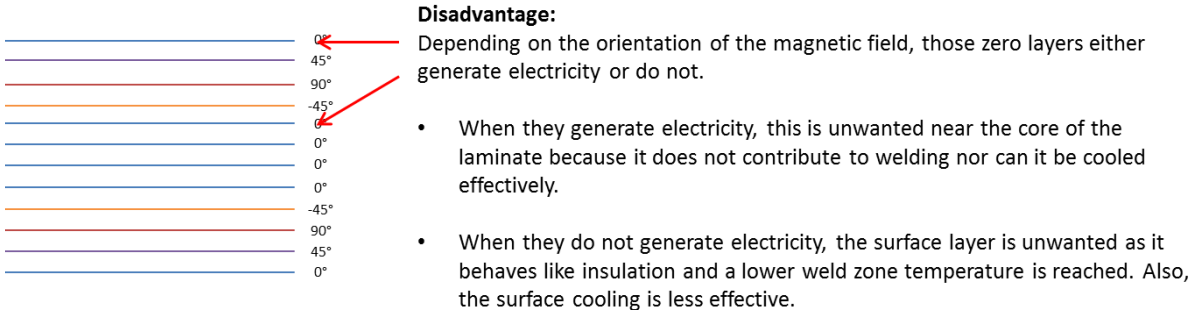

Figure 7.1: Disadvantage of previously used layups

[1]During the preliminary trials it was falsely concluded that the electricity is generated in the fibers perpendicular to the the inductor and that the temperatures measured at the edge are therefore the highest with many fibers perpendicular to the edge. However, the highest temperature at the edge is caused by a more efficient heat transport towards the edge when many layers with fibers perpendicular to the edge are present. The laminates were designed using this faulty theory.

The layups presented in Figures 7.2 to 7.5 were tested in the primary tests. The laminate presented in Figure 7.2 is the common laminate as was already tested. This laminate is used as reference to see if the changes in the laminate layups have the expected effects.

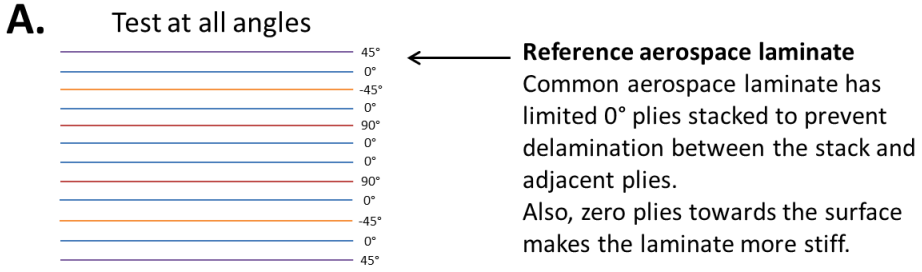

Figure 7.2: Layup A - Common aerospace laminate

Layup B is based on the common aerospace laminate and is presented in Figure 7.3. The layup is kept as close as possible to the common aerospace laminate in order to limit the effects of the change in layup on its properties. The -45° layer has been switched with the 90° layer to improve heating at the surface and limit the heating at the core of the laminate. It is stated with which inductor orientation the most optimal heating is expected. In the picture references are made to the tests that showed that the combinations used either showed much or little edge heating in the preliminary tests.

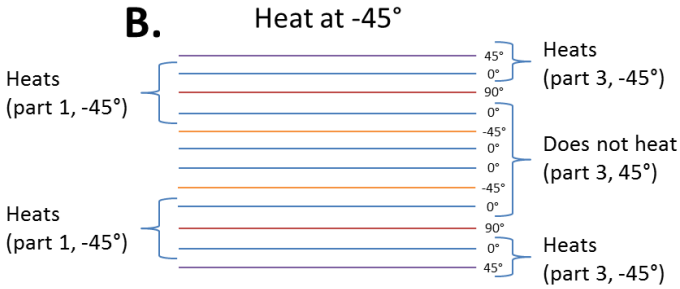

Figure 7.3: Layup B

In Figure 7.4 a layup is shown that is not based on the common aerospace laminate but on part 5 of the preliminary tests. This laminate showed the highest possible temperature increase at the edge of all the test parts in the preliminary tests. However, as already explained in Figure 7.1, the top layer in 0° direction is removed in order to focus the heat generation at the surfaces only.

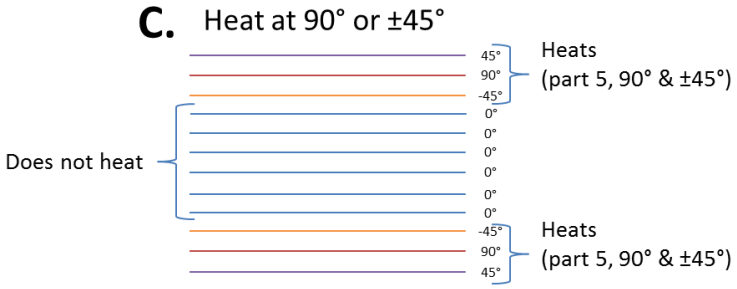

Figure 7.4: Layup C

The final layup that is investigated in the primary tests is shown in Figure 7.5. This layup is similar to layup C but the -45° and 90° layers have been switched. This way, it is tested whether a 45° angle between neighbouring plies results in better heating, or whether 90° angles between (most of the) neighbouring plies results in more heat generation.

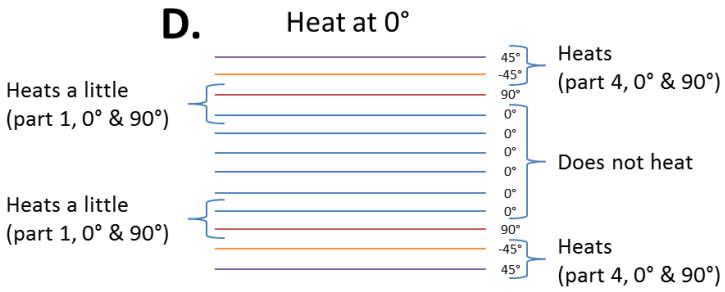

Figure 7.5: Layup D

7.1.2. Preparation

Because no ready made thermocouples of type E with isolation could be purchased, isolated thermocouple wire was ordered from Omega Engineering GmbH, Deckenpfronn, Germany. These wires were welded together using a LABFACILITY L60+ thermocouple & fine wire welder.

Because not all temperatures along the thickness of the laminates were considered interesting, a few thermocouples were left out of the laminate at places where it was considered possible. This allowed for material saving, less tests to be performed and an approximation of the edge effect as the distance between the first thermocouple to the edge is different than the distance between the last thermocouple and the edge in two of the four laminates. The thermocouple location for the four laminates is shown in Figure 7.6. Here, Figure 7.6a shows the picture of part but the same thermocouple configuration is used for part B. The same holds for Figure 7.6b where the figure shows part C but the same configuration is used for part D.

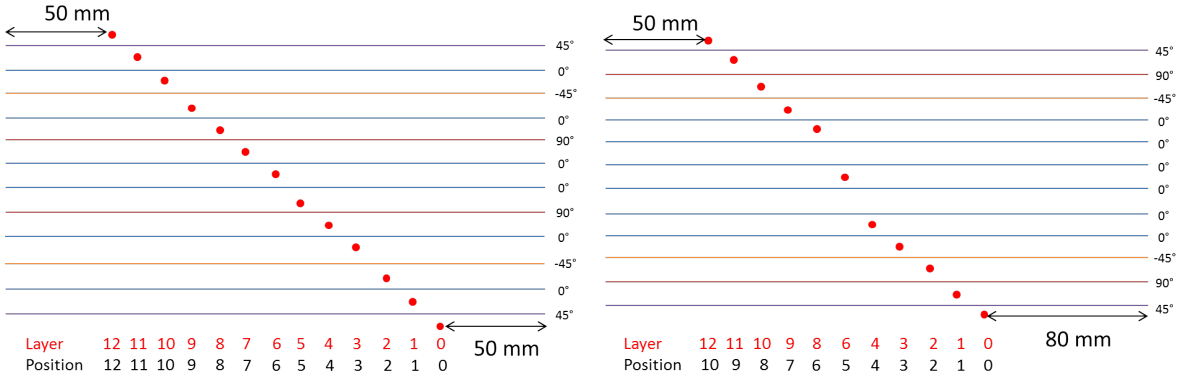

(a) Thermocouple location in part A and B

(b) Thermocouple location in part C and D

Figure 7.6: Thermocouple location

The 0° and 90° layers were cut by hand using a guillotine style paper cutter. The ±45° layers were cut automatically by uploading DXF files, that were generated using CATIA V5, onto a cnc cutter. The thermocouples were, as was described in Section 6.2.2, attached onto the pre-preg material using a soldering iron and a printed positioning grid. At the edge the thermocouple wires were attached with tape.

7.1.3. Procedure

All test parts were tested with an inductor angle of -45°, 0°, 45° and 90° as is further clarified in Figure 7.7. The same inductor settings as for the preliminary trials were used meaning a ramp to 40% voltage for 1 second and maintaining the voltage for 2 seconds. Between the measurements the parts were let to cool down to below 40°C.

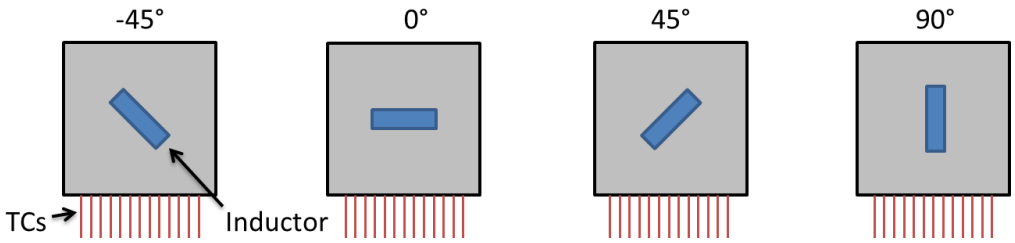

Figure 7.7: Clarification for inductor direction primary tests

The way the temperature profiles are established is explained in Figure 7.8. Each time two plates of the same layup are put below the inductor in the same orientation and position. The part with the thermocouples is the top part. Because the TCs are located next to each other, every TC has to be targeted separately in order for them to receive the same magnetic field. This means that for part A and B thirteen measurements were taken per temperature profile and for part C and D eleven measurements are made.

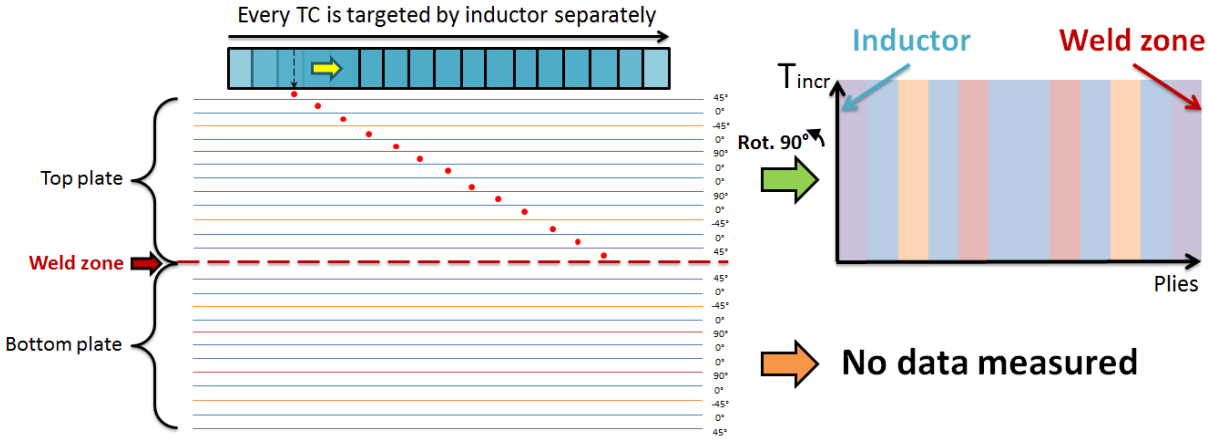

Figure 7.8: Explanation of test-setup and temperature profile graph establishment

As can be seen in Figure 7.8, only the temperature profile of the top plate was measured. The temperature shown is the temperature increase, meaning the temperature at the end of the measurement subtracted by the temperature at the start of the measurement. This way, the effect of starting temperature on the results is minimized. All parts were tested twice; once from the “front” side which is the pressure piece side and once from the “back” side which is the mould side. Theoretically, the measurements from the front and the back side should be equal. However, there are multiple effects that can cause a difference between the values measured. These include but are not limited to:

- Different inductor position
- Different thermocouple position
- Edge effect
- Failure in thermocouple
- Difference in laminate properties

7.1.4. Results

A selection of the temperature profiles measured is presented in this section. In the temperature profiles the layup is shown and the inductor is located at ply zero. The color of the lines for the different inductor orientations are equivalent to the color of layer directions that are parallel to the inductor. In Figures 7.9 and 7.10 respectively, the front and the back temperature profile of part A (the common aerospace laminate) heated with different inductor

orientations is shown. What stands out is that a big difference in the measured temperature increase can be seen for an inductor orientation of 0° w.r.t. the other orientations.

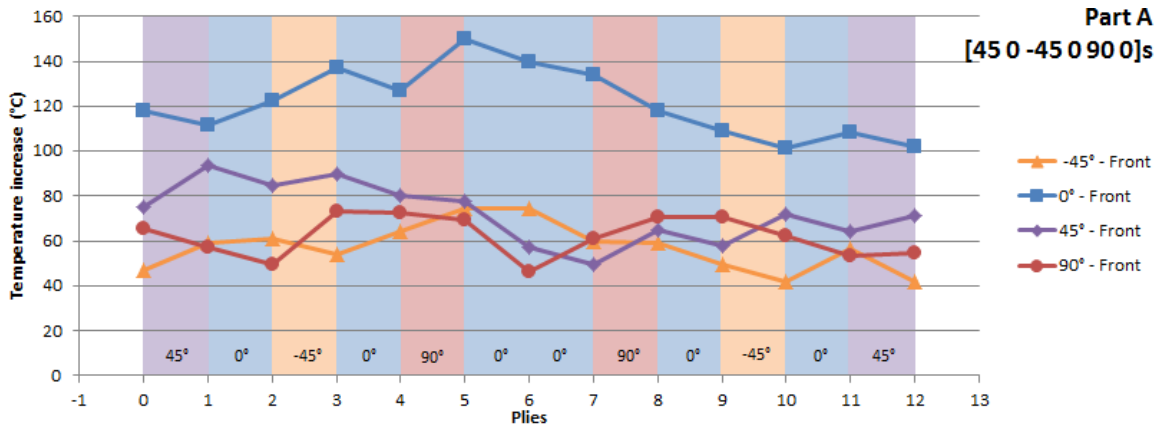

Figure 7.9: Part A front side

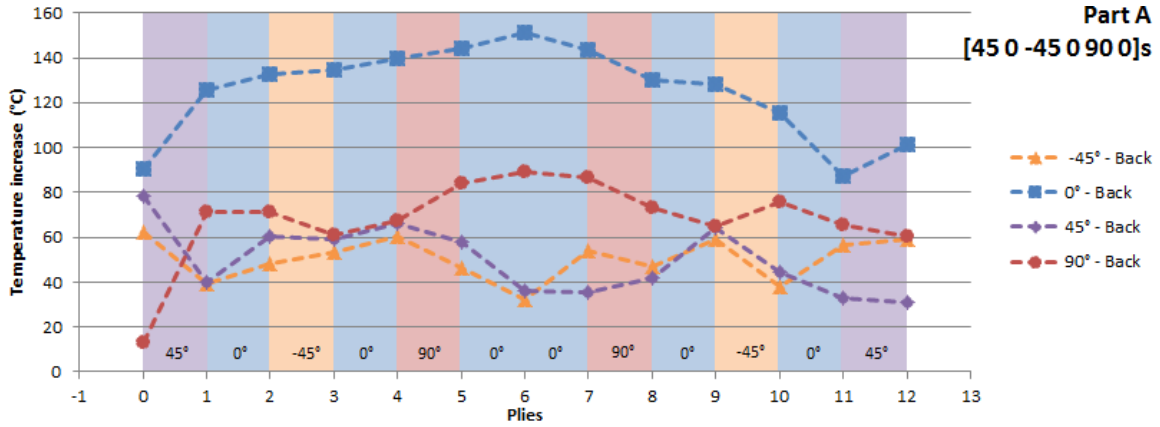

Figure 7.10: Part A back side

In Figures 7.11 and 7.12, the temperature profiles measured for the different inductor orientations are shown for part B. Again, a much higher temperature increase for the 0° layer can be seen. Because interfaces are located across the thickness, and because some error can be found in the measurements, no clear source of heat generation can be pointed out here.

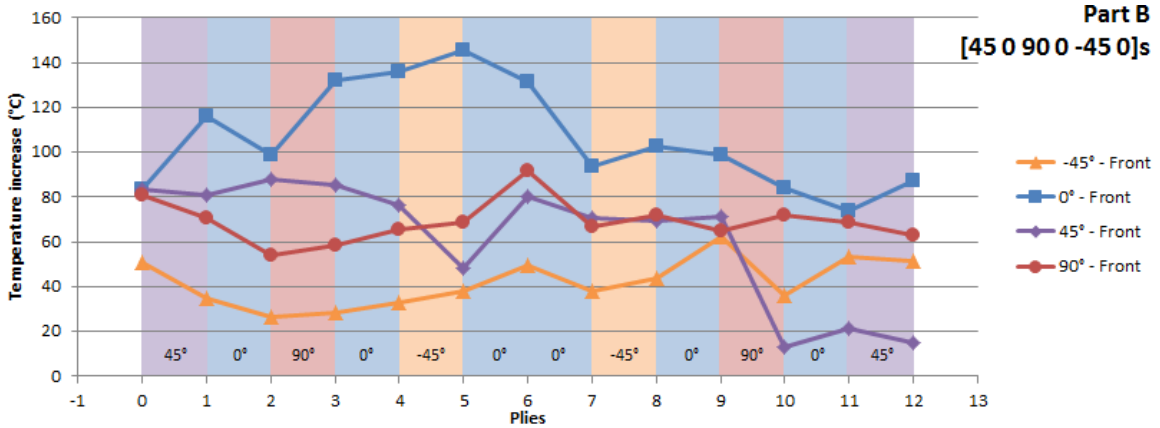

Figure 7.11: Part B front side

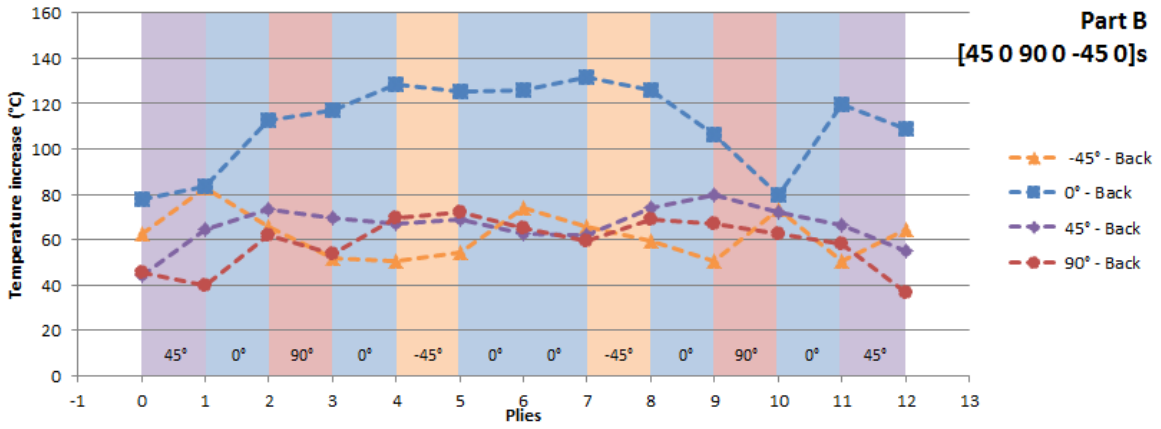

Figure 7.12: Part B back side

Figures 7.13 and 7.14 show the temperature profiles measured for part C. Also here, a difference in the temperature profiles for the different inductor orientations can be seen. An inductor orientation of 0° results in the highest temperature increase, whereas an inductor orientation of 45° results in the lowest temperature increase. Small increases in temperature can be found at the interfaces of the plies with which the inductor aligns.

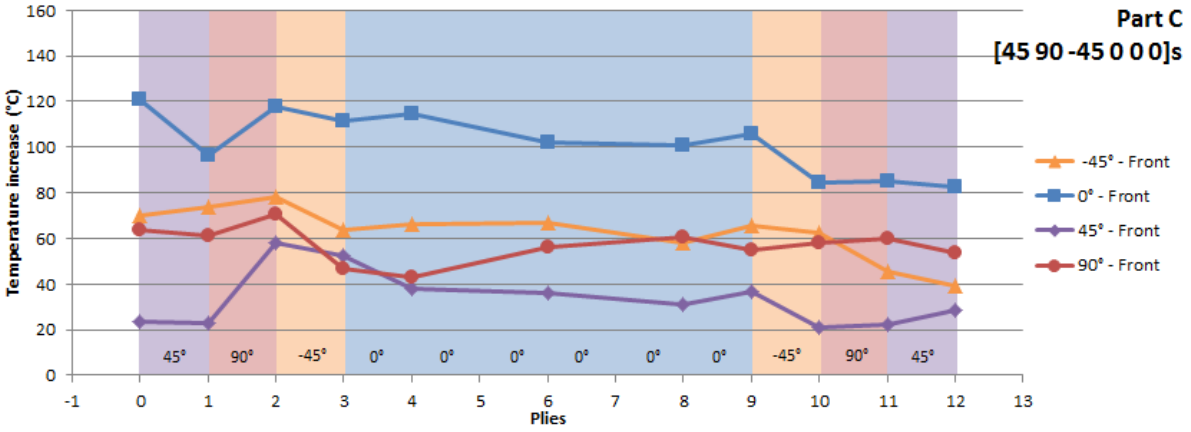

Figure 7.13: Part C front side

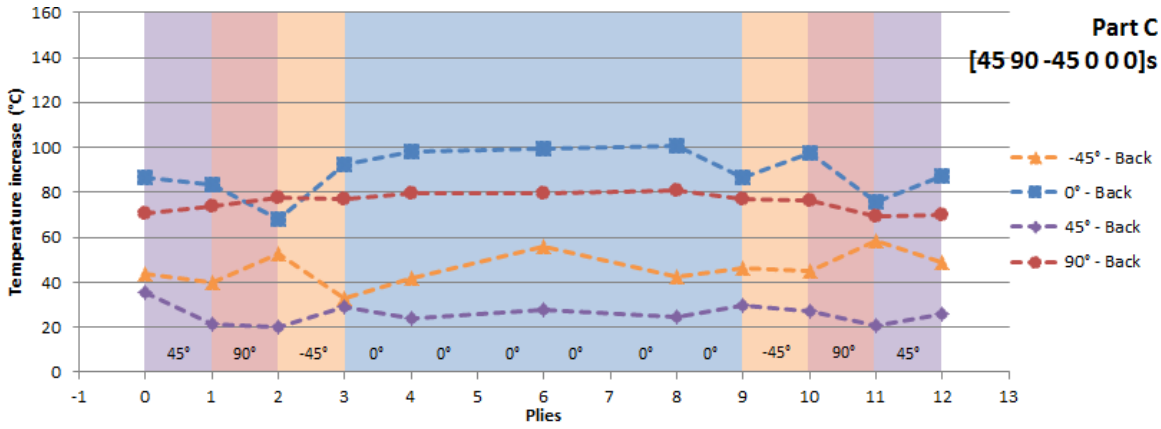

Figure 7.14: Part C back side

In Figures 7.15 and 7.16 the temperature profiles for part D are given. Again a bigger temperature increase for the 0° inductor orientation and a smaller temperature increase for the 45° inductor orientation can be seen. Also here, small increases in temperature can be found at the interfaces of the plies with which the inductor aligns.

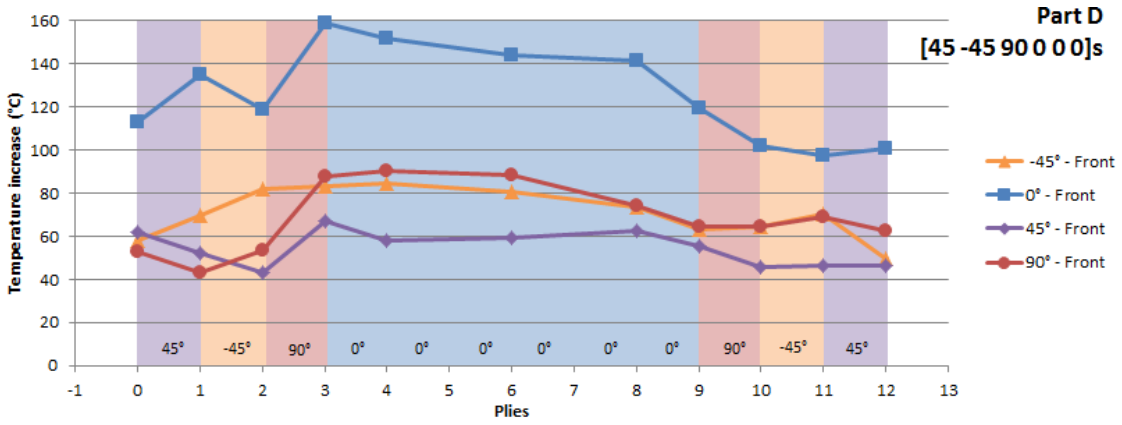

Figure 7.15: Part D front side

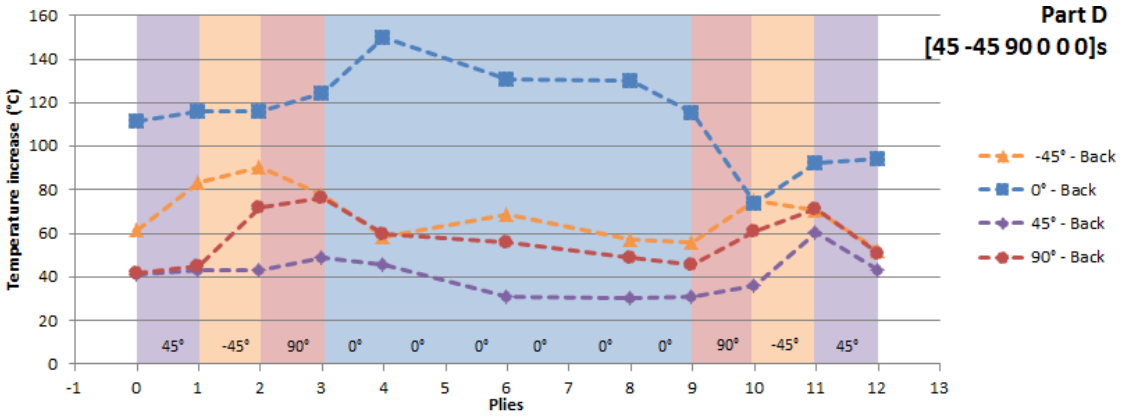

Figure 7.16: Part D back side

7.1.5. Discussion

When looking at the results presented in Figures 7.9 to 7.16, the lines are not always predictable and often a different shape can be found for the measurement done from the front side and from the back side. Therefore, it looks like there is a considerable error present. These errors can be the result of imprecise thermocouple or inductor placement, interaction of the carbon fibers with the unisolated measurement tips or due to the low measuring rate.

When looking at the temperature profiles for parts C and D in Figures 7.13 to 7.16, a trend can be seen that the temperature profile measured from the “front” side show a gradually decreasing temperature over the thickness while the temperature profiles from the “back” side show a more constant temperature profile across the thickness of the part for parts C and D. This can be explained by the edge effect. Parts A and B both have 13 thermocouples and the first and the last thermocouple are both located 50mm away from the edge. Parts C and D, however, have 11 thermocouples only and the first thermocouple is located 50mm away from the edge and the last is located 80mm away from the edge. It was noted that the center of the part heats up more under the same inductor settings than the edge does. An explanation for the difference in temperature profiles for part C and D, using the fact that the center heats up more than the edges, between the “front” measurement and the “back” measurement is illustrated in Figure 7.17.

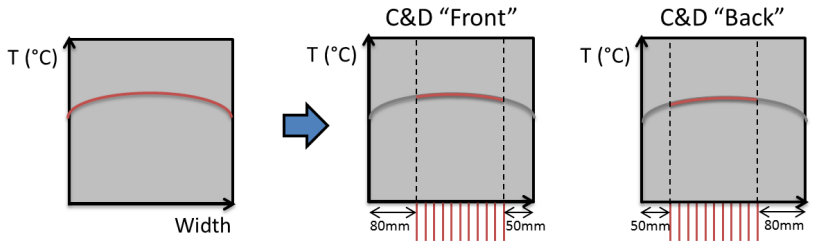

Figure 7.17: Explanation for difference between "front" and "back" profiles for part C and D

The hypothesis described above is confirmed by the data shown in Figure 7.18[2]. Here, a thermocouple was attached to the inductor for a constant position w.r.t. the inductor. The inductor was then moved from one edge to the other, making temperature measurements over the entire width. With this data, a second order polynomial was built which was used to normalize the data for part C which is shown in Figure 7.19.

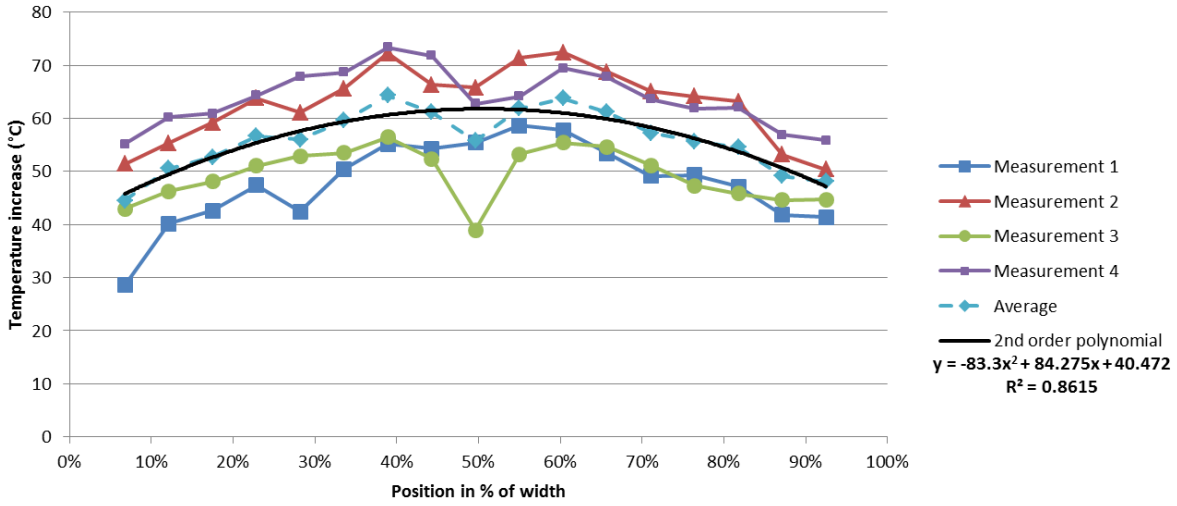

Figure 7.18: Temperature increase profile over width of test part C

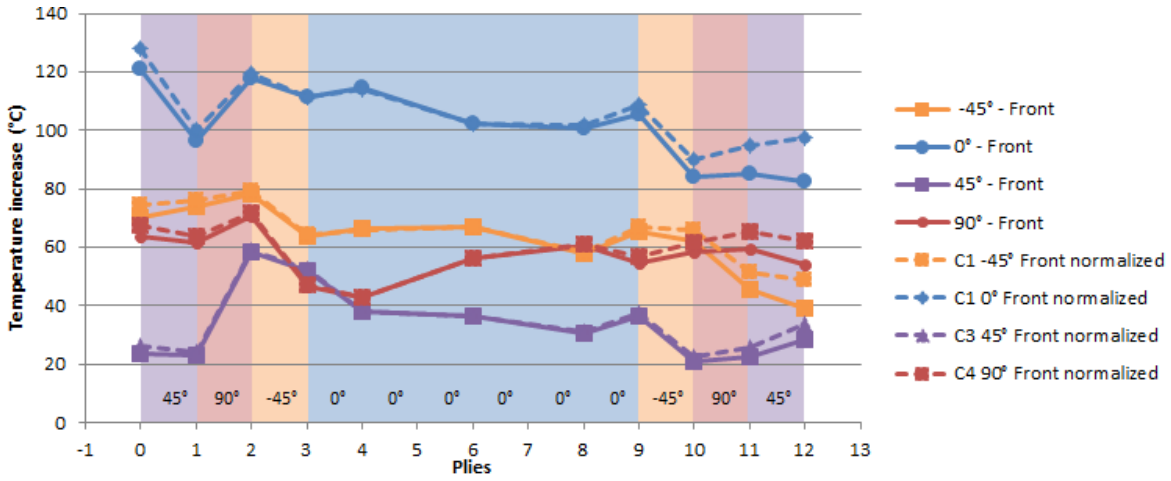

Figure 7.19: Part C normalized

[2]The temperature dip in the center of the plate is caused by four of the six 0° layers being cut in the middle. This was done in order to use material that would otherwise have been thrown away. The laminate used is the bottom laminate without thermocouples and therefore the effect of those cut layers was expected to be small.

As can be seen in Figure 7.19, the temperature profiles improve after normalization. For an inductor orientation of 90°, the temperature at the weld zone is now only 9.5°C cooler than the hottest temperature measured across the thickness. For the non-normalized data, this value was 17°C. However, since the temperature was measured at the surface, it can be the case that the temperature profile within the part differs from the temperature profile at the surface. Also, since the temperature measurements were done 2s after the inductor stopped heating and because the inductor is cooled, it can be the case that the differences in temperature across the width are actually bigger than were measured. This would lead to an even better temperature profile. This, however, has to be investigated further.

When looking at the measurements done, it can be seen that the most heat is generated when the inductor is oriented parallel to most fibers. Also, taking into account the errors, a general trend can be observed that the thermocouples measure a higher value around the plies in the same direction as the inductor. This would mean that the electricity is generated in the fibers parallel to the inductor. This also makes sense as, according to Lenz's law, the eddy currents induced create a magnetic field opposite to the one that generated them [28]. A model of this effect is given in Figure 7.20. In order for the eddy currents to flow, adjacent plies in different orientations are needed such that closed loops can be created.

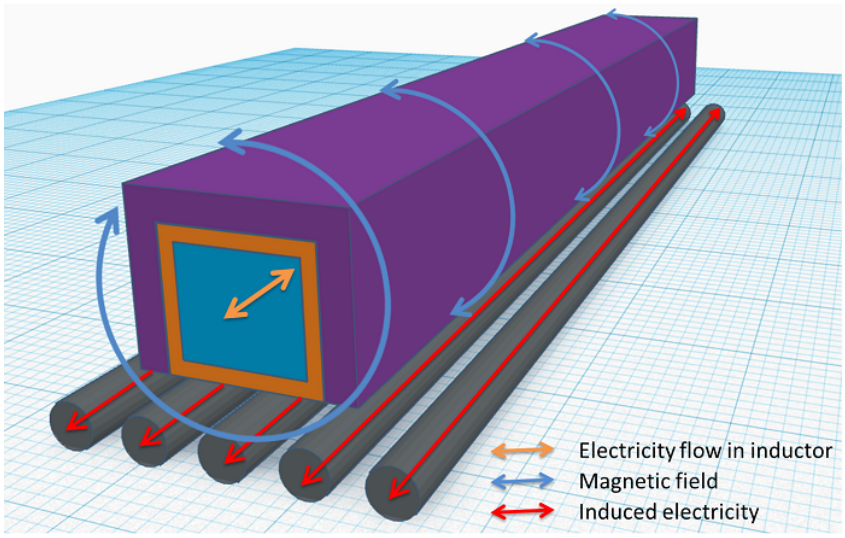

Figure 7.20: Electricity generation model

It was examined which laminate heats up the most in which direction. To this end, to make the data more easy to compare, the average temperature over the total thickness was calculated and is given in Table 7.1. Here, it can be seen that for every laminate, the most heat is generated when the inductor is placed at a 0° angle. This is probably the case because current is induced in the 0° layer for a 0° inductor angle. This induced current might then be conducted towards the interfaces such that the current can flow in a loop.

Table 7.1: Average temperature increase (in °C) for parts in different orientations

	A (°C)	B (°C)	C (°C)	D (°C)
-45°	54	52	46	60
0°	124	109	81	102
45°	61	64	25	40
90°	75	64	59	53

It is expected that the current generated in the 0° layers is either conducted towards the interface or can generate heat in the thick UD block in part C and D. This is expected because otherwise, there is no reason for part C and D to heat up more with an inductor orientation of 0°. Heat in the UD block could be generated by the electricity moving back and forth caused

by the alternating magnetic field leading to Joule losses as is shown in Figure 7.21a or to eddy current flowing in circles due to loop formation caused by material imperfections such as fiber waviness called undulations. The electricity can also be conducted towards the interface as is shown in Figure 7.21b because of the high fiber volume fraction and due to undulations which allows the fibers to touch.

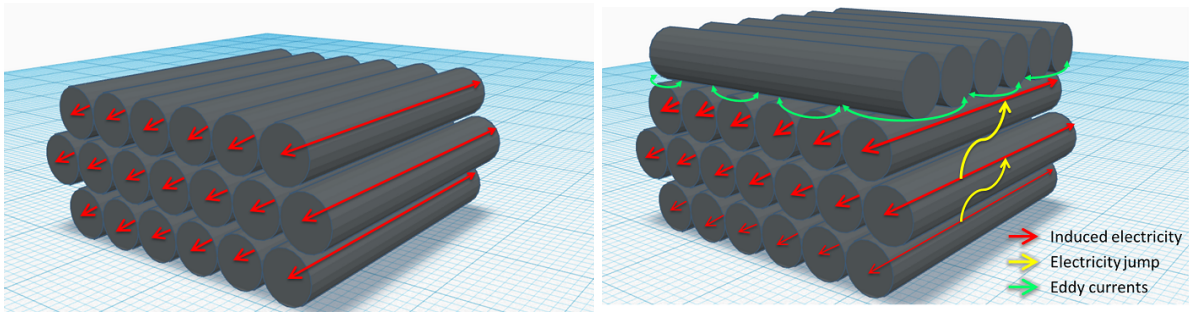

(a) Heating due to Joule losses only

(b) Electricity jumping towards interface

Figure 7.21: Heating mechanisms part C and D for a 0° inductor orientation

When looking at the average temperature increase for the different parts with an inductor orientation of 0°, it can be noted that part D gets hotter than part C, namely 102°C instead of 81°C. This can be caused by a better heating of a 0/90° interface in part D than a 0/-45° interface for part C. A similar observation can be done when comparing the average temperature increase for part A and B with a 0° inductor orientation. Here, part A gets warmer as the more efficient 0/90° interfaces are located closer to the core than for part B. When the interfaces that cause the highest temperature increase are located closer to the core, the cooling of the laminate is less effective and less heat is lost at the surface of the part due to conduction or radiation. Therefore, a part with better heat generation close to the core is likely to have a higher average temperature increase than a part with better heat generation close to the surface. This, however, does not mean that this results in a better temperature profile.

Using the observations that were done in the primary trials, hypotheses were generated that explain the temperature profiles measured. These hypotheses include:

1. Current is induced in the layers parallel to the inductor.
2. Part A and B heat more in the 0° direction than in the other directions because, when the current is induced in the layers parallel to the inductor, a maximum amount of interfaces can be found for the 0° inductor orientation between layers where electricity is induced and neighbouring layers that form loops for eddy currents to flow.
3. Part C and D heat more in the 0° direction than in the other directions because, with an inductor orientation of 0°, the most electricity is induced as half of the layers is parallel to the inductor compared to a sixth of the layers being parallel to the inductor for the other directions. This results in one or a combination of the following phenomena:
   (a) Electricity jumps between parallel fibers towards the interface with a differently oriented ply such that the electricity can flow in loops called eddy currents.
   (b) Joule losses caused by electrons moving back-and-forth heat a stack of UD material with the hairpin inductor used. This is further discussed in Section 10.4.
   (c) Undulations allows for closed loop formation in a stack of UD material such that eddy currents can flow. This is also further discussed in Section 10.4.
4. A 0/90° interface heats better than a 0/45° interface.
5. The measured temperature profiles are not accurate and should show a higher temperature close to the two surfaces because, for the thermocouples close to the surface, the distance to the edge of the part was insufficient in order to exclude edge effects.

As the observation that the parts heat up more with a 0° inductor orientation is in contrast with the results obtained in Chapter 6, this will be further investigated and explained in Chapter 10.

During the preliminary trials and the primary trials, the same voltage settings have been used. When looking at Table 7.1 and comparing these temperature increases to the temperature increases measured during the preliminary trials, it can be noted that the measured temperature increases in the primary trials are much higher than for the preliminary trials. Also this will be further explained in Chapter 10.

7.2. Effect of inductor voltage setting

Using part C of the test parts described in Section 7.1, the effect the voltage has on the temperature profile was investigated. This was done with an inductor orientation of 90° as this resulted in the best temperature profile because the electricity is generated in the layer below the surface, which results in good heat generation close to the weld zone. The measurement was done from the front side. The results of the test can be found in Figure 7.22.

It should be noted that the inductor was regulated via its voltage, not its power. As was already noted in Section 6.3.2, the reason for this is that the power is dependent on both the voltage and current ($P = U \cdot I$). The current is dependent on the impedance which varies for each workpiece. Therefore, for different workpieces, different voltages and currents set when the system is controlled via power. On top of that, it is possible that when regulating by power, the necessary current is not reached even at maximum voltage due to high system impedance. Voltage is the only independent variable and thus the best variable upon which the system can be controlled.

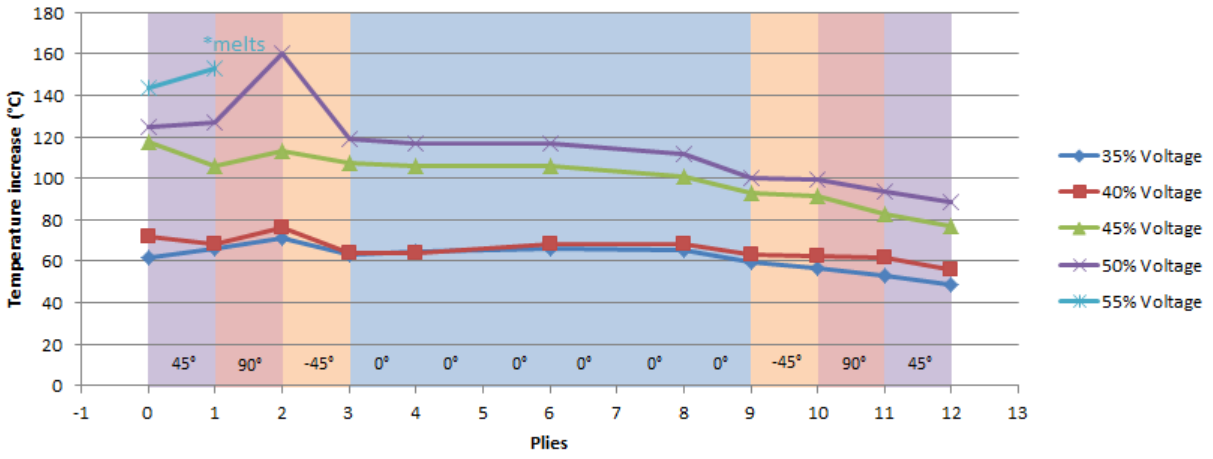

Figure 7.22: Voltage magnetic field - Part C 90° inductor orientation

As can be seen in Figure 7.22, no big change in the temperature profile can be seen with increasing voltage. There only seems to be a peak at the 50% Voltage measurement at ply 2. This, however, is suspected to be a faulty measurement which should be investigated further. It is assumed that increasing the voltage would result in a similar temperature profile during welding.

8

Optimizing temperature profile by using a CFRP susceptor

Because the ideal temperature profile for welding thermoplastic composites has the highest temperature at the weld interface, research is done into how to reach this optimal temperature profile without adding foreign materials like metal susceptors to limit their, often unpredictable, influence on the weld durability. Therefore, in this chapter it is investigated whether a susceptor can be made of carbon fiber which heats up better than the laminate does. In this chapter the preparations including manufacturing procedure are described in Section 8.1, followed by the preliminary test results in Section 8.2, the primary test results in Section 8.3 and a discussion in Section 8.4.

8.1. Preparation

As was explained in Section 3.1.2, carbon fiber heats well when the contact between the fibers is maximized. This can be done by decreasing the thread count, decreasing the titer and increasing the fiber volume content as was stated by Becker and Mitschang [12, 34]. Whether to use UD material or fabric material depends on the FVC used as was explained in Section 3.1.2. Therefore, using the materials available, it was decided to build both woven susceptors and thin-ply susceptors. These thin-ply susceptors are made of very fine UD material in different orientations and therefore should heat up well because they have a lot of crossing points due to which eddy currents can flow in loops. The preparation of the woven and thin-ply susceptor will be explained in Sections 8.1.1 and 8.1.2 respectively.

8.1.1. Fabric susceptors

Susceptor materials were build from dry fibers and PAEK foil. The dry fibers that were used were a 2x2 twill fabric with an areal weight of $200 g/m^2$ and a plain weave fabric with an areal weight of $400 g/m^2$. The PAEK foil had a thickness of $0.1 mm$. The theoretical fiber volume content was calculated with Equation (8.1).

$$FVC = \frac{v_f}{v_c} = \frac{m_f/\rho_f}{m_f/\rho_f + m_m/\rho_m} \tag{8.1}$$

By using available material it was decided to build two laminates with the $200 g/m^2$ fabric because a laminate built with layers of low areal weight should heat up better than a laminate built with layers of high areal weight. One of the laminates with $200 g/m^2$ areal weight was built with one PAEK foil and the other with two PAEK foils resulting in theoretical fiber volume

contents of 53% and 36% respectively. For the $400g/m^2$ fabric, two PAEK film were added resulting in a theoretical fiber volume content of 53%.

The susceptor materials were consolidated in the autoclave using a 5mm thick stainless steel pressure piece for a smooth finish on both sides. The resulting susceptor materials can be seen in Figures 8.1a to 8.1c.

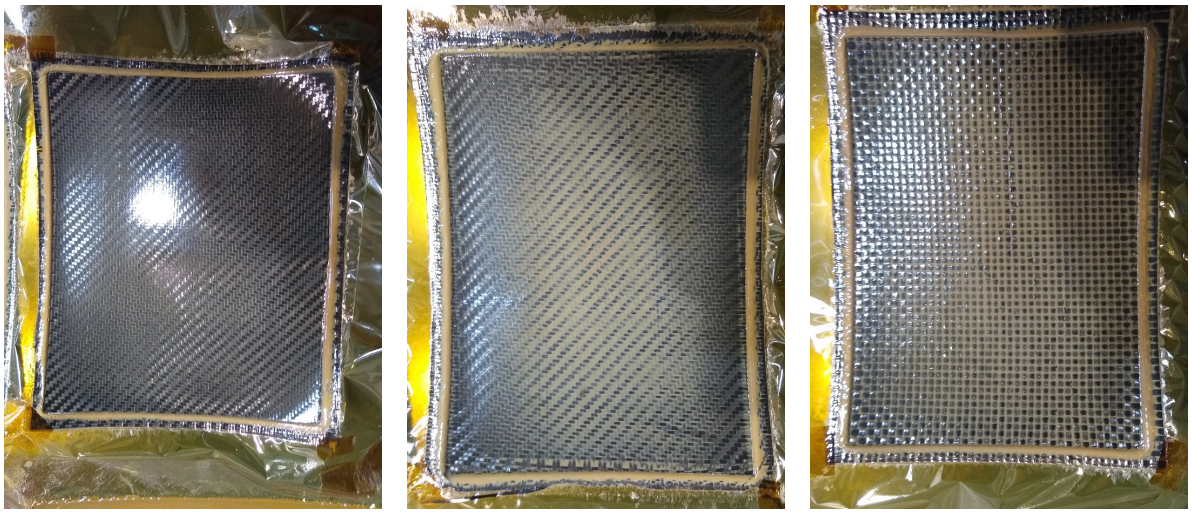

(a) $200g/m^2$ 2x2 twill weave with 1 PAEK foil (b) $200g/m^2$ 2x2 twill weave with 2 PAEK foils (c) $400g/m^2$ plain weave with 2 PAEK foils

Figure 8.1: CFRP susceptor materials

As can be seen in Figures 8.1a to 8.1c, some resin was squeezed out and an edge of excess resin can be found around where the pressure piece was located. This means that the resin content in the resulting composite is a bit lower than was calculated, resulting in a higher fiber volume content. The resulting thickness of the $200g/m^2$ 2x2 twill weave with 1 PAEK foil was 0.22mm. For the $200g/m^2$ 2x2 twill weave with 2 PAEK foils the thickness varied from 0.22mm on the edge to 0.33mm at the center. Finally, for the $400g/m^2$ plain weave with 2 PAEK foils the resulting thickness was 0.53mm.

The resulting fiber volume contents were calculated with Equation (8.2). In order to estimate the error in this measurement, the areas and the weight of the susceptors were measured multiple times. These measurements and the maximum error of the scale (=0.1g) was used to calculate the minimum, maximum and average fiber volume content of the susceptors. Taking the the biggest difference in percentage between the minimum and the average or the maximum and the average resulted in the maximum estimated error.

$$FVC = \frac{v_f}{v_c} = \frac{m_f/\rho_f}{m_f/\rho_f + m_m/\rho_m} = \frac{m_f/\rho_f}{m_f/\rho_f + (m_c - m_f)/\rho_m} \tag{8.2}$$

The theoretical and measured FVCs are given in Table 8.1[1]. Where:

Fabric 1	$200g/m^2$ dry fiber 2x2 twill weave with 1 PAEK foil	$\longrightarrow$	316 ± 5	g/m^2
Fabric 2	$200g/m^2$ dry fiber 2x2 twill weave with 2 PAEK foils	$\longrightarrow$	414 ± 53	g/m^2
Fabric 3	$400g/m^2$ dry fiber plain weave with 2 PAEK foils	$\longrightarrow$	631 ± 89	g/m^2

Notable is that susceptor with the lowest fiber volume content, which is shown in Figure 8.1b, has more matrix material in the center of the composite than near the edges. This can probably

[1]Void content is neglected.
[2]These percentages denote the maximum absolute deviation in FVC meaning that the actual FVC of susceptor 1 can range from 55.3% to 58.7%

Fabric	Theoretical FVC (%)	Measured FVC (%)	Estimated max. meas. error[2] (%)
1	52.9	57	± 1.7
2	36.0	42	± 1.9
3	52.9	57	± 1.3

Table 8.1: Fiber volume content of susceptor materials[1]

be attributed to the fact that the resin near the edge could more easily be squeezed out than the resin in the center. Another explanation could be that the pressure piece was not fully flat.

Because the laminates built consist of one layer of fabric only, the resulting susceptors were not flat as can be seen in Figure 8.2. In Figure 8.2 the susceptors have been turned around such that the face that touched the mould is now at the upper side. From the left to the right, the $200 g/m^2$ 2x2 twill weave with 1 PAEK foil is showed first, followed by the $200 g/m^2$ 2x2 twill weave with 2 PAEK foils in the middle and the $400 g/m^2$ plain weave with 2 PAEK foils at the right.

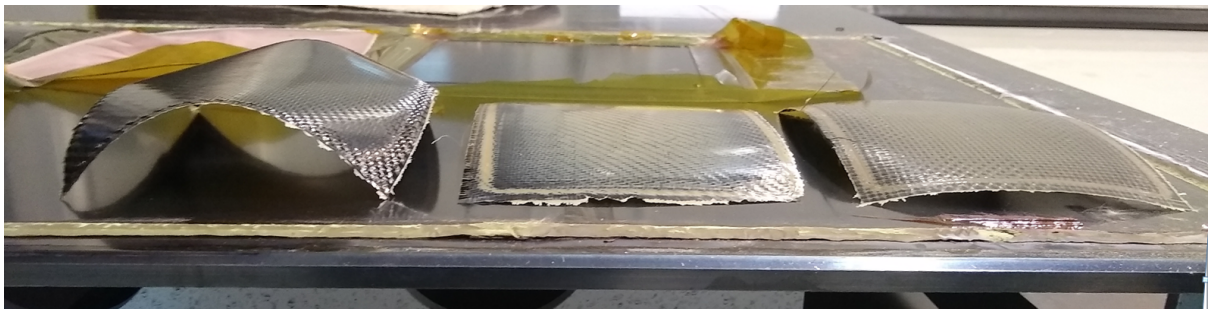

Figure 8.2: Overview curvatures of susceptor materials

After demoulding the susceptors, the edges were cut using a Stanley knife. Even though the susceptor were not perfectly flat, they can easily be flattened out between the test parts using a little pressure. The susceptors were made of PAEK foil with dry fibers because no fabric prepregs were available and only PAEK foil instead of PEKK foil was available. It is expected that using PAEK foil instead of PEKK foil does not have a big influence on the heating rate of the susceptor under induction. This is because the dielectric heating of the material is dependent on the product of the loss tangent ($tan\delta$) and the dielectric constant (ε_r) of the matrix material [39]. This data is given in Table 8.2 and as can be seen, the difference between the product of the values is relatively small.

Table 8.2: Product calculation of loss tangent and dielectric constant for PAEK and PEKK

	$tan\delta$ at 1MHz (-)	ε_r at 1 kHz (-)	$tan\delta \cdot \varepsilon_r$ (-)
PAEK [86]	0.004	3.12	0.0125
PEKK [87]	0.007	2.5	0.0175
PEEK [88]	0.004	3.1	0.0124

Using a susceptor with a different matrix material would have an influence on the weld strength because the matrix of the susceptor is not compatible with the matrix of the test part. This research, however, only investigates the heat generation below its melting point and therefore it is expected that there is little to no influence of the matrix material on the induction heating of the laminates. The same holds for the thin-ply susceptors made with a PEEK matrix that were tested next.

8.1.2. Thin-ply susceptors

The thin-ply susceptor was made of thin-ply PEEK UD tapes of 0.04mm thickness and 1 inch (=2.54cm) in width supplied by the Industrial Technology Centre of Fukui Prefecture (ITCF), Japan. The fibers are the T800SC fibers from Toray Industries Inc., Tokyo, Japan and have a fiber volume fraction of 60%. Because this thin-ply has a thickness of approximately $1/5^{th}$ of the thickness of the material used to build the test parts, it was decided to build a susceptor with five layers such that thickness is approximately the same as that of one ply. The fiber areal weight of one layer of thin-ply is approximately $40 g/m^2$ and therefore the fiber areal weight of the thin-ply susceptor is $200 g/m^2$.

For the thin-ply susceptor it was also investigated whether it is better to gradually change the angle between the plies or whether it is better to maximize the angle between the plies. Therefore, the layups shown in Figures 8.3a and 8.3b were built.

(a) Thin-ply susceptor 1 (b) Thin-ply susceptor 2

Figure 8.3: Thin-ply susceptor layups

It was chosen to put the fibers on the surface of the susceptor perpendicular to the fibers of (most of) the test pieces. This could theoretically further increase the heating rate as Eddy currents can also flow between the surface of the test piece and the surface of the susceptor.

The thin-ply layup process is depicted in Figure 8.4a and the consolidated thin-ply susceptors are shown in Figure 8.4b. For the preliminary tests, a 0/90° sample and a ±45° sample was cut from both the thin-ply susceptor 1 and 2.

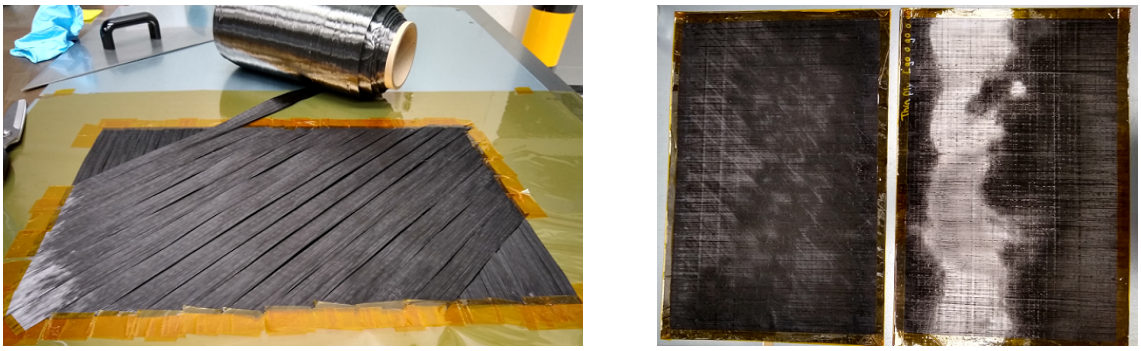

(a) Layup thin-ply (b) Consolidated thin-ply susceptors

Figure 8.4: Thin-ply susceptors

8.2. Preliminary test results

To see whether the susceptors have a positive effect on the temperature profile, the susceptors were put between two test pieces and the temperature profile was measured using an infrared camera. The susceptors were packed between the two common aerospace laminate test pieces at an angle of 90° to the inductor. Section 8.2.1 explains the test results obtained using the fabric susceptors and Section 8.2.2 explains the test results obtained using the thin-ply susceptors.

8.2.1. Fabric susceptors

The fabric susceptors, whose manufacturing procedure was explained in Section 8.1.1, were tested using the infrared camera from the side. Again, a sample size of five was used. The results can be found in Figure 8.5. The different susceptors were both tested at a 45° angle and a 90° angle. Figure 8.5 shows the 45° results and the 90° results can be found in Figure H.3 in Appendix H.

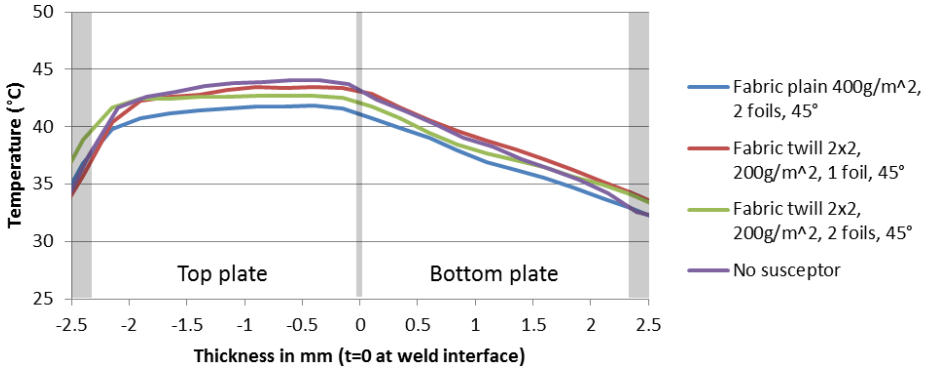

Figure 8.5: Comparison different fabric susceptors 45°

In Figure 8.5 it can be seen that the different susceptors build from fabric do not improve the temperature profile. In fact, the temperature profile without susceptor shows the best temperature profile of all.

8.2.2. Thin-ply susceptors

In the preliminary tests, use was made of the infrared camera to see whether the thin-ply (TP) susceptors increase the temperature at the weld interface. This was done by putting the thin-ply susceptor between two pieces of the common aerospace laminate. The aerospace laminate had an orientation of 90° w.r.t. the inductor and the thin-ply susceptors were tested at 90° and 45°. A sample size of 5 was used and the averages can be found in Figure 8.6. The non-averaged data can be found in Figures H.4 to H.8 in Appendix H. For the calculation of the average of TP 1 45° the outlier, depicted in dark blue in Figure H.5, had been removed from the data.

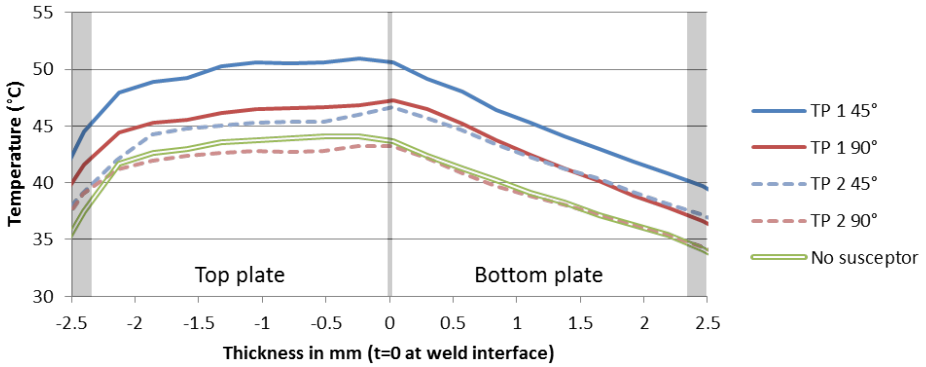

Figure 8.6: Comparison TP1, TP2 and no susceptor

As can be seen in Figure 8.6, all thin-ply susceptors cause a little jump in temperature at the weld interface. This means that the susceptors have the desired effect. In Figure 8.6, the overall temperature is less important than the jump in temperature that can be found at the interface. The global change in temperature is likely to be caused by not waiting long enough between the tests for the test part to cool down enough. The most prominent jump that can be seen is caused by thin-ply 2 in the 45° direction.

8.3. Primary test results

For the primary test results, the temperature increase of the last ply of the top plate was measured five times for each susceptor. The temperature increase of only the last ply was measured to reduce the amount of tests that needed to be performed and therefore allowing the test to be replicated to better know the distribution of the values. The results are shown in Figure 8.7. The error bars denote the 95% confidence interval. Part C was tested.

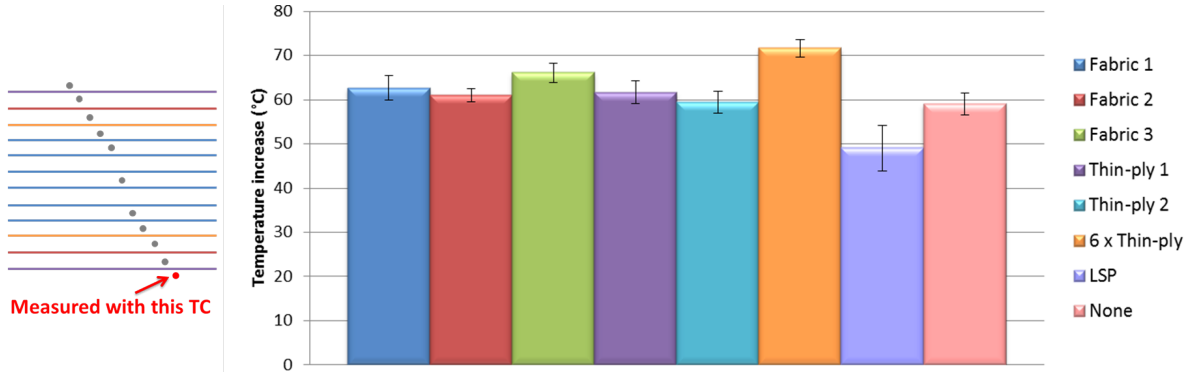

Figure 8.7: Comparison temperature increase of last ply for all susceptors

The last bar in Figure 8.7 named "None" is the temperature increase measured using no susceptor. As can be seen, all bars except for the LSP bar, show a larger temperature increase than without susceptor. This means that the susceptors have a positive influence on the temperature at the weld zone. In order to prove that the increase in temperature for the thin-ply susceptors is not due to inaccuracies in the measurement, six layers of thin-ply were stacked. This resulted in the highest temperature increase of all susceptors meaning that each individual layer indeed contributes to increasing the temperature at the weld interface.

Fabrics 1-3 also show an increase in temperature with a higher temperature increase for increasing fiber volume content (Fabric 1 > Fabric 2) and for increasing thickness or higher fiber weight (Fabric 3 > Fabric 1). It should be noted that all susceptors have a similar fiber areal weight as one layer of the UD material used to build the test parts (200 vs $194 g/m^2$). This excludes fabric 3 with a fiber areal weight of $400 g/m^2$.

The LSP resulted in a decrease in temperature measured at the weld zone. The reason for this is that the LSP reduces the magnetic field that is absorbed by the CFRP. Due to this, and due to the bad contact between the LSP and the TC in the last layer, a lower temperature increase is measured than without susceptor material. This is further explained in Chapter 9.

8.4. Discussion

For the fabric susceptors a noticeable difference was found between the preliminary tests and the primary tests. In contrast to the preliminary tests, in the primary tests the fabric susceptors did show an increased temperature at the weld interface. For the thin-ply susceptors on the other hand, an increase in weld zone temperature was measured in both the preliminary and the primary trials. This can be explained by the difference in thermal conductivity between fabrics and UD material. Joven [89] found that the thermal conductivity of laminates made of unidirectional material were more than twice as high as for laminates made of woven material. It should be noted that the UD laminate investigated by Joven [89] had layers in one direction only meaning that it had double the amount of fibers in the "fiber direction". However, taking this into account, still a better conductivity for UD plies was found than for fabrics. Therefore, heat is better conducted towards the edge for the thin-ply susceptors than for the fabric susceptors and therefore, during the preliminary trials, the thin-ply susceptors showed a temperature jump at the weld interface where the fabric susceptors did not. Further investigations should be performed to test this hypothesis.

9

Welding with LSP

To test how the temperature profile changes when lightning strike protection is added to the laminate, a separate mesh that is not consolidated with the test laminates is used. This way, the same test parts can be used without the need for producing extra test parts. The LSP used is the 3CU7-100FA from Dexmet Corporation, Wallingford, England.

9.1. Preliminary test results

In order to see what effect LSP has on the temperature profile, a piece of LSP was put underneath two stacked test parts. For these tests the common aerospace laminate was used under a 90° angle w.r.t. the inductor. The temperature profile was measured with the infrared camera from the side and the temperature measured at a line over the thickness is depicted in Figure 9.1 for which a sample size of five was used. In Figure 9.2, the temperature profile with LSP is improved using the susceptors TP1 45 and TP2 45 which are the thin-ply susceptors at a 45° angle of which their preparation and effects on temperature profile are explained in Sections 8.1.2 and 8.2.2 respectively.

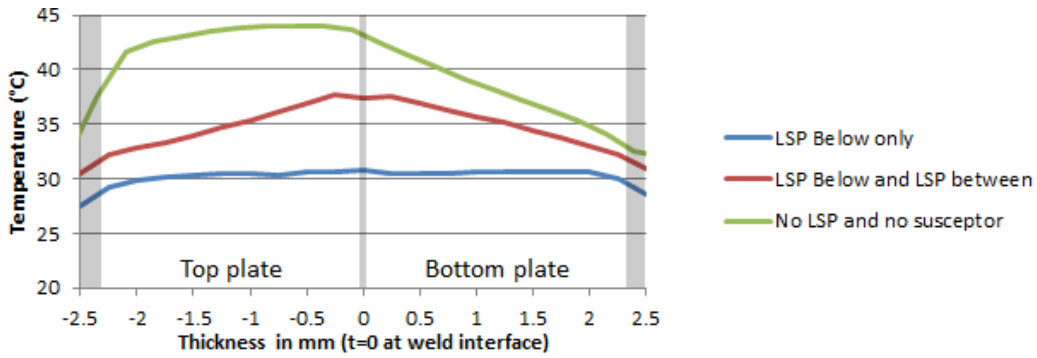

Figure 9.1: Comparison welding with LSP

What can be seen in Figure 9.1 is that the heat generated in the CFRP parts goes down when LSP is added. However, welding with LSP does not seem to be impossible because no big jump in temperature can be found at the location of the LSP. The LSP does heat up and decreases the temperature gradient in the second part which can be seen in Figure 8.6. However, it does not heat so much that the temperature at the LSP is the highest across the laminate thickness. Also, the heating of the LSP can be counteracted by actively cooling this surface. Finally, as can be seen in Figure 9.2, the temperature profile with LSP can be improved by stacking a few layers of thin-ply.

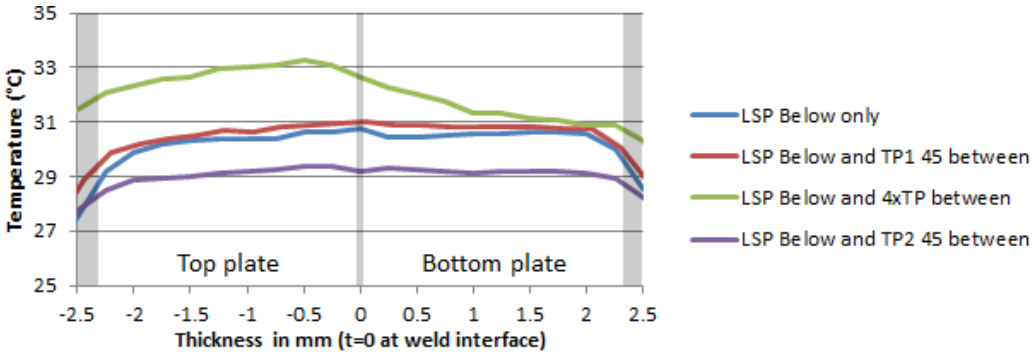

Figure 9.2: Comparison welding with LSP - different susceptors

9.2. Primary test results

During the primary tests, LSP was put below the to-be-welded parts. In Figure 9.3 the results are given for heating the two parts with the same inductor settings with and without LSP.

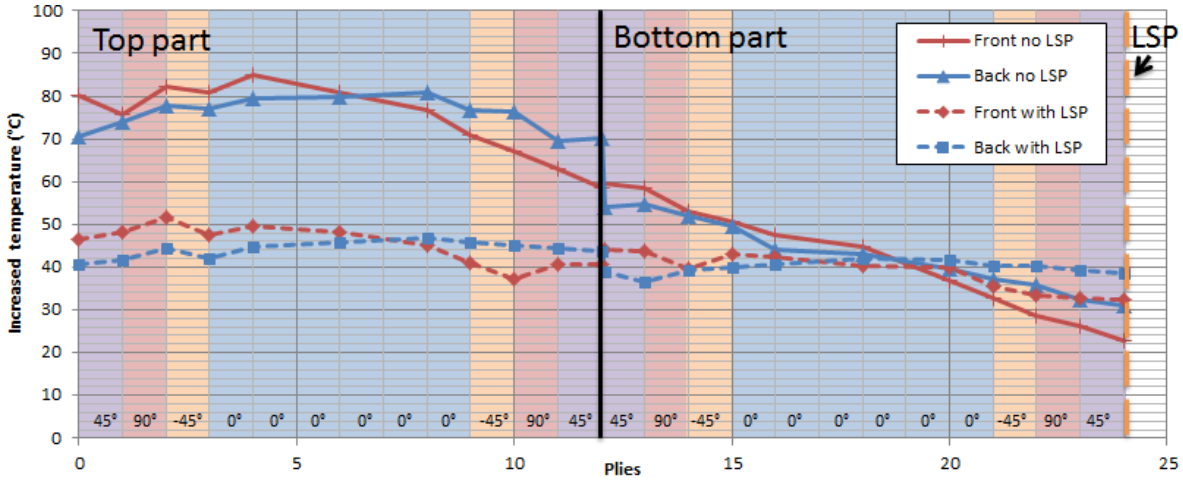

Figure 9.3: Heating with and without LSP

9.3. Discussion

In Figures 9.1 and 9.3 three things stand out. First of all, the temperature increase in the top part goes down when LSP is added. One explanation for this could be that the eddy currents generated within the LSP generate a magnetic field that opposes the magnetic field that created them [28]. This results in a weaker magnetic field throughout the parts and therefore in a lower temperature increase. Another explanation provided by COBES GmbH, Ettenheim, Germany, is that the magnetic field contains a certain amount of energy. Because the eddy currents can flow through copper LSP more easily than through the CFRP, the copper absorbs a lot of this energy and thus less energy is left to heat the CFRP.

The second thing that is noticed in Figures 9.1 and 9.3, is that no peak can be found at the last thermocouple adjacent to the LSP. This can be explained by poor contact between the LSP and the CFRP. Also, since the LSP conducts heat so well, the heat is quickly distributed over the LSP followed by a fast cooling down because of the high surface area of the LSP. Because the temperature is measured 2s after the inductor is switched off, it is possible that the LSP cools down faster than the laminate, resulting in a lower measured temperature.

The third thing standing out in Figures 9.1 and 9.3 is the decreased gradient in the bottom plate when LSP is added. This is due to heat conduction from the LSP into the laminate.

10

Validation

In this chapter the test methods used for the preliminary trials and the primary trials are validated. First, in Section 10.1, the difference found in the magnitude of the temperature increase between the preliminary trials and the primary trials is discussed and further investigations done to find its cause are explained. Then, in order to better understand edge heating and the influence it has on the temperature measured at the side of the laminate, edge heating is further examined in Section 10.2. Next, in Section 10.3, an explanation is discussed for the observation that during the preliminary trials the largest temperature increase was caused by a different inductor orientation than during the primary trials. Finally, tests performed on heating a UD laminate are described in Section 10.4.

10.1. Difference in temperature increase between preliminary trials and primary trials

Because the temperature increase measured during the primary trials were much higher than the temperature increases measured during the preliminary trials, the cause of this difference had to be investigated. To this end, the common aerospace laminate of the preliminary test parts was used to test whether the surface below the inductor becomes hotter when the inductor is placed at the center of the part. This is shown in Figure 10.1.

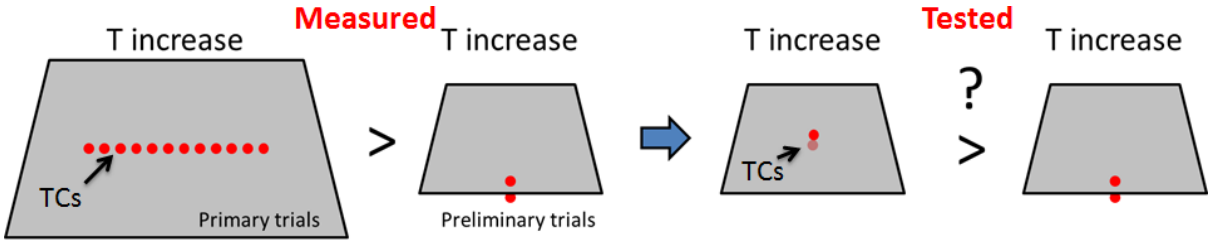

Figure 10.1: Explanation for test at edge versus test at center

The data for the increase in temperature at the edge were taken from the preliminary trials and extra tests were performed to gather data for the temperature increase at the center of part 6. The data can be found in Table 10.1 and shows that the TCs heat up more when the inductor is placed at the center of the part than on the edge. Also, a shift in the orientation resulting in the highest temperature increase takes place. This shift will be further explained in Section 10.2. TC1 is located below the inductor and TC2 is located below the part.

It can be concluded that the measured temperature increase is smaller when the inductor is placed at the edge compared to when the inductor is placed at the center. Investigation of

Table 10.1: Temperature increase center versus edge

	Edge		Center	
	TC1 (°C)	TC2 (°C)	TC1 (°C)	TC2 (°C)
-45	15	11	24	22
0	11	7	56	58
45	13	9	21	19
90	13	8	20	11

both scenarios, at the edge and at the center, is relevant as often parts need to be welded together which have both situations (e.g. skin and stringer).

10.2. Edge heating

An explanation was sought for why the thermocouples show that the part gets hotter when the inductor is placed over the center of the part compared to the edge. An explanation for this could be that the cutting of the plates resulted in delaminations close to the part edges. This hinders the formation of eddy currents due to poor fiber contact and therefore the the edges of the part heat up less than the center of the part does.

To further investigate what happens, the inductor was placed at the edge of part 6 and the infrared camera was used to measure the temperature over the inductor width as is shown in Figure 10.2.

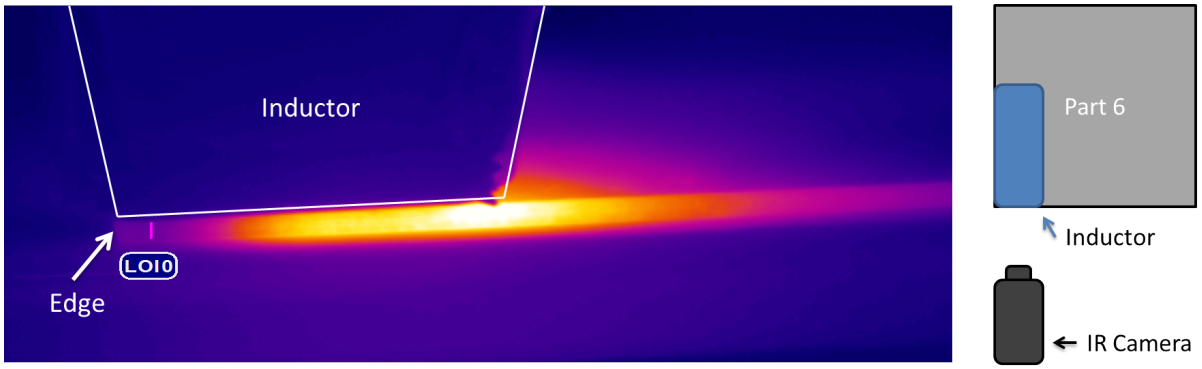

Figure 10.2: Edge heating from side

In Figure 10.2 an interesting fact could be discovered. Namely, the hottest point measured is not directly located underneath the inductor, but more towards the center of the part. All edges for part 6 were tested for both the 0/90° plate as for the ±45° plate. The edges that resulted in a comparable infrared picture are denoted with the same letters in Figure 10.3. The pictures corresponding to the letters shown in Figure 10.3 are shown in Figure 10.4.

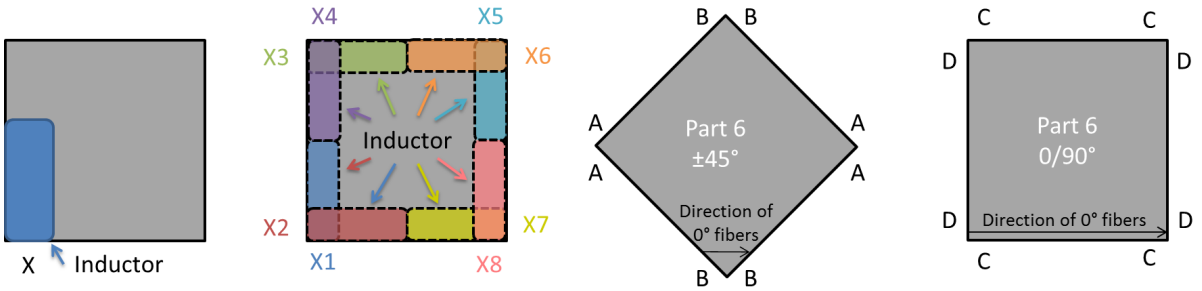

Figure 10.3: Edges that resulted in comparable infrared pictures

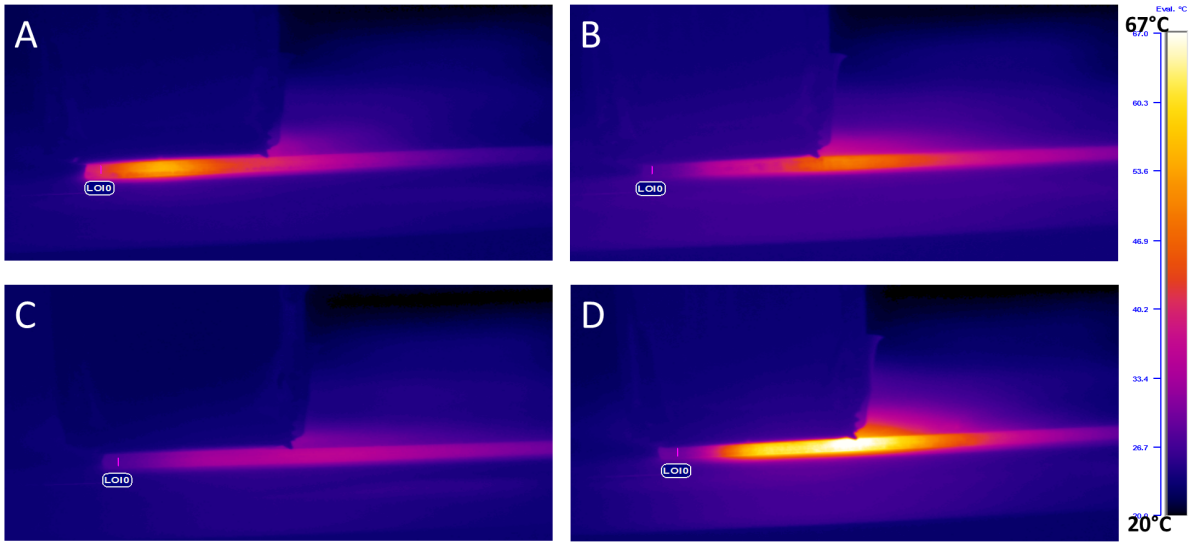

Figure 10.4: Infrared pictures per edge

An explanation for the different heating behaviour of the different corners of the laminate was sought in the fiber direction with respect to each corner. These directions w.r.t. the corners are shown in Figure 10.5. The non-symmetric layers in the corners result in a different heating when the inductor is placed at one edge than at the other edge. In corner A and B two layers are non-symmetric meaning that they have a different orientation w.r.t. the inductor when the inductor is turned 90° (parallel versus perpendicular). The asymmetric layers cancel each other out as there are two of them in corner A and B in the opposite direction. Here it is assumed that the position along the thickness of these layers can be neglected. In the corners named C and D, four layers are non-symmetric of which three are of the same kind. Therefore, this non-symmetry is not cancelled out and when the inductor is placed at one edge of the corner, a different temperature profile is created than for the other edge of the same corner.

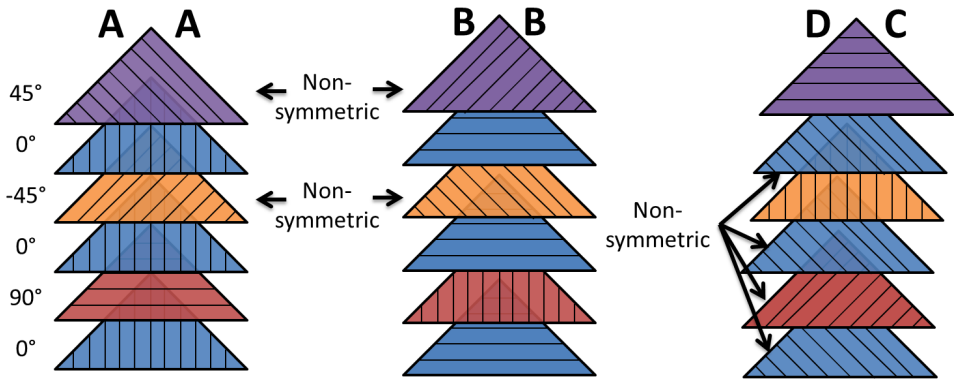

Figure 10.5: Layup w.r.t. corners in the common aerospace laminate (top half of laminate drawn)

When comparing the temperature profiles in Figure 10.4 with the layer direction w.r.t. the corners in Figure 10.5, some conclusions can be drawn. First of all, the edge of corner D gets hottest. In the preliminary trials it was initially concluded that this is caused by current that is induced in the fibers that run perpendicular to the length of the inductor, in this case the blue 0° layers. However, a better explanation for this is that current is not induced in the fibers perpendicular to the inductor, but in the fibers parallel to the inductor. The higher temperature measured in the preliminary trials at the corner with many fibers perpendicular to the edge, is caused by good heat conduction along the fibers [90] and thus towards the side where the temperature is measured. The thermal conductivity perpendicular to the fibers is

approximately four times the thermal conductivity perpendicular to the fibers as is calculated in Appendix I. Corner C seems to heat up the least because of the lack of fibers perpendicular to the edge. This does not mean that the temperature inside the part for configuration C is lower than for configuration D, however, the heat within the part is transported to the edge more efficiently at corner D than at corner C.

A second conclusion that can be made is that the hottest point at edge B is closer to the center of the part than for edge A. This can be explained by the great amount of fibers running towards the corner in corner A and much fewer fibers running towards the corner in corner B. Because the fibers run towards the corner for A, the generated heat is transported into the corner. For corner B this is not the case and much of the heat generated is transported away from the corner. Therefore, it looks like the heat is generated more towards the corner for A and more towards the center of the part for corner B. It is however more likely that this effect is caused by a more efficient heat transportation along the length of the fibers than perpendicular to the fibers.

10.3. Difference in orientation of inductor for highest temperature increase in the preliminary trials and the primary trials

It was noticed that the inductor orientation resulting in the highest temperature increase was different for the preliminary trials than for the primary trials. In the preliminary trials the highest temperature increase for the common aerospace laminate was reached with an inductor orientation of -45° and the lowest temperature increase with an inductor orientation of 0°. This is in contrast to the highest temperature increase measured for the common aerospace laminate during the primary tests for an inductor orientation of 0° and the lowest temperature increase for an inductor orientation of -45°.

Fibers need a certain length before eddy currents start to flow. Therefore, at the edge little to no heat is generated as is supported by the findings in Section 10.1. With the infrared camera the temperature at the edge was measured, meaning that most of the measured temperature increase is a result of heat conducted from a point within the part where the fibers are long enough for eddy currents to flow. The more efficient the heat can be conducted towards the edge, the higher the temperature increase at the edge will be. Because heat is conducted far better along the length of the fibers than perpendicular to the fibers [90], as is also calculated in Appendix I, the heat is best conducted towards the edge when there are as many fibers perpendicular to the edge as possible. This is why the temperature increase measured at the side is the highest for the case when as many fibers are perpendicular to the edge as possible. The highest temperature increase at the center can be measured for the 0° inductor orientation because electricity is induced in the fibers parallel to the inductor and, contrary to heating at the edge, no problems with electricity flow due to cut fibers arise at the center.

To exclude the possibility that the difference is caused by the thermocouple orientation w.r.t. the inductor, tests have been performed that measure the temperature below the inductor at the center of the plate with the thermocouple oriented perpendicular and parallel to the inductor. No evident difference in heating behavior of the two configurations could be found.

10.4. UD heating

The temperature increase with different voltage settings was measured for a uni-directional laminate. The test-setup used is shown in Figure 10.6. The UD laminate that was used is a 21mm thick thermoset based laminate having a glass fiber layer at the side. In Figure 10.7a the temperature increase for the UD laminate is plotted for different voltage settings and in Figure 10.7b this temperature increase compared to the temperature increase measured for part 6, the common aerospace laminate with layup (45 0 -45 0 90 0)s, is shown.

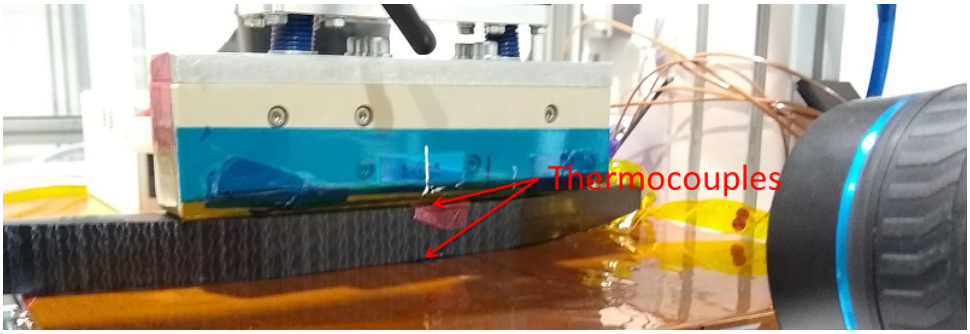

Figure 10.6: UD test-setup

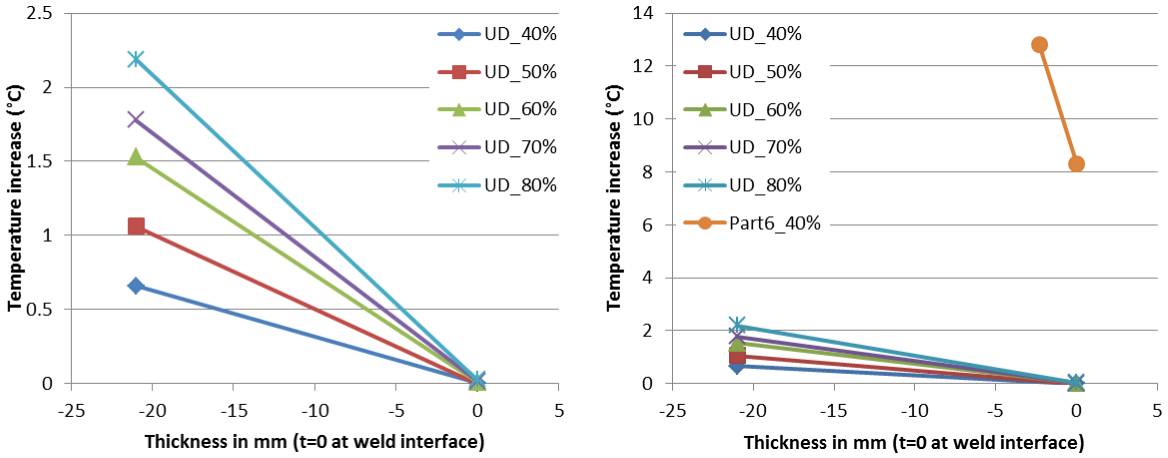

(a) T_{incr} UD laminate

(b) T_{incr} UD lam. vs part 6

Figure 10.7: UD heating for different voltage settings compared to heating of common aerospace laminate

As can be seen in Figure 10.7b, the UD laminate heats up much less than the common aerospace laminate. Even when the voltage is doubled compared to that of the common aerospace laminate, the UD laminate heats up very little. Therefore it is concluded that part C and D do not heat up due to Joule losses in the UD block at the core of the laminate as was shown in Figure 7.21a. Also, as the UD laminate hardly heated up, undulations in the laminate tested did not allow for large-scale closed loop formation such that eddy currents flow and therefore generate heat.

11

Conclusions

The aim of this thesis was to find how induction heating can be used to selectively heat the weld zone of multidirectional carbon fiber laminates with and without using a carbon fiber susceptor material. To this end, three sub-questions were investigated.

First of all, it was investigated whether specific plies in multidirectional CFRP laminates could be heated by manipulation of the magnetic field. It was concluded that the orientation of the magnetic field has a big influence on the heating of the laminate and that this orientation can be used to heat plies with fibers parallel to the hairpin inductor. Required for this are differently oriented adjacent plies which allow eddy currents to flow. Adjacent plies with a difference in orientation of 90° heat up better than adjacent plies with a difference in orientation of 45°. The average temperature increase was shown to differ, up to a factor two for some laminates, when a different orientation of magnetic field was used. No prominent change in the temperature profile could be discovered by increasing the power, with the exception of a larger temperature increase for increasing power.

Second of all, research was done into whether carbon fiber material can be used as susceptor material in order to increase the temperature at the weld interface. To this end, different susceptors were made of fabrics and thin-plies. In the primary tests, all of them resulted in a higher temperature increase at the weld interface than when no susceptor was used. It was concluded that susceptors made of carbon fiber can be used to improve the temperature profile, but more research is needed to optimize the susceptors and to test what thickness is required for considerable improvement of the temperature profile.

Finally, tests were performed to give an outlook on whether it is possible to inductively weld parts with lightning strike protection. The results showed a total decrease in heating of the laminates. At the side of the LSP no peak temperature was measured. However, this is likely to be caused by the poor contact between the LSP and the laminate in which the thermocouple is consolidated.

12

Recommendations

This research showed potential in increasing the temperature at the weld zone relative to the rest of the laminate by using the magnetic field orientation to target plies close to the weld zone or by using a susceptor made of carbon fiber. To further develop these techniques, more research has to be performed. The main recommendations are listed in this chapter.

- During this thesis the test parts were heated to below their melting temperature only. It still needs to be investigated whether the heat profiles found can be extrapolated to above the melting temperature of the matrix.
- The tests that were performed with lightning strike protection were done without the lightning strike protection being consolidated into the laminate. This is likely to have a major effect on the temperature measured at the lightning strike protection due to bad heat conductance into the laminate. It is recommended to perform the tests again with lightning strike protection consolidated into the part.
- When placing the inductor at the edge of the the part, the surface below got less hot than when the inductor was placed at the center of the part. Since the reason why this happens is not yet fully understood, more research has to be done in order to be able to predict it. Also the effect this has on common welding configurations such as a skin/stringer combination can be more extensively researched.
- In the primary tests it was found that for parts C and D, which have six adjacent zero degree layers which theoretically do not heat because no closed loop are available for eddy currents to flow, showed that the temperature at the core of the laminate was often higher than the temperature near the surface. This is likely due to the fact that the thermocouples close to the surface were located close to the edge in the test part. It was found that when putting the inductor close to the edge, the part below heats up much less than when the inductor is put at the center of the part. Therefore, it is likely that when the thermocouples close to the surface were located farther away from the edge, the temperature readings would be much higher resulting in temperature profiles with a high temperature close to the two surfaces and a lower temperature at the core for parts C and D. This was also supported by the asymmetry in the thermocouples in parts C and D resulting in a more decreasing temperature gradient when measuring from the “front” side than when measuring from the “back” side. It is therefore recommended to build new laminates which are larger such that the edge effect becomes smaller or to distribute the thermocouples through the laminate differently such that its effect can be estimated.
- There seems to be an error in the temperature readings of some thermocouples. These can be the consequence of a failure in the thermocouple, a mistake or inaccuracy in placement of the thermocouple, an error induced on the readings due to contact with the

carbon fibers at the measuring tip or something else. The reason for this error needs to be further investigated such that more precise measurements of the temperature profile across the thickness can be done.

- Currently the program only measures the temperature 15 times over a measuring time of 7s. As this is much less than the hardware is capable of, the program in LabVIEW must be written poorly. It is therefore recommended to write a program that can gather more data during the measuring time in order to get more accurate results and to be able to better see the noise.
- Interesting could be to measure the temperature for multiple seconds after the inductor is switched off. This way, it can be investigated how the heat dissipates across the laminate thickness.
- Laminates were built with one thickness only such that they could be compared easily. To see whether the findings are also valid for different part thicknesses, these have to be tested too.
- Different frequencies result in a different penetration depth in the laminate. This can be used to create a homogeneous heating across the laminate thickness such that the top laminate will not melt before the weld interface does, or to reach such a penetration depth that the lightning strike protection hardly heats up.
- The technique used in this thesis is a non-continuous process which can be used for some aircraft parts such as clips. In order to perform long welds on aircraft parts, research has to be done into how to make this process continuous or sequential.
- Research into advanced surface cooling could enhance the current process. When more energy can be extracted from the top laminate, a better temperature profile will be created such that the temperature at the weld zone will be higher than anywhere else along the thickness of the to-be-welded parts.

Bibliography

[1] Martin Gagné and Daniel Therriault. Lightning strike protection of composites. *Progress in Aerospace Sciences*, 64:1 – 16, 2014.

[2] Thomas Forstner, Christoph Sommitsch, and Fabian Fischer. Induktionsschweißen von carbonfaserverstärktem polyamid 66 im automobilen karosseriebau. *Zeitschrift Kunststofftechnik*, 14(4):233–278, 6 2018.

[3] Oliver Schieler. *Auswahl einer Fügetechnologie für faserverstärkte Thermoplaste im Helikopterbau*. doctoralthesis, Technische Universität Kaiserslautern, 2015.

[4] C. Ageorges, L. Ye, and M. Hou. Advances in fusion bonding techniques for joining thermoplastic matrix composites: a review. *Composites Part A: Applied Science and Manufacturing*, 32(6):839 – 857, 2001.

[5] Patrice Gouin O'Shaughnessey, Martine Dubé, and Irene Villegas. Modeling and experimental investigation of induction welding of thermoplastic composites and comparison with other welding processes. *Journal of Composite Materials*, 50, 01 2016.

[6] Irene Villegas. Process and performance evaluation of ultrasonic, induction and resistance welding of advanced thermoplastic composites. *J. Thermoplast. Compos.*, 26:1007–1024, 01 2012.

[7] Arnt R. Offringa. Thermoplastic composites—rapid processing applications. *Composites Part A: Applied Science and Manufacturing*, 27(4):329 – 336, 1996. 4th International Conference on Automated Composites.

[8] Francesca Lionetto, Silvio Pappadà, Giuseppe Buccoliero, and Alfonso Maffezzoli. Finite element modeling of continuous induction welding of thermoplastic matrix composites. *Materials & Design*, 120:212 – 221, 2017.

[9] Anahi Pereira da Costa, Edson Cocchieri Botelho, Michelle Leali Costa, Nilson Eiji Narita, and JosÃ© Ricardo Tarpani. A Review of Welding Technologies for Thermoplastic Composites in Aerospace Applications. *Journal of Aerospace Technology and Management*, 4: 255 – 265, 09 2012.

[10] R Vodicka. Thermoplastics for airframe applications: a review of the properties and repair methods for thermoplastic composites. *DSTO Aeronautical and Maritime Research Laboratory*, 10 1996.

[11] Hexply 8552® expoxy matrix (180°C /356°F curing matrix). Internet. Accessed on 02-04-2019 at: https://www.hexcel.com/Resources/DataSheets/Prepreg?lC=Epoxy.

[12] Stephan Becker and Peter Mitschang. Influences of laminate parameters on the induction heating behavior of cfrpc. In *ECCM18 - 18th European Conference on Composite Materials*, 08 2018.

[13] Tian Zhao, Charlotte Broek, Genevieve Palardy, Irene Villegas, and R Benedictus. Towards robust sequential ultrasonic spot welding of thermoplastic composites: Welding process control strategy for consistent weld quality. *Composites Part A: Applied Science and Manufacturing*, 109, 03 2018.

[14] Keita Goto, Kenta Imai, Masahiro Arai, and Takashi Ishikawa. Shear and tensile joint strengths of carbon fiber-reinforced thermoplastics using ultrasonic welding. *Composites Part A: Applied Science and Manufacturing*, 116:126 – 137, 2019.

[15] Ginger Gardiner. Peek vs. pekk vs. paek and continuous compression molding. *CompositesWorld*, July 2018.

[16] Debdatta Ratna. *Handbook of thermoset resins*. ISmithers Shawbury, UK, 2009.

[17] C.C.M. Ma, N.H. Tai, S.H. Wu, S.H. Lin, J.F. Wu, and J.M. Lin. Creep behavior of carbon-fiber-reinforced polyetheretherketone (peek) [±45]4s laminated composites (i). *Composites Part B: Engineering*, 28(4):407 – 417, 1997.

[18] Zachary August, G Ostrander, J Michasiow, and David Hauber. Recent developments in automated fiber placement of thermoplastic composites. *SAMPE J*, 50:30–37, 03 2014.

[19] Yoshitomo Furushima, Christoph Schick, and Akihiko Toda. Crystallization, recrystallization, and melting of polymer crystals on heating and cooling examined with fast scanning calorimetry. *Polymer Crystallization*, page e10005, 08 2018.

[20] R Velthuis. Induction welding technology - joining fiber reinforced thermoplastic polymer (composites) for aerospace applications. In *54th International Astronautical Congress of the International Astronautical Federation*, 09 2003.

[21] Oliver Schieler, Uwe Beier, and Peter Mitschang. Control of the through-thickness temperature distribution in carbon composite aerospace parts during induction welding. *Journal of Thermoplastic Composite Materials*, 11 2017.

[22] Lars Moser. *Experimental Analysis and Modeling of Susceptorless Induction Welding of High Performance Thermoplastic Polymer Composites*. doctoralthesis, Technische Universität Kaiserslautern, 2012.

[23] T.J. Ahmed, D Stavrov, Harald Bersee, and Adriaan Beukers. Induction welding of thermoplastic composites - an overview. *Composites Part A: Applied Science and Manufacturing*, 37:1638–1651, 10 2006.

[24] Reiner Rudolf. *Entwicklung einer neuartigen Prozess- und Anlagentechnik zum wirtschaftlichen Fugen von thermoplastischen Faser-Kunststoff-Verbunden*. doctoralthesis, Technische Universität Kaiserslautern, 2000.

[25] Silvio Pappadà, Andrea Salomi, Jeanette Montanaro, Alessandra Passaro, Antonio Caruso, and Alfonso Maffezzoli. Fabrication of a thermoplastic matrix composite stiffened panel by induction welding. *Aerospace Science and Technology*, 43:314 – 320, 2015.

[26] D. Stavrov and H.E.N. Bersee. Resistance welding of thermoplastic composites-an overview. *Composites Part A: Applied Science and Manufacturing*, 36(1):39 – 54, 2005.

[27] M. Dubé, P. Hubert, A. Yousefpour, and J. Denault. Fatigue failure characterisation of resistance-welded thermoplastic composites skin/stringer joints. *International Journal of Fatigue*, 31(4):719 – 725, 2009.

[28] Raymond L. Cook Valery Rudnev, Don Loveless. *Handbook of Induction Heating: Theoretical Background*, chapter 3, pages 51–138. CRC Press, 2017.

[29] Reiner Rudolf, P Mitschang, and M Neitzel. Induction heating of continuous carbon-fibre-reinforced thermoplastics. *Composites Part A-applied Science and Manufacturing - COMPOS PART A-APPL SCI MANUF*, 31:1191–1202, 11 2000.

[30] Stephan Becker, D Maurer, Miro Duhovic, and P Mitschang. Quality-controlled continuous induction welding of cfrp composites. *JEC Composites Magazine*, 52:40–43, 01 2015.

[31] P. Mitschang, M. Hümbert, and L. Moser. Susceptorless continuous induction welding of carbon fiber reinforced thermoplastics. *ICCM-Proceedings*, 2013.

[32] Martina Hümbert and Peter Mitschang. Characterization and modification of the temperature distribution during continuous induction welding. In *ECCM16 - 16th European Conference on Composite Materials*, 06 2014.

[33] Thomas Bayerl, Miro Duhovic, Peter Mitschang, and Debes Bhattacharyya. The heating of polymer composites by electromagnetic induction – a review. *Composites Part A: Applied Science and Manufacturing*, 57:27 – 40, 2014.

[34] Stephan Becker and Peter Mitschang. Influences of textile parameters on the induction heating behavior of CFRPC. In *21st International Conference on Composite Materials*, 08 2017.

[35] M. Duhovic, P. Mitschang, and M. Maier. Advances in simulating the processing of composite materials by electromagnetic induction. *9th European LS-DYNA Conference*, 2013.

[36] Cobes. Linearinkuktor, linear, 1-wdg, l=170mmm, June 2013. Zeichnungsnummer: 366 0002.

[37] Miro Duhovic, P L'Eplattenier, I Caldichoury, P Mitschang, and M Maier. Advanced 3d finite element simulation of thermoplastic carbon fiber composite induction welding. *16th European Conference on Composite Materials, ECCM 2014*, 01 2014.

[38] S Yarlagadda, Hee joong Kim, John Gillespie Jr, NB Shevchenko, and BK Fink. A study on the induction heating of conductive fiber reinforced composites. *Journal of Composite Materials*, 36:401–421, 01 2002.

[39] S. Becker and P. Mitschang. Influencing the induction heating of textilereinforced cfrp by laminate parameters [beeinflussung der induktionserwärmung von textilverstärktem cfk durch laminatparameter]. *Zeitschrift Kunststofftechnik/Journal of Plastics Technology*, 2019(3):210–244, 2019. cited By 0.

[40] John Jackowski, Robert Goldstein, and Valentin Nemkov. Induction process and coil design for welding of carbon fiber reinforced thermoplastics. *International SAMPE Technical Conference*, 01 2014.

[41] F. Ohlsson. 8 - weight reduction by optimized reinforcement structures. In J. Njuguna, editor, *Lightweight Composite Structures in Transport*, pages 191 – 215. Woodhead Publishing, 2016. ISBN 978-1-78242-325-6.

[42] C.M. Worrall and R.J. Wise. Novel induction heating technique for joining of carbon fibre composites. *16th European Conference on Composite Materials, ECCM 2014*, 01 2014.

[43] Bruce K. Fink, Roy L. McCullough, and John W. Gillespie Jr. A local theory of heating in cross-ply carbon fiber thermoplastic composites by magnetic induction. *Polymer Engineering & Science*, 32(5):357–369, 1992.

[44] M Hagenbeek, J Vilà Bramon, and Irene Villegas. Controlling the edge effect using a bypass conductor for induction welding of carbon fibre thermoplastic composites. In *In Proceedings of the 18th European Conference on Composite Materials*, 06 2018.

[45] Jon S. Wilson. *Sensor technology handbook*. Elsevier, 2005. ISBN 0-7506-7729-5.

[46] João Crisóstomo and Rui Pitarma. *The Importance of Emissivity on Monitoring and Conservation of Wooden Structures Using Infrared Thermography*, pages 1–16. 01 2019. ISBN 978-953-51-8286-3.

[47] *Data Acquisition and Signal Conditioning Course Manual*. National Instruments Corporation, april 2008 edition. Course Software Version 8.5, Part Number 320733M-01.

[48] Omega. Thermocouple sensors - what is a thermocouple? Internet, August 2018. Accessed on 27-05-2019 at: https://www.omega.com/en-us/resources/thermocouples.

[49] Omega. Unisolierte feindraht-thermoelemente aus wolfram/rhenium, platin/rhodium und standardlegierungen. Internet. Accessed on 04-06-2019 at: https://www.omega.de/temperature/pdf/IRCO_CHAL_P13R_P10R.pdf.

[50] H.M. Hashemian. *Sensor Performance and Reliability*. ISA, 2005. ISBN 978-1-55617-897-9.

[51] A. Smalcerz and R. Przylucki. Impact of electromagnetic field upon temperature measurement of induction heated charges. *International Journal of Thermophysics*, 34(4): 667–679, Apr 2013.

[52] Jacob Fraden. *Handbook of Modern Sensors*. Springer, fifth edition edition, 2015.

[53] OMEGA Engineering GmbH. Temperature measurement in electromagnetic environments. Internet, September 2018. Accessed on 09-12-2019 at: https://www.omega.com/en-us/resources/temperature-measurement-in-electromagnetic-environments.

[54] Jon S. Wilson. *Sensor Technology Handbook*. Elsevier, 2005. ISBN 978-0-7506-7729-5.

[55] C. Franco, J. Acero, R. Alonso, C. Sagues, and D. Paesa. Inductive sensor for temperature measurement in induction heating applications. *IEEE Sensors Journal*, 12(5):996–1003, May 2012.

[56] Rouhollah Dermanaki Farahani and Martine Dubé. Novel heating elements for induction welding of carbon fiber/polyphenylene sulfide thermoplastic composites. *Advanced Engineering Materials*, 19(11):1700294, 2017.

[57] Muhammad Muddassir. *Development of nano/micro hybrid susceptor sheet for induction heating applications*. PhD thesis, Technischen Universität Kaiserslautern, 2016.

[58] E Rodriguez-Senín and Irene Villegas. Effect of mesh configuration on the induction welding process of thermoplastic composites. *16th European Conference on Composite Materials, ECCM 2014*, 01 2014.

[59] S Yarlagadda, Bruce K. Fink, and John Gillespie Jr. Design of a resistive susceptor for uniform heating during induction bonding of composites. *Journal of Thermoplastic Composite Materials*, 11:321–337, 07 1998.

[60] Martine Dubé, Pascal Hubert, Jan N.A.H. Gallet, Darko Stavrov, Harald E.N. Bersee, and Ali Yousefpour. Fatigue performance characterisation of resistance-welded thermoplastic composites. *Composites Science and Technology*, 68(7):1759 – 1765, 2008.

[61] Thomas Bayerl, Ralf Schledjewski, and Peter Mitschang. Induction heating of thermoplastic materials by particulate heating promoters. *Polymers and Polymer Composites*, 20:333–342, 05 2012.

[62] Kenneth B. Tamayo. *Magnetic properties of solids*. Materials Science and Technologies. Nova Science Publishers, Incorporated, 2009.

[63] CARBON.EE. Carbon fiber- all patterns explained. Internet, April 2015. Accessed on 10-04-2019 at: https://www.carbon.ee/en/n/carbon-fiber-all-patterns-explained.

[64] Hexcel. Woven reinforcements. Internet. Accessed on 11-04-2019 at: https://www.hexcel.com/Resources/DataSheets/Reinforcements/Woven-Reinforcements.

[65] R. Amacher, J. Cugnoni, J. Botsis, L. Sorensen, W. Smith, and C. Dransfeld. Thin ply composites: Experimental characterization and modeling of size-effects. *Composites Science and Technology*, 101:121 – 132, 2014.

[66] B. Hannemann, S. Backe, S. Schmeer, F. Balle, and U.P. Breuer. Metal fiber incorporation in carbon fiber reinforced polymers (cfrp) for improved electrical conductivity [steigerung der elektrischen leitfähigkeit von kohlenstofffaserverstärkten kunststoffen (cfk) durch integration von metallfasern]. *Materialwissenschaft und Werkstofftechnik*, 47(11):1015–1023, 2016.

[67] Andrzej Katunin, Katarzyna Krukiewicz, Roman Turczyn, Przemysław Sul, Andrzej Łasica, and Marcin Bilewicz. Synthesis and characterization of the electrically conductive polymeric composite for lightning strike protection of aircraft structures. *Composite Structures*, 159:773 – 783, 2017.

[68] Johannes Rehbein, Peter Wierach, Thomas Gries, and Martin Wiedemann. Improved electrical conductivity of ncf-reinforced cfrp for higher damage resistance to lightning strike. *Composites Part A: Applied Science and Manufacturing*, 100:352 – 360, 2017.

[69] Anders Larsson. The interaction between a lightning flash and an aircraft in flight. *Comptes Rendus Physique*, 3(10):1423 – 1444, 2002.

[70] Andrzej Katunin. Lightning strike protection of aircraft composite structures: Analysis and comparative study. *Fatigue of Aircraft Structures*, 2016:49–54, 12 2016.

[71] Andrzej Katunin and Katarzyna Krukiewicz. Preliminary analysis of thermal response of dielectric and conducting composite structures during lightning strike. *Composites Theory and Practice*, 16:8–14, 03 2016.

[72] Dexmet corporation. Lightning strike protection - microgrid for composite aircraft, wind turbine blades and structures. Accessed on 17-12-2019 at: https://cdn.thomasnet.com/ccp/10111169/29002.pdf.

[73] S. Palagummi and F.-G. Yuan. 8 - magnetic levitation and its application for low frequency vibration energy harvesting. In Fuh-Gwo Yuan, editor, *Structural Health Monitoring (SHM) in Aerospace Structures*, pages 213 – 251. Woodhead Publishing, 2016. ISBN 978-0-08-100148-6.

[74] Tahira J. Ahmed. An experimental investigation into resistance and induction welding for aerospace structures: A comparison. *47th AIAA/ASME/ASCE/AHS/ASC Structures, Structural Dynamics, and Materials Conference*, 2006.

[75] S.S.M. Tavares, M.R. da Silva, J.M. Neto, S. Miraglia, and D. Fruchart. Ferromagnetic properties of cold rolled aisi 304l steel. *Journal of Magnetism and Magnetic Materials*, 242-245:1391 – 1394, 2002. Proceedings of the Joint European Magnetic Symposia (JEMS'01).

[76] Valery Rudnev. Joining components by induction heating, part i. *Heat treating progress*, 5:19–22, 03 2005.

[77] Noesis Solutions. Optimus theoretical background. Technical report, Noesis, 2016.

[78] R. Saidur, N.A. Rahim, and M. Hasanuzzaman. A review on compressed-air energy use and energy savings. *Renewable and Sustainable Energy Reviews*, 14(4):1135 – 1153, 2010. ISSN 1364-0321.

[79] *Induktionsgenerator Serie i-Class 10-12kW*. Cobes GmbH, C.-D.-Magirus-Strasse 1, 79367 Weisweil, Germany, 800 0026.01_ba edition, August 2018.

[80] Ebay. National instruments ni 9213 16ch thermocouple input 250 vrms cat ii ni9213. Internet. Accessed on 18-12-2019 at: https://www.ebay.com/p/1122911588.

[81] The Modal Shop. National instruments. Internet. Accessed on 18-12-2019 at: http://www.modalshop.com/rental/National-Instruments?ID=294.

[82] Christos Kassapoglou. *Design and Analysis of Composite Structures: with Applications to Aerospace Structures.* WILEY, 2013.

[83] Pietro Tadini, Nathan Grange, Khaled Chetehouna, Nicolas Gascoin, Samuel Senave, and Isabelle Reynaud. Thermal degradation analysis of innovative pekk-based carbon composites for high-temperature aeronautical components. *Aerospace Science and Technology*, 65:106 – 116, 2017. ISSN 1270-9638.

[84] Kanbkam. Philips steam iron, blue - gc1440/26. Internet. Accessed on 04-11-2019 at: https://www.kanbkam.com/sa/en/philips-steam-iron-blue-gc144026-29597750.

[85] M. Duhovic, M. Hümber, P. Mitschang, and M. Maier. Further advances in simulating the processing fo composite materials by electromagnetic induction. *13th International LS-DYNA Users Conference*, 2014.

[86] Solvay asking more from chemistry. Avaspire paek. Datasheet.

[87] Arkema. Kepstan by arkema - technical data - 6000 series. Datasheet.

[88] Victrex High Performance Polymers. Victrex® peek 450g. Internet, July . Accessed on 17-12-2019 at: https://www.victrex.com/ /media/datasheets/victrex_tds_450g.pdf.

[89] Ronald Joven. Thermal properties of carbon fiber/epoxy composites with different fabric weaves. 01 2012.

[90] Tian Tian and Kevin D. Cole. Anisotropic thermal conductivity measurement of carbon-fiber/epoxy composite materials. *International Journal of Heat and Mass Transfer*, 55 (23):6530 – 6537, 2012. ISSN 0017-9310.

[91] Bhyrav Mutnuri. Thermal conductivity characterization of composite materials. Online, December 2019.

[92] J. Caruso and C. Chamis. Assessment of simplified composite micromechanics using three-dimensional finite-element analysis. *J. Compos. Technol. Res.*, 8, 02 1986.

[93] Toho Tenax Europe GmbH. Carbon ud hs 194 gsm. Internet. Accessed on 11-12-2019 at: http://ase.au.dk/fileadmin/www.ase.au.dk/Filer/Laboratorier_og_vaerksteder/Komposit-lab/Fiber/Carbon/Carbon_UD_HS__194_gsm__Tenax-E_HTS45_E23_-_TDS.pdf.

[94] M-Base. General polyetherketoneketone (pekk). Internet. Accessed on 11-12-2019 at: https://matmatch.com/materials/mbas044-general-polyetherketoneketone-pekk-.

A

Graphs by Schieler [3, 21]

Figure A.1 shows the temperature increase in °C after 5s of heating with a power of 99% for different radii of thermocouples. It can be seen that the smaller the radius is, the less they are heated up. This means that the error produced by using thermocouples in an electromagnetic field gets smaller by decreasing thermocouple diameter.

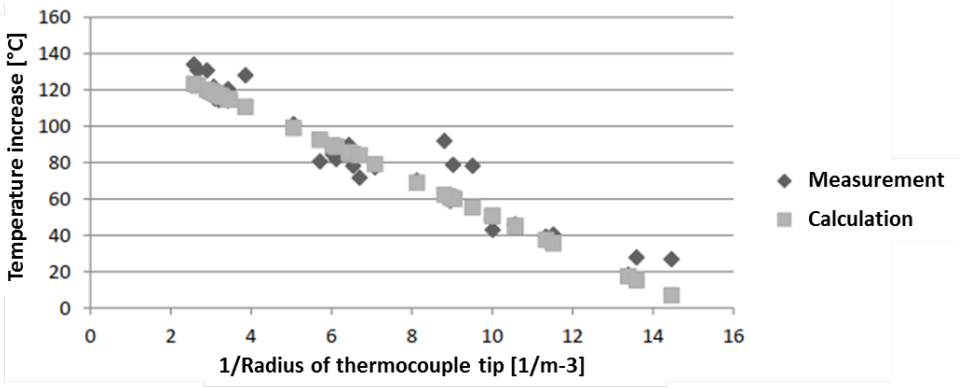

Figure A.1: Influence of wire diameter on the heating of a thermocouple [3]

Figure A.2 shows the through-thickness temperature profile when altering the air jet temperature. No obvious movement of the maximum temperature away from the coil can be seen, meaning that according to this test, lowering the air jet temperature was not effective.

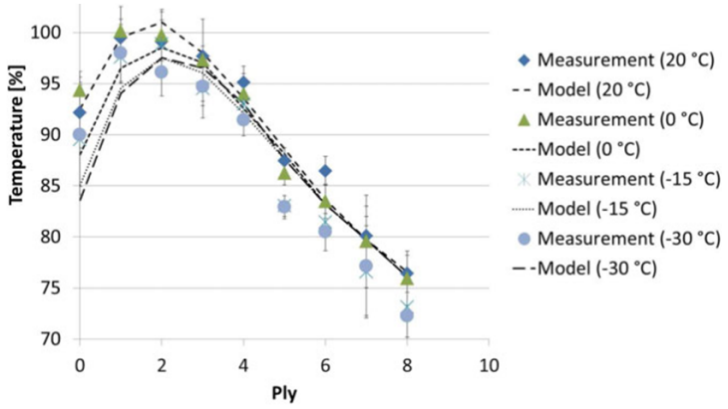

Figure A.2: Through-thickness temperature profile with varying air jet temperature by Schieler et al. [21]

B

Graphs by Becker and Mitschang [34]

Figure B.1 shows the experimental setup using infrared cameras used by Becker and Mitschang [34]. The temperature on both the side of the inductor and on the other side was measured. No through-the-thickness temperature measurements were performed.

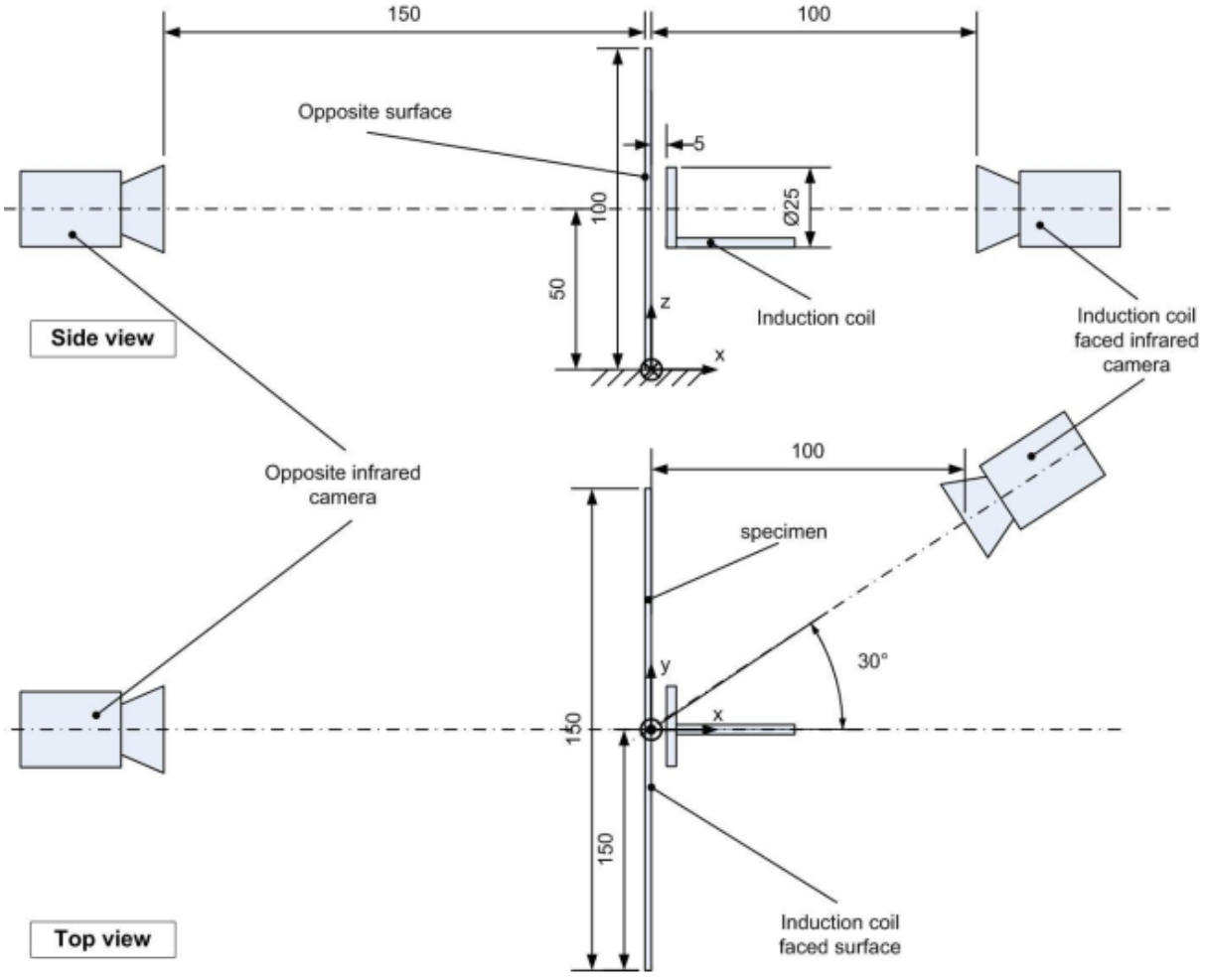

Figure B.1: Experimental setup by Becker and Mitschang [34]

Figure B.2 shows the measured fiber volume content and thickness of the laminates built and used by Becker and Mitschang [34]. These FVCs and thicknesses both have an influence on the heating rate of the laminates. Note that both y-axes are cut.

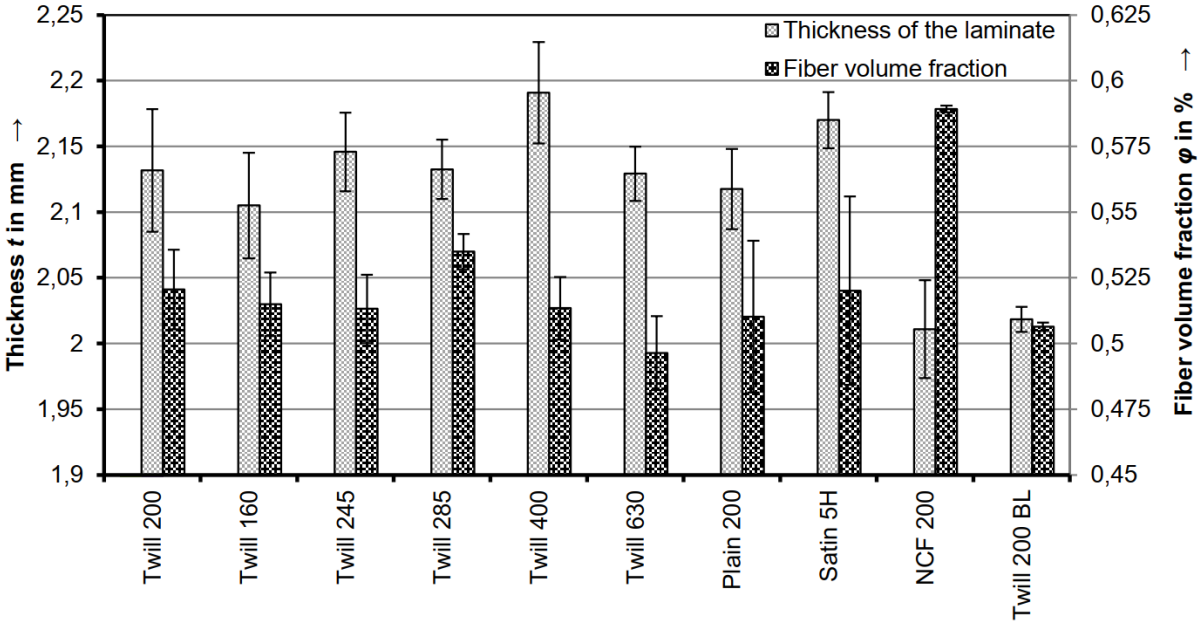

Figure B.2: Fiber volume content and thickness of tested laminates [34]

Figure B.3 shows a laminate design proposed by Becker and Mitschang [34] that theoretically would heat up more at the weld interface compared to near the coil. It would be difficult to automate the production of such a laminate with AFP or ATL because of the different materials that need to be disposed. Also, as the laminate is not symmetric, problems due to coupling effects are likely to arise. As to the best of the author's knowledge, results on the effectiveness of this laminate design have not been published.

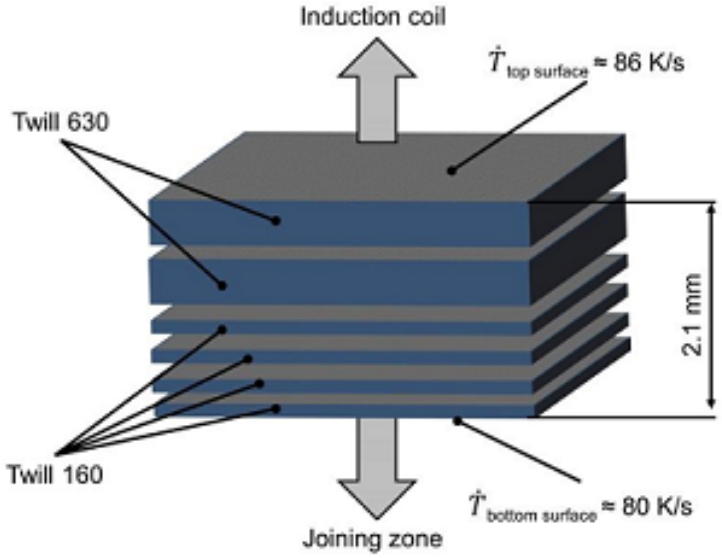

Figure B.3: Optimal laminate according to Becker and Mitschang [34]

C

Graph by Rudolf et al. [29]

Figure C.1 shows the heating time of different laminates made with different carbon fiber materials until a temperature of 300°C was reached [29]. This was done for two coil orientations of 0°and 90°respectively. The tests were stopped after 120 s when the laminates did not reach 300°C before this time. In this case, no bar was drawn.

Here: pw = plain weave, s = satin weave, f = fleece, ud = uni directional, p = polymer interlayer

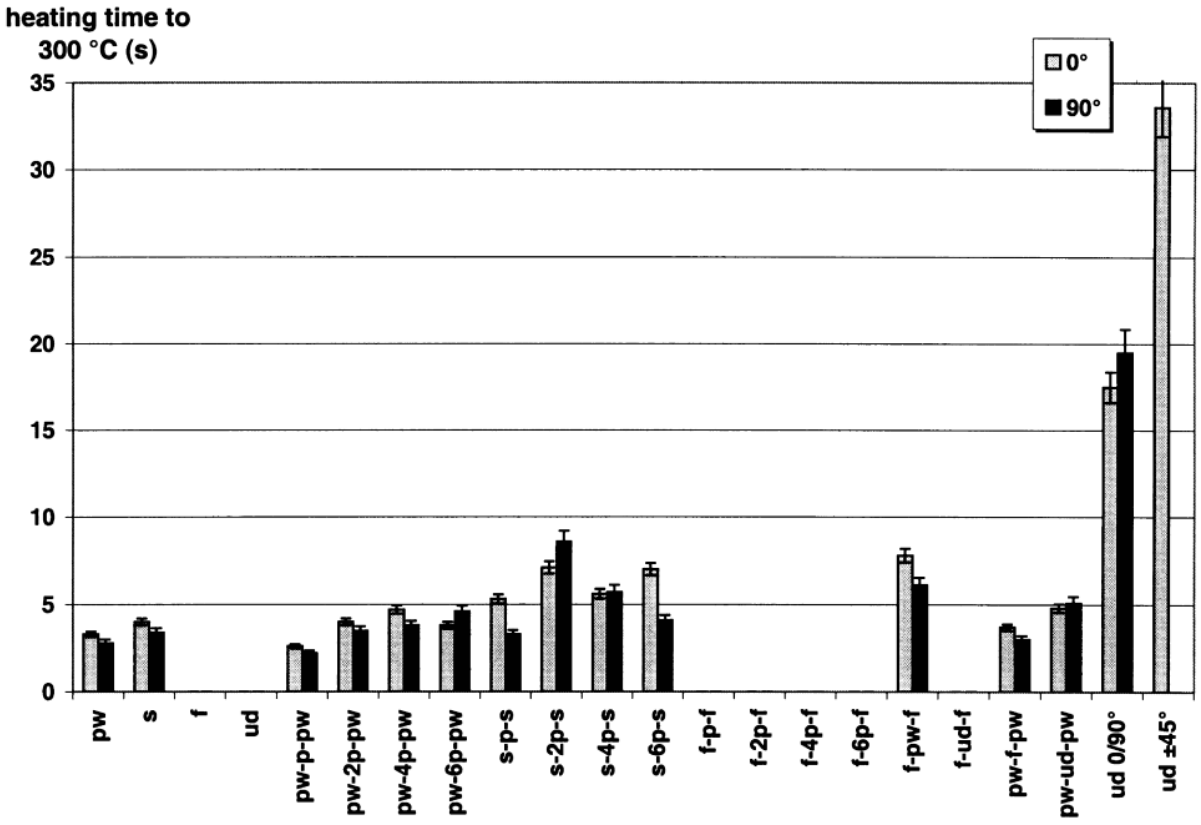

Figure C.1: Time to heat to 300°C for different laminates [29]

D

Design resolution

Table D.1 shows the design resolution of different fractional factorial designs. Here [77]:

- Resolution III - Two-factor interactions confound the main effects
- Resolution IV - Two-factor interactions confound each other
- Resolution V - Three-factor interactions confound two-factor interactions.

Number of Factors, k	Design Specification	Design Resolution	Number of Experiments
3	2^{3-1}	III	4
4	2^{4-1}	IV	8
5	2^{5-1}	V	16
5	2^{5-2}	III	8
6	2^{6-1}	VI	32
6	2^{6-2}	IV	16
6	2^{6-3}	III	8

Table D.1: Design resolution summary [77]

E

LabVIEW

LabVIEW is a program from National Instruments that can be used to acquire the data from sensors and to write programs on what to do with this data. Because the thermocouples are placed in a line and not directly on top of each other, measuring with all the thermocouples at the same time would result in errors due to a different magnetic field for each thermocouple. Therefore, it was decided to build two programs.

In the first program, the thermocouples that are relevant for that test can be selected. The data measured by these thermocouples are then saved to text files. Extra information such as the frequency used, the power, the time that the inductor was on and general notes can be saved to the text file. Also, the current date and time are saved. There is an option to measure with two test plates simultaneously. The data measured by the top plate is then saved in a different file than the data for the bottom plate. A picture of the front end of the LabVIEW program can be found in Figure E.1.

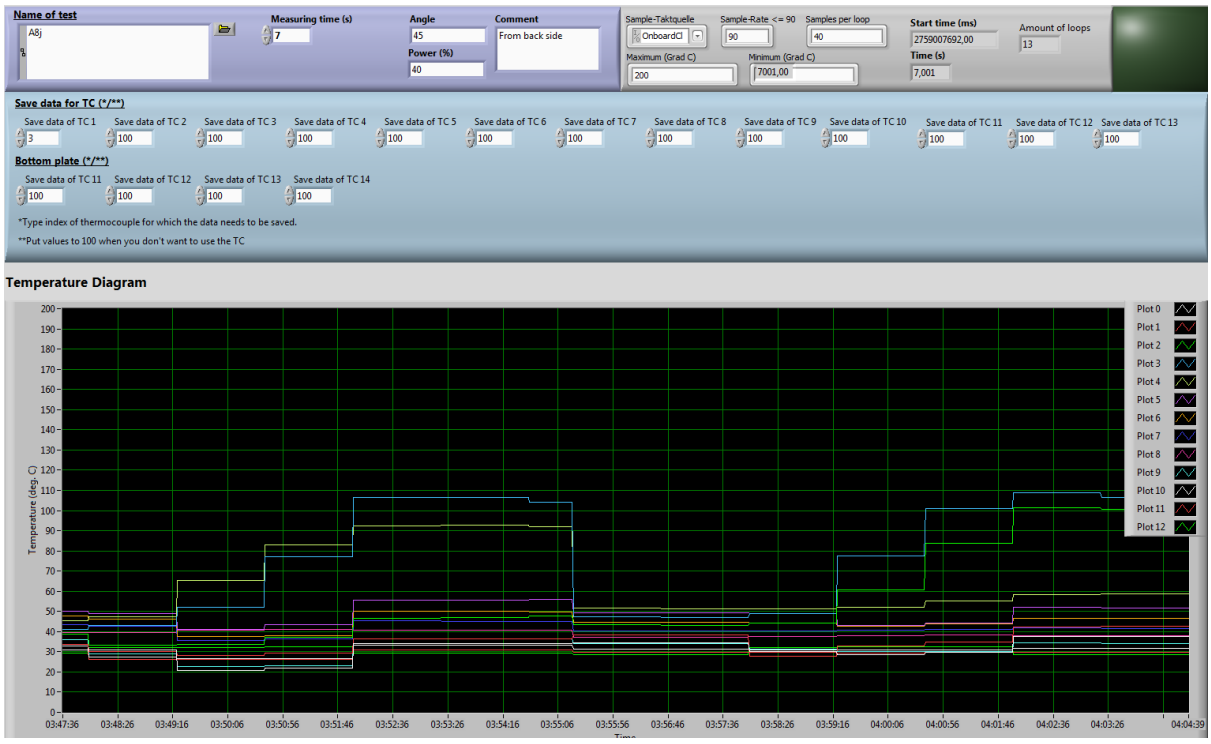

Figure E.1: Front end LabVIEW program - measuring and saving data

The second program puts the data of the different measurements that are stored in different files together. With this assembled data, three graphs are made. The first graph shows the temperature difference between the start of the measurement and the end of the measurement for each thermocouple on their respective location across the thickness of the laminate. This respective location is based on the part number that has to be selected before merging the files. The second graph shows the final temperature of each thermocouple on their location along the thickness of the laminate. Finally, the third graphs shows the temperature over time for each thermocouple. The graphs produced are saved automatically. A picture of the front end of the second LabVIEW program can be found in Figure E.2.

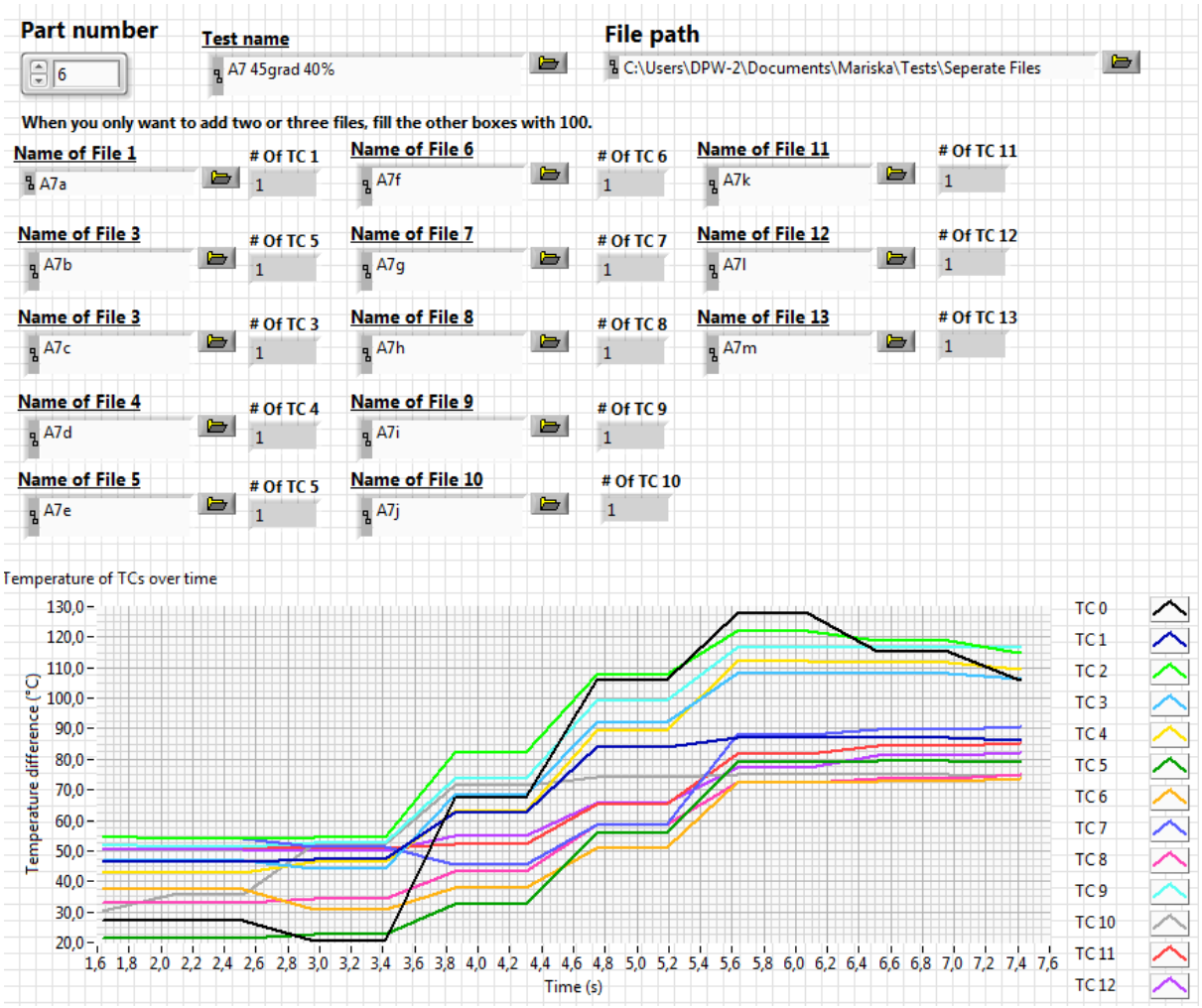

Figure E.2: Front end LabVIEW program - merge files and create graphs

F

Thermocouple calibration

As was explained in Section 2.2.2, thermocouples have a maximum limit of error. For type E thermocouples this is 1.7°C or 0.5%. For the special, or more accurate type, this limit is 1.0°C or 0.4%. These errors will not form a problem as it is expected that, depending on the test piece and the heating parameters, the temperatures found at different locations across the thickness will vary with more than 10°C during the primary tests [31, 32, 34].

In order to validate the temperature measured by the thermocouples, some thermocouples were calibrated. For the preliminary tests, two thermocouples of type E were calibrated and one thermocouple of type T and K were calibrated for comparison. The calibration was done by averaging 10 measurements with a 1Hz measuring frequency. For the preliminary tests, these temperature levels ranged from 30°C to 180°C with increments of 50°C. The limit of 180°C was chosen in order to allow for easy and safe insulation of the thermocouple wires. For the primary tests, glass fibre insulated thermocouples were used and they were calibrated for 50°C until 350°C with 50°C increments. The upper limit of this range was determined by the range of the calibration oven. This calibrated range just includes the melting temperature of 340°C. The calibration oven can be seen in Figure F.1a.

(a) Calibration with Beamex FB350

(b) Preliminary tests

(c) Primary tests

Figure F.1: Close-up of calibration machine and isolation thermocouples

For the unsheathed thermocouples in the preliminary tests, the wires had to be isolated such that they did not make contact outside of the measurement tip in the calibration machine (Beamex FB350). As can be seen in Figure F.1b, the isolation had to be small such that it

would fit in the calibration machine. For the primary tests, the thermocouples were isolated already as can be seen in Figure F.1c.

The isolation was done using a double-sided tape and a normal tape both resistant to temperatures up to 200°C. The two thermocouple wires were adhered to the two sides of the double-sided tape after which it was isolated from the surroundings with one-sided tape. The excess tape was cut away.

The calibration was performed in NI MAX from National Instruments and the results can be found in Figure F.2 and Figure F.3 for the preliminary tests and the primary tests respectively. On the y-axis the difference between the measured temperature by the thermocouple and the temperature provided by the calibration oven is plotted. This difference shows the error in the thermocouple measurement.

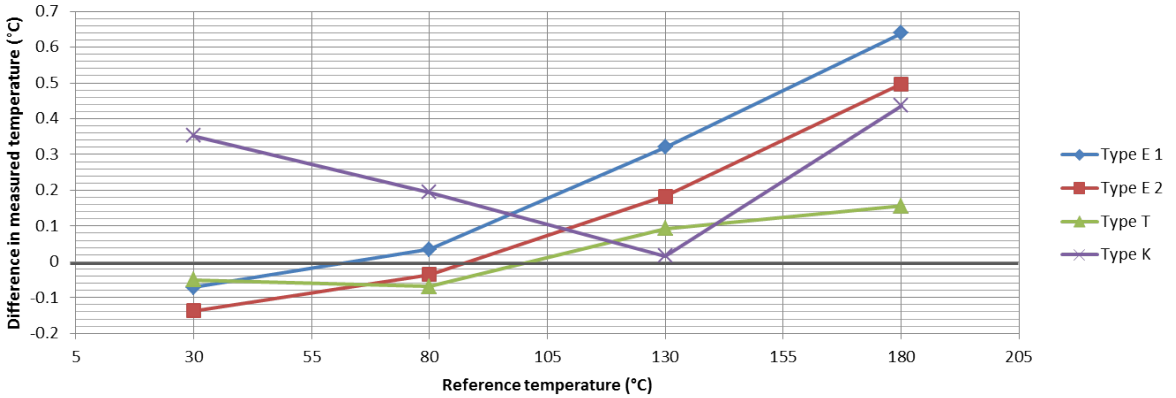

Figure F.2: Calibration thermocouples preliminary tests

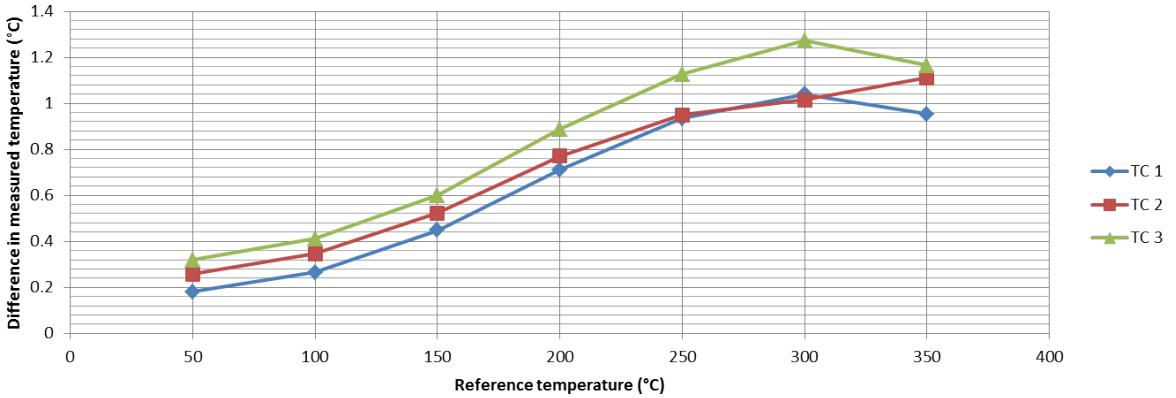

Figure F.3: Calibration type E thermocouples primary tests

As can be seen in Figures F.2 and F.3, the difference between the measured temperatures by the thermocouples and the temperature inside the oven were all well below the maximum error of 1.7°C or 0.5%. In the acquired results, except for type K, a trend can be noticed that for increasing temperature, the difference between the measured temperature and the reference temperature increases.

G

Temperature increase of preliminary test parts per inductor orientation

In Figures G.1 to G.4 the temperature increase measured with the thermocouples in the preliminary tests described in Section 6.3.2 can be found for each inductor orientation. The inductor orientation convention can be found in Figure 6.20. The data was collected with a sample size of five for which the thermocouples were changed and relocated and the part was moved and turned under the inductor. The error bars show a 95% confidence interval. For part 2, no ±45° samples were cut and therefore data on heating part 2 in the ±45° direction is missing.

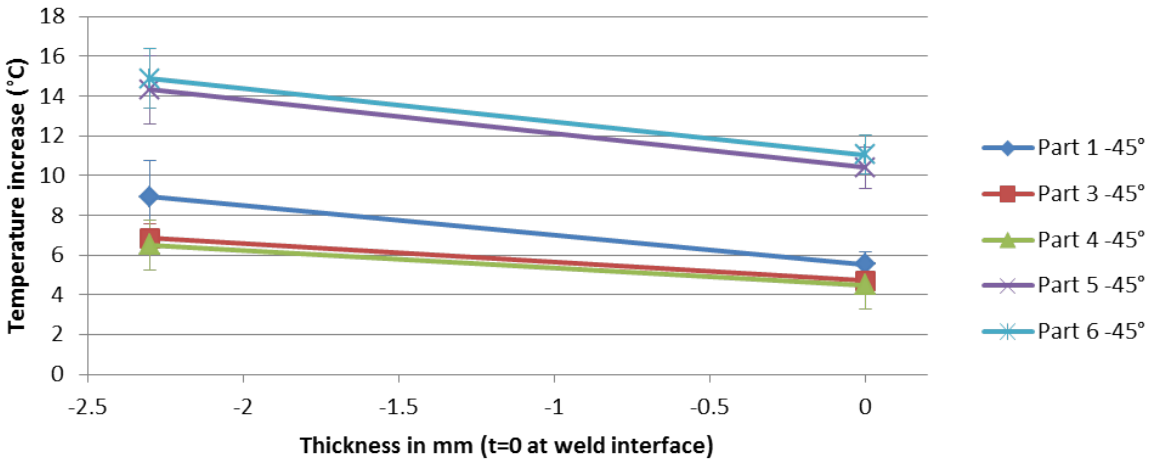

Figure G.1: Temperature increase for each part for an inductor orientation of -45°

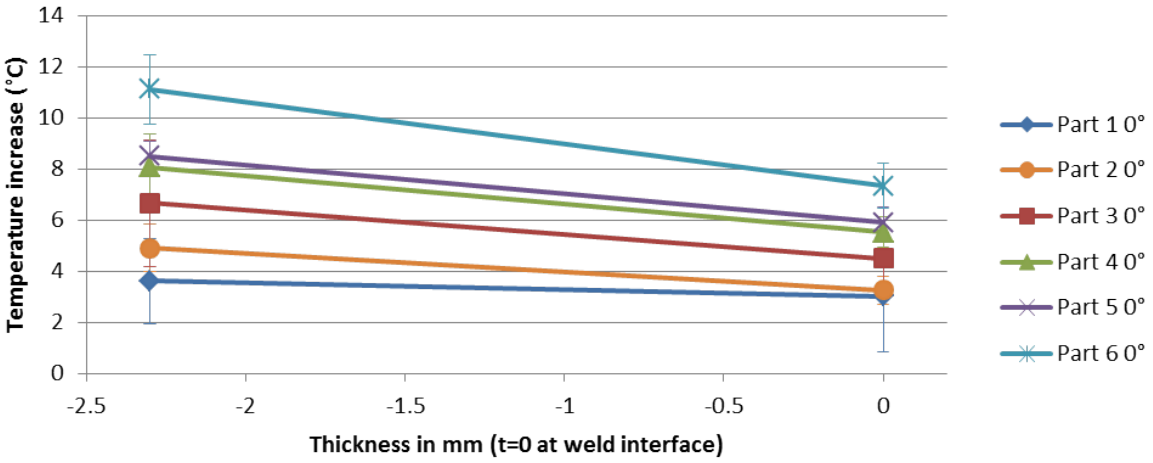

Figure G.2: Temperature increase for each part for an inductor orientation of 0°

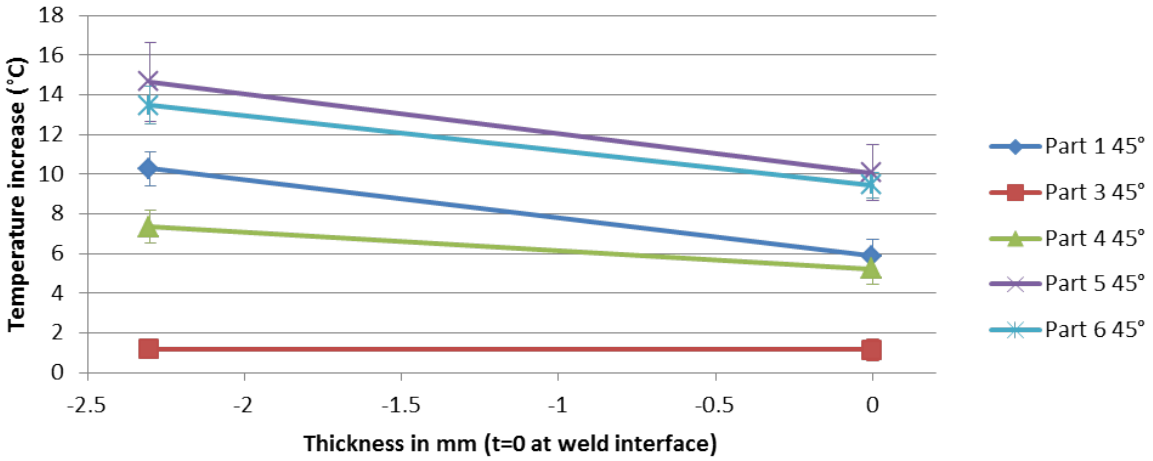

Figure G.3: Temperature increase for each part for an inductor orientation of 45°

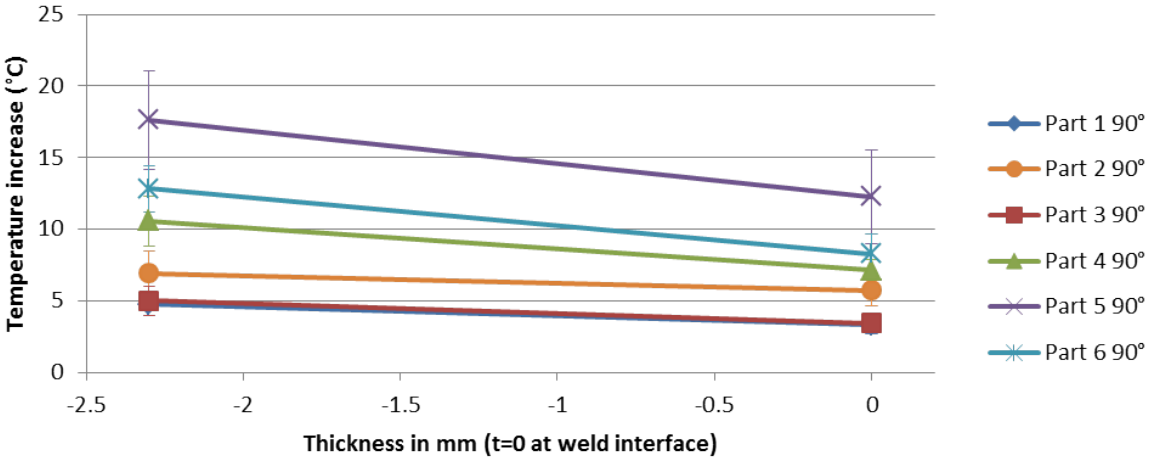

Figure G.4: Temperature increase for each part for an inductor orientation of 90°

Preliminary tests – non-averaged data

In this appendix the non-averaged data measured with the infrared camera during the preliminary trials is given.

In Figures H.1 and H.2, the non-averaged data of what influence the first plate has on the heating of the second plate and what influence the second plate has on the heating of the first plate are shown respectively. The data has been measured with an infrared camera.

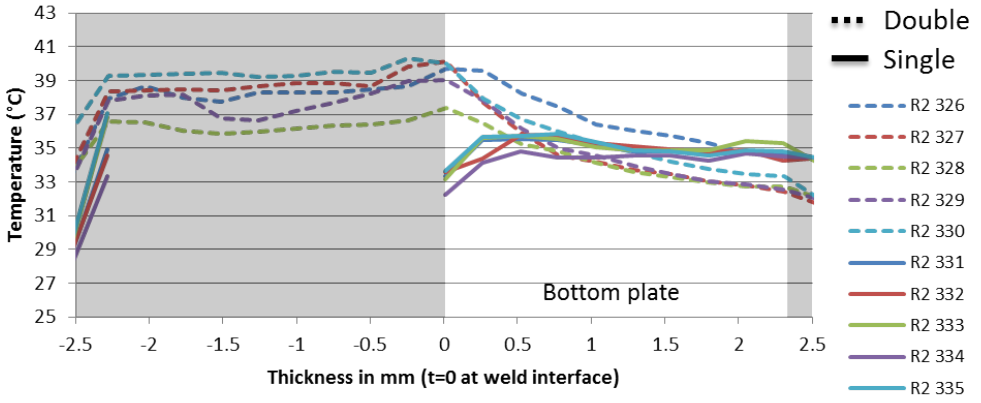

Figure H.1: Temperature profile across thickness - influence first plate on second plate - not averaged

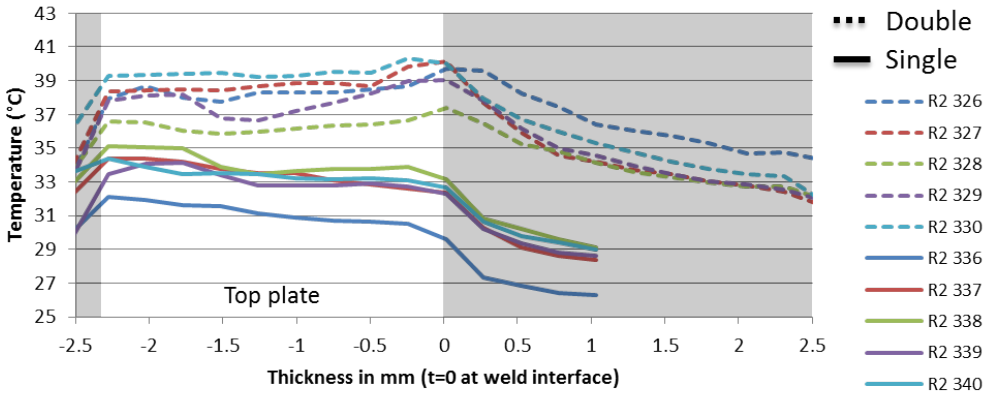

Figure H.2: Temperature profile across thickness - influence second plate on first plate - not averaged

In Figure H.3 the temperature profiles for the different fabric susceptors with a 90° angle w.r.t. the inductor are shown.

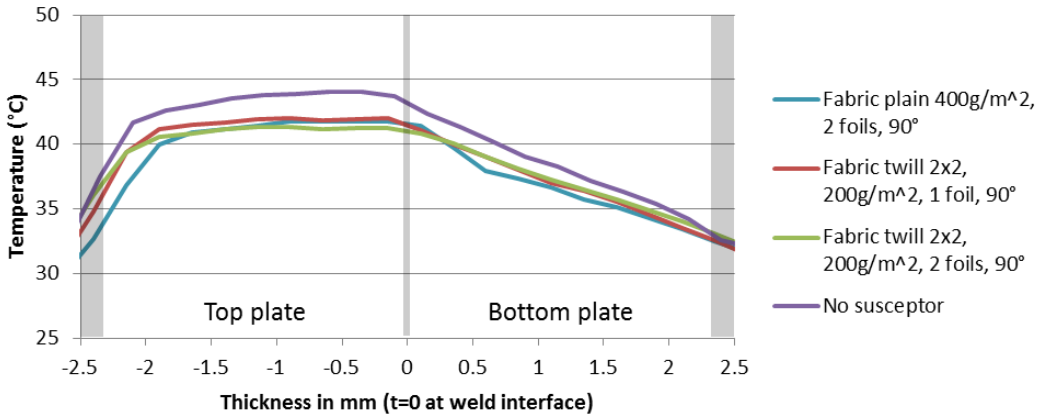

Figure H.3: Comparison different fabric susceptors 90°

In Figures H.4 to H.8 the temperature profiles for using no susceptor, the thin-ply susceptor with layup (90 0 90 0 90) in the 45° and 90° direction and the thin-ply susceptor with layup (90 45 0 45 90) in the 45° and 90° direction respectively. P6 and P7 stand for part 6 and 7 which both have the same layup (45 0 -45 0 90 0)s and therefore should produce the same results.

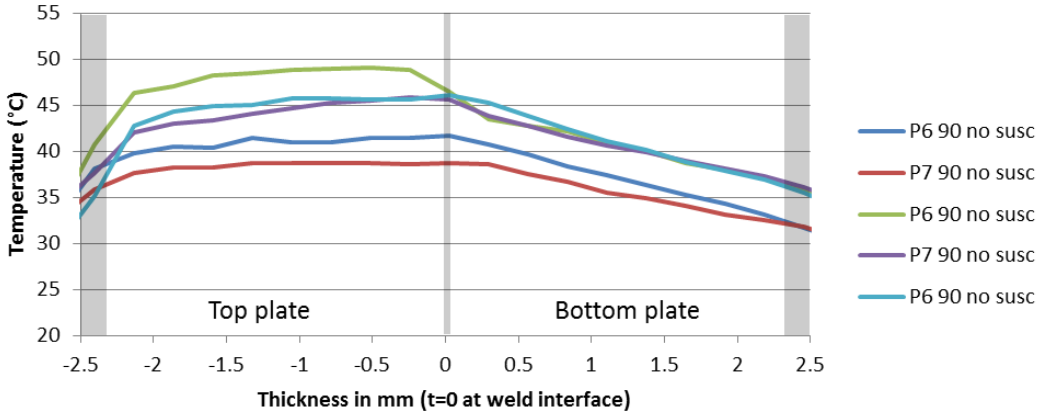

Figure H.4: Part 6 90° no susceptor

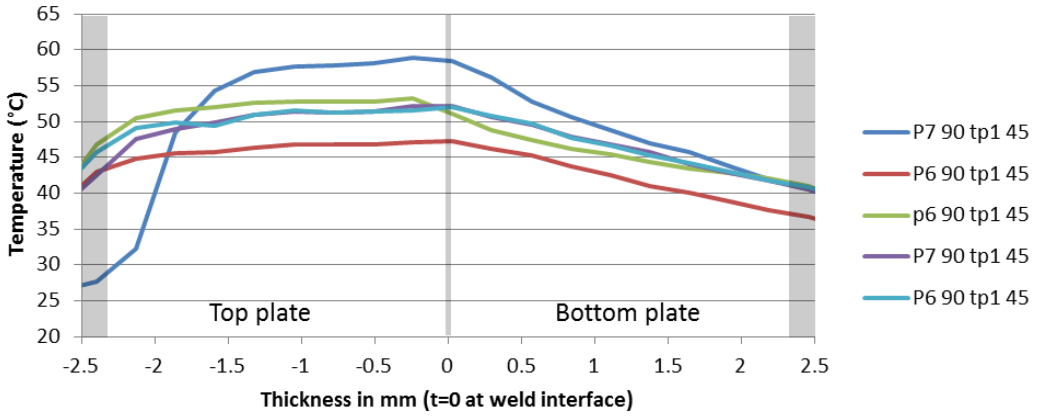

Figure H.5: Part 6 90° thin-ply 1, 45°

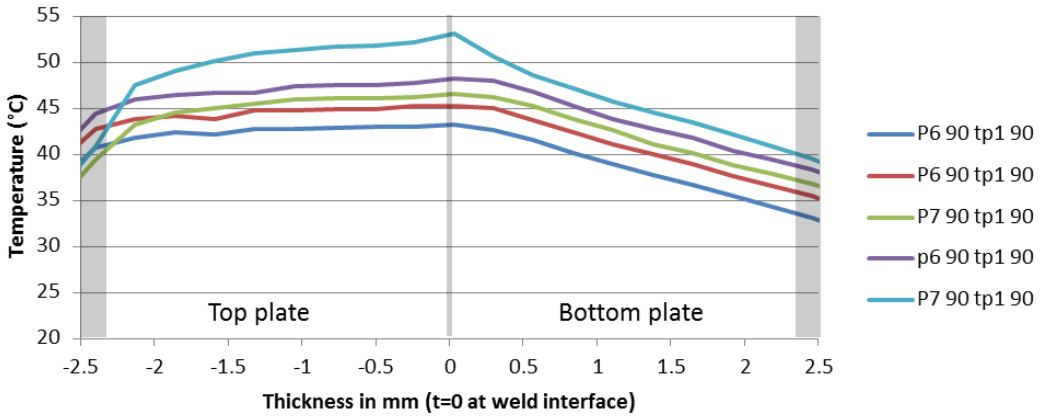

Figure H.6: Part 6 90° thin-ply 1, 90°

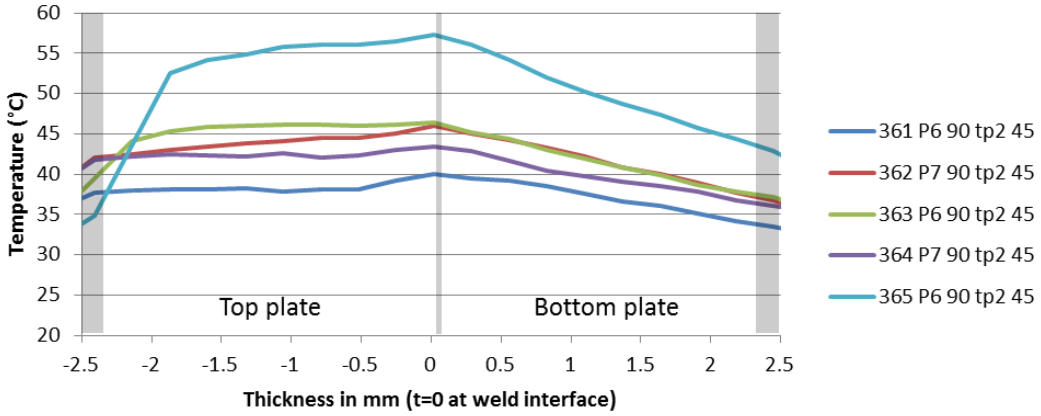

Figure H.7: Part 6 90° thin-ply 2, 45°

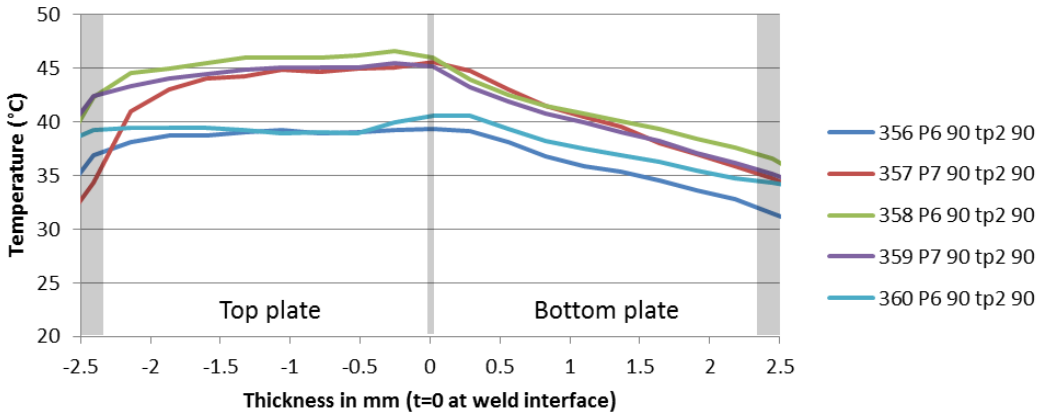

Figure H.8: Part 6 90° thin-ply 2, 90°

Calculating thermal conductivity perpendicular and parallel to the fibers

With the rule of mixtures the thermal conductivity K_p parallel to the fibers can be calculated using Equation (I.1) [91].

$$K_p = K_f \cdot V_f + (1 - V_f) \cdot K_m \tag{I.1}$$

Where: K_f is the thermal conductivity of the fibers, K_m is the thermal conductivity of the matrix and V_f is the fiber volume content.

Again with the rule of mixtures, the lower limit of the thermal conductivity transverse from the fibers can be calculated with Equation (I.2) [91].

$$K_t = \left(\frac{V_f}{K_f} + \frac{1 - V_f}{K_m} \right)^{-1} \tag{I.2}$$

Because the relation between the conductivity parallel and perpendicular to the fibers determines the way the heat is conducted, not the lower limit of thermal conductivity perpendicular to the fibers, but a estimation of the real value is relevant. This estimation can be done using Equation (I.3) proposed by Caruso and Chamis [92]:

$$K_t = 1 - \sqrt{V_f} \cdot K_m + \frac{\sqrt{V_f} \cdot K_m}{1 - \sqrt{V_f} \cdot (1 - \frac{K_m}{K_f})} \tag{I.3}$$

Using $K_f = 10 W/m \cdot K$ [93], $K_m = 0.24 W/m \cdot K$ [94] and $V_f = 58\%$, the K_p and K_t where calculated as follows:

$$K_p = 10 \cdot 0.58 + (1 - 0.58) \cdot 0.24 = 5.9 W/m \cdot K$$

$$K_t = 1 - \sqrt{0.58} \cdot 0.24 + \frac{\sqrt{0.58} \cdot 0.24}{1 - \sqrt{0.58} \cdot (1 - \frac{0.24}{10})} = 1.5 W/m \cdot K$$

It is therefore predicted that the composite conducts heat 5.9/1.5 = 3.9 times as good in the direction of the fibers compared to perpendicular to the fibers.